Nuclear Energy Density Functional methods for the modelling of heavy nuclei

Michael Bender

CNRS/IN2P3, IP2I Lyon, Villeurbanne, France

Ecole Joliot Curie 2026: Theory to shape experiments
held 13-18 September 2026 at Saint-Pierre d'Oléron, France

What to expect from this course

- The concept of static self-consistent mean-field methods
- zoology of effective interactions / energy density functionals for that purpose
- A glimpse of "beyond-mean-field models"
- Overview of phenomena that can be described with such methods
- Guidance about how to connect the output of mean-field/beyond-mean-field codes to experimental observations

From the nuclear many-body problem . . .

Nuclear many-body Hamiltonian composed of one-body kinetic energy, two-body interaction, three-body-interaction, etc

$$\hat{H} = \sum_{i,j} t_{ij}\, a_i^\dagger a_j + \frac{1}{2} \sum_{i,j,m,n} v_{ijmn}\, a_i^\dagger a_j^\dagger a_n a_m + \frac{1}{6} \sum_{i,j,k,l,m,n} v_{ijklmn}\, a_i^\dagger a_j^\dagger a_k^\dagger a_n a_m a_l + \ldots$$

Solve the eigenvalue problem

$$\hat{H}|\Phi_n\rangle = E_n|\Phi_n\rangle$$

All observables and transition matrix elements are then calculated as

$$O = \langle\Phi_n|\hat{O}|\Phi_n\rangle$$

$$T(\Phi_i \to \Phi_f) = \langle\Phi_f|\hat{O}|\Phi_i\rangle$$

The many-body eigenstates $|\Phi_n\rangle$ can be developed into A-body Slater determinants (which are the simplest form of anti-symmetrised Fermionic many-body wave function).
One possibility is to define them as particle-hole excitations on top of a single reference Slater determinant $|\Psi_r\rangle$

$$|\Phi_r\rangle = \prod_{i=1}^{A} a_k^\dagger |-\rangle$$

as

$$|\Phi_n\rangle = c_0|\Phi_r\rangle + \sum_{ph} c_{ph} a_p^\dagger a_h|\Phi_r\rangle + \sum_{pp'hh'} c_{pp'hh'}\, a_p^\dagger a_{p'}^\dagger a_{h'} a_h|\Phi_r\rangle$$

$$+ \sum_{pp'p''hh'h''} c_{pp'p''hh'h''}\, a_p^\dagger a_{p'}^\dagger a_{p''}^\dagger a_{h''} a_{h'} a_h|\Phi_r\rangle + \ldots$$

Other expansions of $|\Phi_n\rangle$ are possible and might be more advantageous for specific applications.

- Can be solved exactly for very light nuclei (through mapping on various clever few-body of many-body techniques that converge to exact low-lying eigenstates)
- The modern *ab-initio* paradigm to the nuclear many-body problem is to have systematically improvable expansions for $\hat{H}$ and $|\Phi_n\rangle$.
- Starting point for all kinds of approximate many-body methods (shell model, algebraic models, collective models . . .) that focus on effective degrees of freedom working with an effective Hamiltonian expressed in the relevant degrees of freedom.

. . . to self-consistent mean field models

Mean-field approximation to the "exact" nuclear many-body problem:

1. Keep your personal favorite form of "bare" Hamiltonian $\hat{H}$ (that is not unique)
2. Make the *ansatz* that the nuclear many-body wave function is a single Slater determinant $|\mathrm{SD}\rangle$
3. Use Ritz' variational principle to search for the Slater determinant $|\mathrm{SD}\rangle$ that gives the largest binding

$$\delta E = \delta \frac{\langle \mathrm{SD}|\hat{H}|\mathrm{SD}\rangle}{\langle \mathrm{SD}|\mathrm{SD}\rangle} = 0$$

Some further comments

- Limits calculation to the lowest nuclear state (reachable from given initial conditions within a given variational space)
- Why this is a "mean-field approximation" will become clear in what follows
- Works often reasonably well in atomic physics for many atoms, molecules, etc
- Tried with the "bare" nuclear Hamiltonians of the day in the 1960s. Explains qualitatively certain aspects of nuclear structure, but completely fails on a quantitative level.
- The strong nuclear interaction leads to in-medium correlations that cannot be neglected. (Example: short-range repulsion that makes that the probability to find a nucleon is not independent on where the other nucleons are)
- The effective interaction also has to absorb the global trend of the coupling to surface modes that are not explicitly treated in mean-field models
- Predictive self-consistent mean-field calculations of nuclei have to be done with (usually phenomenological) effective in-medium interactions adjusted to properties of nuclei and/or nuclear matter.

A few further comments on Slater determinants

The one-body density matrix in a single-particle basis is

$$\rho_{ij} = \langle \Phi | \hat{a}_j^\dagger \hat{a}_i | \Phi \rangle$$

Similarly, one can define a two-body density matrix

$$\rho^{(2)}_{ijmn} = \langle \Phi | a_i^\dagger a_j^\dagger a_n a_m | \Phi \rangle$$

In the single-particle basis that builds the Slater determinant – which is called its "natural basis" – the one-body density matrix is diagonal

$$\rho_{ij} = \langle \mathrm{SD} | \hat{a}_j^\dagger \hat{a}_i | \mathrm{SD} \rangle = \rho_{ii}\delta_{ij} = \begin{cases} 1 & \text{of } i \text{ is occupied ("hole state")} \\ 0 & \text{of } i \text{ is empty ("particle state")} \end{cases}$$

(In arbitrary single-particle bases, ρ_{ij} is in general a full matrix with complex matrix elements).
The square of the one-body density matrix of a Slater determinant is idempotent

$$\sum_m \rho_{im}\rho_{mj} = \rho_{ij}$$

or

$$\rho^2 = \rho \otimes \rho = \rho$$

which is a specificity of Slater determinants and implies that Slater determinants are *independent particle states*, i.e. the probability to find one nucleon does not depend on where the other nucleons are.

With this, all matrix elements between *many-body operators* (such as the Hamiltonian, but not only) of a Slater determinant can be expressed solely through one-body density matrices.

Even more comments on Slater determinants

$$\langle \mathbf{x}_1, \mathbf{x}_2, \cdots, \mathbf{x}_A | \mathrm{SD} \rangle = \frac{1}{\sqrt{A!}} \begin{vmatrix} \psi_1(\mathbf{x}_1) & \psi_1(\mathbf{x}_2) & \cdots & \psi_1(\mathbf{x}_A) \\ \psi_2(\mathbf{x}_1) & \psi_2(\mathbf{x}_2) & \cdots & \psi_2(\mathbf{x}_A) \\ \cdots & \cdots & \cdots & \cdots \\ \psi_A(\mathbf{x}_1) & \psi_A(\mathbf{x}_2) & \cdots & \psi_A(\mathbf{x}_A) \end{vmatrix}$$

The one-body density matrix in coordinate space is

$$\rho(\mathbf{x}, \mathbf{x}') = \langle \Phi | \hat{a}^\dagger_{x'} \hat{a}_x | \Phi \rangle$$

Again, for the density matrices of Slater determinants one has

$$\int \mathrm{d}^3 x'' \, \rho(\mathbf{x}, \mathbf{x}'') \rho(\mathbf{x}'', \mathbf{x}') = \rho(\mathbf{x}, \mathbf{x}')$$

In nuclear physics, one usually deals with three types of coordinates

$$\mathbf{x} = (\mathbf{r}, \sigma; q) \qquad \int \mathrm{d}^3 x = \int \mathrm{d}^3 r \sum_{\sigma = \pm 1} \sum_{q = p, n}$$

which are position, spin and isospin / nucleon species.

Note: sum practitioners use $\sigma = \pm 1/2$ and $\tau = \pm 1$ or $\tau = \pm 1/2$ instead. Note also, that in most of the nuclear physics literature, the neutron has isospin projection $1/2$, whereas in most of the particle physics literature, the neutron has isospin projection $-1/2$. (With this convention, the majority of nuclei has positive isospin projection).

The full density matrices of protons and neutrons are (assuming that $|\Phi\rangle = |\Phi_p\rangle \otimes |\Phi_n\rangle$ as usually done)

$$\rho_q(\mathbf{r}\sigma, \mathbf{r}'\sigma') \equiv \langle \Phi | \hat{a}^\dagger_{\mathbf{r}'\sigma' q} \hat{a}_{\mathbf{r}\sigma q} | \Phi \rangle$$

from which one can construct the non-local densities

$$\rho_q(\mathbf{r}, \mathbf{r}') \equiv \sum_\sigma \rho_q(\mathbf{r}\sigma, \mathbf{r}'\sigma)$$

$$s_{q,\kappa}(\mathbf{r}, \mathbf{r}') \equiv \sum_{\sigma\sigma'} \rho_q(\mathbf{r}\sigma, \mathbf{r}'\sigma') \langle \sigma' | \hat{\sigma}_\kappa | \sigma \rangle$$

Symmetry breaking

- With the exception of homogeneous isotropic infinite matter, independent particle states are incompatible with the symmetries of the nuclear Hamiltonian, that are conserved by the eigenstates of the exact Hamiltonian.
- Phenomenology tells us that the "exact" nuclear part of the Hamiltonian seems to be invariant under translations, rotations, parity, Galilean or Lorentz transformations, time-reversal, and time-translation, and to only weakly depend on transformations in isospin space.
- Electromagnetic interactions are of course not invariant under transformations in isospin space
- Effective interactions and energy density functionals for mean-field calculations are constructed to conserve these symmetries, such that the total energy conserves these symmetries.
- However, a Slater determinant that minimises the total energy will in general break many of the symmetries of the interaction. (Known as "symmetry dilemma", first formulated by Löwdin for atomic physics)
- This is less dramatic than it sound, as it permits the interpretation of nuclear phenomena through symmetry-breaking shapes, i.e. the geometry of the arrangement of nucleons.

Nuclear two-body Hamiltonian with pure two-body force

$$\hat{H} = \sum_{i,j} t_{ij}\, a_i^\dagger\, a_j + \frac{1}{2} \sum_{i,j,m,n} v_{ijmn}\, a_i^\dagger\, a_j^\dagger\, a_n a_m$$

Slater-determinant expectation value

$$E^{\mathrm{HF}} = \sum_{i=1}^{A} t_{ii} + \frac{1}{2} \sum_{i,k=1}^{A} \left(v_{ikik} - v_{ikki} \right)$$

where one usually uses a shorthand $\bar{v}_{ikik} = v_{ikik} - v_{ikki}$ for anti-symmetrised matrix elements.

Variation $\delta E^{\mathrm{HF}} = 0$ under constraint of orthonormality of single-particle wave functions leads to HF equation that can be expressed in several equivalent forms.

$$[h, \rho] = 0 \qquad \Leftrightarrow \qquad \hat{h}\, \psi_j = \epsilon_j\, \psi_j$$

with

$$h_{ik} = \frac{\delta E^{\mathrm{HF}}}{\delta \rho_{ki}} \qquad \text{with} \qquad h_{ii} = \epsilon_i = t_{ii} + \sum_{k=1}^{A} \left(v_{ikik} - v_{ikki} \right)$$

in the basis that diagonalises both h_{ji} and ρ_{ij}. With that

$$E^{\mathrm{HF}} = \tfrac{1}{2} \sum_{i=1}^{A} \left(t_{ii} + \epsilon_i \right)$$

for a Slater determinant that solves the HF equation.

There are very few self-consistent mean-field approaches that use effective three-body forces.

In the context of nuclear mean-field approaches one in general adds a density-dependent part $v[\rho]$ to the two-body force

$$\hat{H} = \sum_{i,j} t_{ij} a_i^\dagger a_j + \frac{1}{2} \sum_{i,j,m,n} \left(v_{ijmn} + v[\rho]_{ijmn} \right) a_i^\dagger a_j^\dagger a_n a_m$$

which yields

$$E^{\mathrm{HF}} = \sum_{i=1}^{A} t_{ii} + \frac{1}{2} \sum_{i,k=1}^{A} \left(v_{ikik} - v_{ikki} \right) + \frac{1}{2} \sum_{i,k=1}^{A} \left(v[\rho]_{ikik} - v[\rho]_{ikki} \right)$$

$$h_{ii} = \epsilon_i = t_{ii} + \sum_{k=1}^{A} \left(v_{ikik} + v[\rho]_{ikik} - v_{ikki} - v[\rho]_{ikki} \right) + \tfrac{1}{2} \sum_{k=1}^{A} \left[\left(\frac{\delta v[\rho]}{\delta \rho} \right)_{ikik} - \left(\frac{\delta v[\rho]}{\delta \rho} \right)_{ikki} \right]$$

and thereby adds a "rearrangement energy" to the single-particle Hamiltonian. With that

$$E^{\mathrm{HF}} = \tfrac{1}{2} \sum_{i=1}^{A} \left(t_{ii} + \epsilon_i \right) - \tfrac{1}{4} \sum_{k=1}^{A} \left[\left(\frac{\delta v[\rho]}{\delta \rho} \right)_{ikik} - \left(\frac{\delta v[\rho]}{\delta \rho} \right)_{ikki} \right]$$

for a Slater determinant that solves the HF equation.

A similar rearrangement energy also emerges from 3-body and higher-order many-body forces.

Heenen and Godefroid, Scholarpedia, 7(10):10545. http://dx.doi.org/10.4249/scholarpedia.10545

In coordinate space, this schematically becomes for a two-body potential $v[\rho](\mathbf{r}-\mathbf{r}')$ (ignoring spin and isospin)

$$E = -\frac{\hbar^2}{2m}\sum_{k=1}^{A}\Psi_k^\dagger(\mathbf{r})\Delta\Psi_k(\mathbf{r}) + \frac{1}{2}\sum_{j,k=1}^{A}\iint \mathrm{d}^3r\,\mathrm{d}^3r'\;\Psi_j^\dagger(\mathbf{r})\,\Psi_k^\dagger(\mathbf{r}')\,v[\rho](\mathbf{r}-\mathbf{r}')\,\left[\Psi_j(\mathbf{r})\,\Psi_k(\mathbf{r}') - \Psi_j(\mathbf{r}')\,\Psi_k(\mathbf{r})\right]$$

$$= E_{\mathrm{kin}} + \iint \mathrm{d}^3r\,\mathrm{d}^3r'\;\rho(\mathbf{r})\,v[\rho](\mathbf{r}-\mathbf{r}')\,\rho(\mathbf{r}') - \iint \mathrm{d}^3r\,\mathrm{d}^3r'\;\rho(\mathbf{r},\mathbf{r}')\,v[\rho](\mathbf{r}-\mathbf{r}')\,\rho(\mathbf{r}',\mathbf{r})$$

and

$$\varepsilon_k\Psi_k(\mathbf{r}) = -\frac{\hbar^2}{2m}\Delta\Psi_k(\mathbf{r}) + \int \mathrm{d}^3r'\;v[\rho](\mathbf{r}-\mathbf{r}')\,\rho(\mathbf{r}')\,\Psi_k(\mathbf{r})$$

$$- \int \mathrm{d}^3r'\;v[\rho](\mathbf{r}-\mathbf{r}')\,\rho(\mathbf{r},\mathbf{r}')\,\Psi_k(\mathbf{r}')$$

$$+ \iint \mathrm{d}^3r'\,\mathrm{d}^3r''\left(\frac{\delta v[\rho](\mathbf{r}'-\mathbf{r}'')}{\delta\rho(\mathbf{r})}\right)\left[\rho(\mathbf{r}')\,\rho(\mathbf{r}'') - \rho(\mathbf{r}',\mathbf{r}'')\,\rho(\mathbf{r}'',\mathbf{r}')\right]$$

$$= -\frac{\hbar^2}{2m}\Delta\Psi_k(\mathbf{r}) + U_{\mathrm{dir}}(\mathbf{r})\,\Psi_k(\mathbf{r}) + \int \mathrm{d}^3r'\;U_{\mathrm{ex}}(\mathbf{r},\mathbf{r}')\,\Psi_k(\mathbf{r}') + U_{\mathrm{rea}}(\mathbf{r})\,\Psi_k(\mathbf{r})$$

Why is there a density dependence?

- Weisskopf [NP3 (1957) 423] pointed out that any pure two-body interaction (irrespective of its form) fitted to reproduce (at the mean-field level) the empirical values for $\rho_{\rm sat}$ and E/A of homogeneous symmetric and spin-symmetric infinite nuclear matter necessarily leads to $m_0^*/m \approx 0.4$, which is incompatible with empirical data. For a modern analysis see [Davesne, Navarro, Meyer, Bennaceur, Pastore, PRC 97 (2018) 044304].

$\Rightarrow$ need for higher-order terms in the density matrix when aiming at a description of nuclear properties (at the mean-field level with effective interactions built for that purpose). But what kind of terms is missing that describes which physics phenomenon?

- Numerically treatable 3-body forces proposed in the past lead to a number of practical problems, see the introduction to [Sadoudi, Duguet, Meyer, Bender, PRC 88 (2013) 064326] and also [Guillon, Bender, Bennaceur, da Costa, arXiv:2607.01190v1] for reviews of the various numerical and phenomenological issues.
- Already very simple forms of density dependence lead to excellent phenomenology.

In the context of self-consistent mean-field models, it has become customary to call the total energy an *Energy Density Functional* (EDF).

One has to distinguish several cases of such energy density functionals:

- *Pseudopotential-based functionals* are strictly and without approximation/omission derived as the HF or HFB expectation value of an *ansatz* for an underlying effective nucleon-nucleon interaction that serves as the generator of the functional.
- *General functionals* are set up as an *ansatz* for a combination of one-body densities that satisfies the symmetries of the exact nuclear Hamiltonian (or even more symmetries), often motivated by the formalism of *Density Functional Theory* as used for atoms, molecules, and condensed matter.

  Note: In spite of popular belief, nuclear EDF calculations are not Kohn-Sham calculations covered by the Hohenberg-Kohn theorem (i.e. conceptually they are different from DFT for electronic systems, although the equations that are solved might look exactly the same).
- *Hybrid functionals* are a combination of the two concepts: the overall structure is usually related to a generator, but, driven by numerical and/or phenomenological considerations, some terms are manipulated/omitted/added/...

This classification applies to all kinds of nuclear energy density functionals.

Energy functional

$$\mathcal{E} = \mathcal{E}_{\text{kin}} + \mathcal{E}_{\text{strong}} + \mathcal{E}_{\text{Coul}} + \mathcal{E}_{\text{pair}} - \mathcal{E}_{\text{corr}}$$

where

- $\mathcal{E}_{\text{kin}}$: free kinetic energy
- $\mathcal{E}_{\text{strong}}$: model of the effective in-medium strong interaction between nucleons (in the particle-hole channel)
- $\mathcal{E}_{\text{pair}}$: model of the effective in-medium electromagnetic interaction between nucleons
- $\mathcal{E}_{\text{pair}}$: model of the effective in-medium interaction between nucleons (in the particle-hole channel)
- $\mathcal{E}_{\text{corr}}$: approximation and/or model of spurious zero-point energies related to working with Slater determinants instead of correlated many-body wave functions (centre-of-mass correction, rotational correction, vibrational correction, . . .)

$$
\begin{aligned}
\mathcal{E}_{\text{Skyrme}} = \int \mathrm{d}^3 r \sum_{t=0,1} \Big\{ & C_t^{\rho\rho}[\rho_0]\, \rho_t(\mathbf{r})\, \rho_t(\mathbf{r}) + C_t^{\rho\tau}\left[\rho_t(\mathbf{r})\, \tau_t(\mathbf{r}) - \mathbf{j}_t(\mathbf{r}) \cdot \mathbf{j}_t(\mathbf{r})\right] \\
& + C_t^{\rho\Delta\rho}\, \rho_t(\mathbf{r}) \Delta\rho_t(\mathbf{r}) + C_t^{ss}[\rho_0]\, \mathbf{s}_t(\mathbf{r}) \cdot \mathbf{s}_t(\mathbf{r}) + C_t^{s\Delta s}\, \mathbf{s}_t \cdot \Delta \mathbf{s}_t(\mathbf{r}) \\
& + C_t^{sT}\left(\mathbf{s}_t \cdot \mathbf{T}_t - \sum_{\mu,\nu=x,y,z} \mathbf{J}_{\mu\nu;t} \mathbf{J}_{\mu\nu;t}\right) \\
& + C_t^{\rho\nabla J}\left[\rho_t(\mathbf{r}) \boldsymbol{\nabla} \cdot \mathbf{J}_t(\mathbf{r}) + \mathbf{s}_t(\mathbf{r}) \cdot \nabla \times \mathbf{j}_t(\mathbf{r})\right] \\
& + C_t^{sF}\left[\mathbf{s}_t(\mathbf{r}) \cdot \mathbf{F}_t(\mathbf{r}) - \tfrac{1}{2} \sum_{\mu,\nu=x,y,z} \mathbf{J}_{\mu\nu;t}(\mathbf{r}) \mathbf{J}_{\nu\mu;t}(\mathbf{r}) - \tfrac{1}{2} \sum_{\mu,\nu=x,y,z} \mathbf{J}_{\mu\mu;t}(\mathbf{r}) \mathbf{J}_{\nu\nu;t}(\mathbf{r})\right] \\
& + C_t^{\nabla s \nabla s}\left[\nabla \cdot \mathbf{s}_t(\mathbf{r})\right]\left[\nabla \cdot \mathbf{s}_t(\mathbf{r})\right] \Big\}
\end{aligned}
$$

- objects in red are coupling constants
- objects in blue are time-even local densities
- objects in green are time-odd local densities
- Some combinations of terms are required by Galilean invariance.
- Summation is over isoscalar ($t = 0$) and isovector ($t = 1$) densities, for example

$$\rho_0(\mathbf{r}) = \rho_p(\mathbf{r}) + \rho_n(\mathbf{r})$$
$$\rho_1(\mathbf{r}) = \rho_p(\mathbf{r}) - \rho_n(\mathbf{r})$$

Local densities

$$\rho_q(\mathbf{r}) = \rho_q(\mathbf{r},\mathbf{r}')\big|_{\mathbf{r}=\mathbf{r}'} \qquad \text{density}$$

$$\tau_q(\mathbf{r}) = \nabla\cdot\nabla'\,\rho_q(\mathbf{r},\mathbf{r}')\big|_{\mathbf{r}=\mathbf{r}'} \qquad \text{kinetic density}$$

$$J_{q,\mu\nu}(\mathbf{r}) = -\tfrac{\mathrm{i}}{2}\left(\nabla_\mu - \nabla'_\mu\right) s_{q,\nu}(\mathbf{r},\mathbf{r}')\big|_{\mathbf{r}=\mathbf{r}'} \qquad \text{spin current}$$

$$\mathbf{s}_q(\mathbf{r}) = \mathbf{s}_q(\mathbf{r},\mathbf{r}')\big|_{\mathbf{r}=\mathbf{r}'} \qquad \text{spin density}$$

$$\mathbf{T}_q(\mathbf{r}) = \boldsymbol{\nabla}\cdot\boldsymbol{\nabla}'\,\mathbf{s}_q(\mathbf{r},\mathbf{r}')\big|_{\mathbf{r}=\mathbf{r}'} \qquad \text{spin kinetic density}$$

$$F_{q,\mu}(\mathbf{r}) = \tfrac{1}{2}\sum_\nu(\nabla_\mu\nabla'_\nu + \nabla_\nu\nabla'_\mu)\,s_{q,\nu}(\mathbf{r},\mathbf{r}')\big|_{\mathbf{r}=\mathbf{r}'} \qquad \text{other spin kinetic density}$$

$$\mathbf{j}_q(\mathbf{r}) = -\tfrac{\mathrm{i}}{2}\left(\nabla_\mu - \nabla'_\mu\right)\rho_q(\mathbf{r},\mathbf{r}')\big|_{\mathbf{r}=\mathbf{r}'} \qquad \text{current density}$$

The expectation values of the components of angular momentum can be calculated from the local spin density and and the current

$$\langle\hat{\mathbf{J}}\rangle = \int d^3r\,\left[\mathbf{r}\times\mathbf{j}_0(\mathbf{r}) + \tfrac{1}{2}\mathbf{s}_0(\mathbf{r})\right]$$

- finite angular momentum of a system implies that time-odd densities are non-zero
- In such systems there will be contributions from time-odd terms to the energy (but potentially also others)

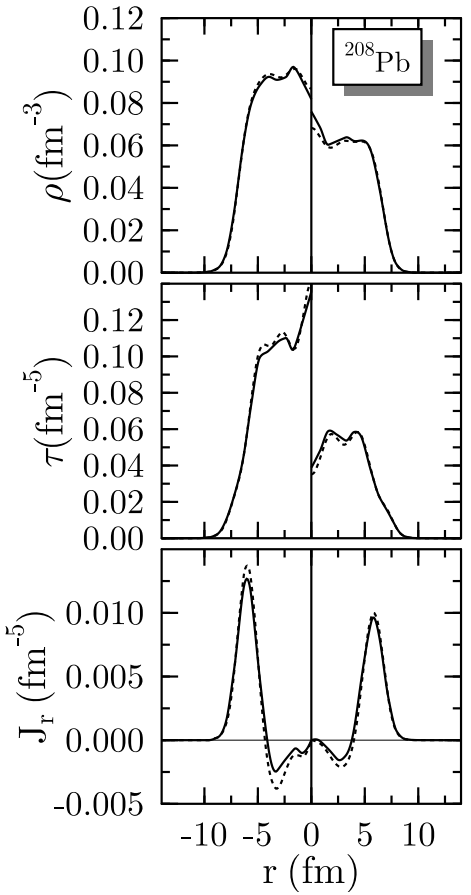

Right: neutron (left panels) and proton (right panels) densities of the time-even ground state of ^{208}Pb as obtained with two different Skyrme interactions (solid and dotted lines).

Energy functional from a "density-dependent Skyrme force"

$$\mathcal{E}_{\text{Skyrme}} = \langle \text{SD} | \hat{t} + \hat{v}^{\text{central}} + \hat{v}^{\text{LS}} + \hat{v}^{\text{tensor}} | \text{SD} \rangle$$

- central

$$\begin{aligned}\hat{v}^{\text{central}} &= t_0 \,(1 + x_0 \hat{P}_\sigma)\, \delta + \tfrac{1}{6}\, t_3 \,(1 + x_3 \hat{P}_\sigma)\, \rho^\alpha \;\delta \\ &+ \tfrac{1}{2}\, t_1 \,(1 + x_1 \hat{P}_\sigma)(\hat{\mathbf{k}}^{\dagger 2}\, \delta + \delta\, \hat{\mathbf{k}}^2) \\ &+ t_2 \;(1 + x_2 \hat{P}_\sigma)\, \hat{\mathbf{k}}^\dagger \cdot \delta\, \hat{\mathbf{k}}\end{aligned}$$

- spin-orbit

$$\hat{v}^{\text{LS}} = \mathrm{i} W_0 \,(\hat{\boldsymbol{\sigma}}_1 + \hat{\boldsymbol{\sigma}}_2) \cdot \hat{\mathbf{k}}^\dagger \times \delta\, \hat{\mathbf{k}}$$

- tensor

$$\begin{aligned}\hat{v}^{\text{tensor}} &= \tfrac{1}{2}\, t_e \left\{ \left[3(\hat{\boldsymbol{\sigma}}_1 \cdot \hat{\mathbf{k}}^\dagger)(\hat{\boldsymbol{\sigma}}_2 \cdot \hat{\mathbf{k}}^\dagger) - (\hat{\boldsymbol{\sigma}}_1 \cdot \hat{\boldsymbol{\sigma}}_2)\,(\hat{\mathbf{k}}^\dagger)^2 \right] \delta + \text{h.c.} \right] \right\} \\ &+ \tfrac{1}{2}\, t_o \left\{ \left[3(\hat{\boldsymbol{\sigma}}_1 \cdot \hat{\mathbf{k}}^\dagger)\, \delta\, (\hat{\boldsymbol{\sigma}}_2 \cdot \hat{\mathbf{k}}) + 3(\hat{\boldsymbol{\sigma}}_2 \cdot \hat{\mathbf{k}}^\dagger)\, \delta\, (\hat{\boldsymbol{\sigma}}_1 \cdot \hat{\mathbf{k}}) - 2(\hat{\boldsymbol{\sigma}}_1 \cdot \hat{\boldsymbol{\sigma}}_2)\, \hat{\mathbf{k}}^\dagger \cdot \delta \hat{\mathbf{k}} \right] \right\}\end{aligned}$$

- $\delta \equiv \delta(\mathbf{r} - \mathbf{r}')$
- $\hat{\mathbf{k}} \equiv -\frac{\mathrm{i}}{2}(\nabla_1 - \nabla_2)$
- $\hat{P}_\sigma$: spin exchange operator

Single-particle Hamiltonian

The single-particle Hamiltonian is given by

$$\hat{h}_q = -\boldsymbol{\nabla}\cdot B_q(\mathbf{r})\boldsymbol{\nabla} + U_q(\mathbf{r}) - \tfrac{\mathrm{i}}{2}\sum_{\mu,\nu=x}^{z}[W_{q,\mu\nu}(\mathbf{r})\nabla_\mu\sigma_\nu + \nabla_\mu\sigma_\nu W_{q,\mu\nu}(\mathbf{r})]$$
$$-\boldsymbol{\nabla}\cdot[\hat{\boldsymbol{\sigma}}\cdot\mathbf{C}_q(\mathbf{r})]\boldsymbol{\nabla} - \boldsymbol{\nabla}\cdot\mathbf{D}_q(\mathbf{r})\,\hat{\boldsymbol{\sigma}}\cdot\boldsymbol{\nabla} + \mathbf{S}_q(\mathbf{r})\cdot\hat{\boldsymbol{\sigma}} - \tfrac{\mathrm{i}}{2}[\mathbf{A}_q(\mathbf{r})\cdot\boldsymbol{\nabla} + \boldsymbol{\nabla}\cdot\mathbf{A}_q(\mathbf{r})]$$

with

$$U_q(\mathbf{r}) \equiv \delta\mathcal{E}/\delta\rho_q(\mathbf{r})$$
$$B_q(\mathbf{r}) = \hbar^2/2m_q^*(\mathbf{r}) \equiv \delta\mathcal{E}/\delta\tau_q(\mathbf{r})$$
$$W_{q,\mu\nu}(\mathbf{r}) \equiv \delta\mathcal{E}/\delta J_{q,\mu\nu}(\mathbf{r})$$
$$\mathbf{A}_q(\mathbf{r}) \equiv \delta\mathcal{E}/\delta\mathbf{j}_q(\mathbf{r})$$
$$\mathbf{S}_q(\mathbf{r}) \equiv \delta\mathcal{E}/\delta\mathbf{s}_q(\mathbf{r})$$
$$\mathbf{C}_q(\mathbf{r}) \equiv \delta\mathcal{E}/\delta\mathbf{T}_q(\mathbf{r})$$
$$\mathbf{D}_q(\mathbf{r}) \equiv \delta\mathcal{E}/\delta\mathbf{F}_q(\mathbf{r})$$

- objects in blue are time-even local potentials or densities
- objects in green are time-odd local potentials or densities

Variations and Extensions

Not all (in fact very few) parameter sets of the Skyrme EDF are constructed as *pseudoportential-based functionals* that relate all coupling constants C_t^{AB} of the functional to the t_i, w_i, W_0 of the Skyrme generator

- Most parameter sets do not consider genuine two-body tensor interactions, $t_o = t_e = 0$ and/or $C_t^{sF} = C_t^{\nabla s \nabla s}$
- The majority of parameter sets set $C_t^{sT} = 0$ although such terms are necessarily generated by the two-body Skyrme generator (such that they are hybrid or general EDFs)
- Many practitioners also modify $C^{ss}[\rho_0]_t$, $C_t^{s\Delta s}$, either setting them to zero or values suggested by phenomenology (such that they use hybrid or general EDFs)
- Pairing energy is usually generated differently.
- Coulomb exchange is usually treated in "Slater approximation" (which is a local approximation to the non-local exchange term that is exact in homogeneous infinite matter)

Various extensions of the standard form have been tried

- multiple density dependences of same type with different powers
- additional density dependence of terms with gradients
- three-body terms with two gradients
- Higher-order terms in gradients. In modern jargon, the above form is "next-to-leading order (NLO) in gradients", containing terms without and with two gradients. There are efforts to build extended Skyrme EDFs with four (N2LO) and six (N3LO) gradients. Note: There is no reason to expect that this refers to a hierarchy in physical relevance, but it nevertheless refers a hierarchy in computational complexity.

Effective interaction:

$$
\begin{aligned}
v_{\text{Gogny}} = & \sum_{i=1}^{2} \left(W_i + B_i P_\sigma - H_i P_\tau - M_i P_\sigma P_\tau\right) e^{-(\mathbf{r}-\mathbf{r}')_{12}^2/\mu_i^2} \\
& + t_0 \left(1 + x_0 P_\sigma\right) \rho^\alpha(\mathbf{R}_{12}) \delta(\mathbf{r}_{12}) \\
& + \mathrm{i} W_{LS} \left(\boldsymbol{\sigma}_1 + \boldsymbol{\sigma}_2\right) \cdot \mathbf{k}'_{12} \times \delta(\mathbf{r}_{12}) \mathbf{k}_{12}.
\end{aligned}
$$

Energy functional (in the particle-hole channel)

$$
\begin{aligned}
E_{\text{pot}} = & \iint \mathrm{d}^3 r \, \mathrm{d}^3 r' \sum_{t=0,1} \sum_{i=1}^{2} e^{-(\mathbf{r}-\mathbf{r}')^2/\mu_i^2} \Big[A_{it}^{\rho\rho} \, \rho_t(\mathbf{r}) \, \rho_t(\mathbf{r}') + A_{it}^{ss} \, \mathbf{s}_t(\mathbf{r}) \cdot \mathbf{s}_t(\mathbf{r}') \\
& \qquad + B_{it}^{\rho\rho} \, \rho_t(\mathbf{r}, \mathbf{r}') \, \rho_t(\mathbf{r}', \mathbf{r}) + B_{it}^{ss} \, \mathbf{s}_t(\mathbf{r}, \mathbf{r}') \cdot \mathbf{s}_t(\mathbf{r}', \mathbf{r}) \Big] \\
& + \int \mathrm{d}^3 r \left[\tfrac{3}{8} \, t_0 \, \rho_0^2(\mathbf{r}) - \tfrac{1}{4} \, t_0 \left(\tfrac{1}{2} + x_0\right) \rho_1^2(\mathbf{r}) - \tfrac{1}{4} \, t_0 \left(\tfrac{1}{2} - x_0\right) \mathbf{s}_0^2(\mathbf{r}) - \tfrac{1}{8} \, t_0 \, \mathbf{s}_1^2(\mathbf{r}) \right] \rho_0^\alpha(\mathbf{r}) \\
& + \int \mathrm{d}^3 r \Big[- \tfrac{3}{4} \, W_0 \left(\rho_0(\mathbf{r}) \nabla \cdot \mathbf{J}_0(\mathbf{r}) + \mathbf{j}_0(\mathbf{r}) \cdot \nabla \times \mathbf{s}_0(\mathbf{r})\right) \\
& \qquad - \tfrac{1}{4} \, W_0 \left(\rho_1(\mathbf{r}) \nabla \cdot \mathbf{J}_1(\mathbf{r}) + \mathbf{j}_1(\mathbf{r}) \cdot \nabla \times \mathbf{s}_1(\mathbf{r})\right) \Big],
\end{aligned}
$$

$\Rightarrow$ non-local single-particle Hamiltonian

$$
\begin{aligned}
h_q(\mathbf{r}\sigma,\mathbf{r}'\sigma') &= \frac{\delta E}{\delta\rho_q(\mathbf{r}'\sigma',\mathbf{r}\sigma)} \\
&= T(\mathbf{r}\sigma,\mathbf{r}'\sigma') + \Gamma_{q,\mathrm{dir}}(\mathbf{r}\sigma,\mathbf{r}'\sigma') + \Gamma_{q,\mathrm{exc}}(\mathbf{r}\sigma,\mathbf{r}'\sigma') \\
&= T(\mathbf{r}\sigma,\mathbf{r}'\sigma') + \Gamma_{q,\mathrm{dir}}(\mathbf{r}\sigma,\mathbf{r}\sigma') + \Gamma_{q,\mathrm{exc}}(\mathbf{r}\sigma,\mathbf{r}'\sigma')
\end{aligned}
$$

The contribution from one of the central finite-range interaction $v_j(\mathbf{r}-\mathbf{r}') = e^{-(\mathbf{r}-\mathbf{r}')^2/\mu_j^2}$ is

$$
\begin{aligned}
\Gamma_{q,\mathrm{dir}}(\mathbf{r}\sigma,\mathbf{r}'\sigma') &= \delta(\mathbf{r}-\mathbf{r}')\,\delta_{\sigma\sigma'}\int \mathrm{d}^3r''\, v_j(\mathbf{r}-\mathbf{r}'')\sum_{q'}\Big[(W-H\delta_{qq'})\rho_{q'}(\mathbf{r}'') + (B-M\delta_{qq'})\rho_{q'}(\mathbf{r}''\sigma,\mathbf{r}''\sigma)\Big] \\
&\quad + \delta(\mathbf{r}-\mathbf{r}')\,\delta_{\sigma-\sigma'}\int \mathrm{d}^3r''\, v_j(\mathbf{r}-\mathbf{r}'')\sum_{q'}(B-M\delta_{qq'})\rho_{q'}(\mathbf{r}''\sigma,\mathbf{r}''-\sigma) \\
\Gamma_{q,\mathrm{exc}}(\mathbf{r}\sigma,\mathbf{r}'\sigma') &= v_j(\mathbf{r}-\mathbf{r}')\sum_{q'}\Big\{\delta_{\sigma\sigma'}\Big[(M-B\delta_{qq'})\sum_{\sigma''}\rho_{q'}(\mathbf{r}\sigma'',\mathbf{r}'\sigma'') + (H-W\delta_{qq'})\,\rho_{q'}(\mathbf{r}\sigma,\mathbf{r}'\sigma)\Big] \\
&\quad + \delta_{\sigma-\sigma'}(H-W\delta_{qq'})\,\rho_{q'}(\mathbf{r}\sigma,\mathbf{r}'-\sigma)\Big\}.
\end{aligned}
$$

Dobaczewski et al, PRC 53 (1996) 2809

- In spite of the complicated expression, the direct term is a (spin- and isospin-dependent) local potential $U(\mathbf{r})$ that is obtained from the convolution of local densities with the finite-range function.
- The exchange potential is non-local
- The contributions from the density-dependent term and the spin-orbit term

The Fayans functional

formulated in terms of dimensionless density

$$x_t(\mathbf{r}) \equiv \frac{\rho_t(\mathbf{r})}{\rho_{\rm sat}}$$

The functional:

$$E = E^{\rm kin} + E^{\rm v} + E^{\rm s} + E^{\rm ls} + E^{\rm coul} + E^{\rm pair}$$

Its particle-hole part is given by

$$\begin{aligned}
E^{\rm v} &= \tfrac{1}{3}\,\epsilon_F\,\rho_{\rm sat}\int {\rm d}^3r \left\{ a^v_+ \frac{1-h^v_{1+}\left[x_0(\mathbf{r})\right]^\sigma}{1+h^v_{2+}\left[x_0(\mathbf{r})\right]^\sigma}\left[x_0(\mathbf{r})\right]^2 + a^v_+ \frac{1-h^v_{1-}x_0(\mathbf{r})}{1+h^v_{2-}x_0(\mathbf{r})}\left[x_1(\mathbf{r})\right]^2 \right\} \\
E^{\rm s} &= \tfrac{1}{3}\,\epsilon_F\,\rho_{\rm sat}\int {\rm d}^3r \frac{a^s_+\, r_s^2\left[\boldsymbol{\nabla} x_0(\mathbf{r})\right]^2}{1+h^s_\nabla\, r_s^2\left[\boldsymbol{\nabla} x_0(\mathbf{r})\right]^2} \\
E^{\rm ls} &= \frac{4\epsilon_F\, r_s^2}{3\rho_{\rm sat}}\int {\rm d}^3r \left[\kappa\rho_0(\mathbf{r})\boldsymbol{\nabla}\cdot\mathbf{J}_0(\mathbf{r}) + \kappa'\rho_1(\mathbf{r})\boldsymbol{\nabla}\cdot\mathbf{J}_1(\mathbf{r}) + g\left[\mathbf{J}_0(\mathbf{r})\right]^2 + g'\left[\mathbf{J}_1(\mathbf{r})\right]^2\right]
\end{aligned}$$

- Constructed in a "general functional"
- $m^*/m = 1$ by construction
- cannot be related to pseudo-potential

Fayans et al, Nucl. Phys. A 676, 49 (2000)

Reinhard et al, PRC95, 064328 (2017)

Other energy density functionals

There are also many other forms of EDFs that I will not address in detail

Various classifications are possible

- relativistic / non-relativistic
- contact interactions / finite-range interactions
- Finite-range interactions with Gaussians / Yukawa functions
- These can be ph Hartree + pair EDF hybrids / Hartree + exchange + pair EDF hybrids / Hartree + exchange + pairing pseudopotential-based EDFs
- density-dependent two-body interactions / many-body forces

Namedropping

- Barcelona-Catania-Paris-Milano functional (BCPM)
- SeaLL
- relativistic Walecka-type
- relativistic point-coupling models

Hartree-Fock-Bogoliubov: quasiparticle operators

Include pairing correlations in the mean-field modeling

$\Rightarrow$ Hartree-Fock-Bogoliubov

Define (non-normalised) quasiparticle vacuum

$$|\mathrm{HFB}\rangle = \prod_{\mu} \beta_\mu |-\rangle \qquad \text{with} \qquad \beta_\mu |\mathrm{HFB}\rangle = 0$$

of quasiparticles defined through a Bogoliubov transformation W

$$\beta_\mu = \sum_n \left(U^*_{n\mu} c_n + V^*_{n\mu} c^\dagger_n \right) \quad , \quad \beta^\dagger_\mu = \sum_n \left(V_{n\mu} c_n + U_{n\mu} c^\dagger_n \right)$$

which in matrix form becomes

$$\begin{pmatrix} \beta \\ \beta^\dagger \end{pmatrix} = \begin{pmatrix} U^\dagger & V^\dagger \\ V^T & U^T \end{pmatrix} \begin{pmatrix} c \\ c^\dagger \end{pmatrix} = \mathcal{W}^\dagger \begin{pmatrix} c \\ c^\dagger \end{pmatrix}$$

Unitarity of W leads to

$$U^\dagger U + V^\dagger V = \left(U^\dagger U + V^\dagger V \right)^* = 1$$
$$V^T U + U^T V = \left(V^T U + U^T V \right)^* = 0$$
$$V V^\dagger + U^* U^T = \left(V V^\dagger + U^* U^T \right)^* = 1$$
$$U V^\dagger + V^* U^T = \left(U V^\dagger + V^* U^T \right)^* = 0$$

odd-even staggering of binding energies

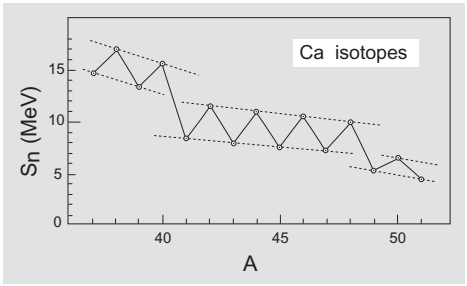

qualitative difference between spectra of even-even and odd-A nuclides

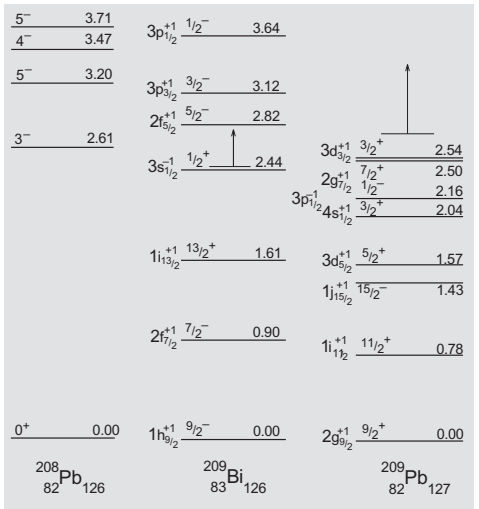

There are now 3 types of density matrices

$$\rho_{ij} \equiv \frac{\langle\Phi|c_j^\dagger c_i|\Phi\rangle}{\langle\Phi|\Phi\rangle} \quad , \quad \kappa_{ij} \equiv \frac{\langle\Phi|c_j c_i|\Phi\rangle}{\langle\Phi|\Phi\rangle} \quad , \quad \kappa_{ij}^* \equiv \frac{\langle\Phi|c_i^\dagger c_j^\dagger|\Phi\rangle}{\langle\Phi|\Phi\rangle}$$

They can be combined to a generalized density matrix

$$\mathcal{R} \equiv \begin{pmatrix} \rho & \kappa \\ -\kappa^* & 1-\rho^* \end{pmatrix} = \begin{pmatrix} V^* V^T & V^* U^T \\ U^* V^T & U^* U^T \end{pmatrix}$$

with

$$\mathcal{R}^2 = \mathcal{R}$$

which implies

$$\rho\rho - \kappa\kappa^* = \rho \quad , \quad \rho\kappa - \kappa\rho^* = 0$$

Note that

$$\rho_{\mu\nu}^* = \rho_{\nu\mu} \quad , \quad \kappa_{\mu\nu} = -\kappa_{\nu\mu},$$

$\mathcal{R}$ is diagonal in any quasiparticle basis

$$\tilde{\mathcal{R}} = \mathcal{W}^\dagger \mathcal{R} \mathcal{W} = \begin{pmatrix} 0 & 0 \\ 0 & 1 \end{pmatrix}$$

There are again "empty" quasiparticle states with eigenvalue 0 and "occupied" quasiparticle states with eigenvalue 1.

Even-even, odd and odd-odd nuclei

According to the Bloch-Messiah-Zumino theorem,

$$\mathcal{W} = \mathcal{D}\,\bar{\mathcal{W}}\,\mathcal{C} = \begin{pmatrix} D & 0 \\ 0 & D^* \end{pmatrix} \begin{pmatrix} \bar{U} & \bar{V} \\ \bar{V} & \bar{U} \end{pmatrix} \begin{pmatrix} C & 0 \\ 0 & C^* \end{pmatrix}$$

there exists a " canonical" single-particle basis of the Bogoliubov transformation, in which the quasiparticle vacuum takes the (normalised) form

$$|\mathrm{HFB}\rangle = \prod_{\substack{k>0 \\ k\neq b}} \left(u_k + v_k a_k^\dagger a_{\bar{k}q}^\dagger\right) \prod_b a_b^\dagger |-\rangle\,.$$

and in which the density matrices take the simple form

$$\rho = \begin{pmatrix} 1 & & & & & \\ & \ddots & & & & \\ & & v_k^2 & & & \\ & & & v_{\bar{k}}^2 & & \\ & & & & \ddots & \\ & & & & & 0 \end{pmatrix}, \qquad \kappa = \begin{pmatrix} 0 & & & & & 0 \\ & \ddots & & & & \\ & & 0 & u_k v_k & & \\ & & u_{\bar{k}} v_{\bar{k}} & 0 & & \\ & & & & \ddots & \\ 0 & & & & & 0 \end{pmatrix}$$

Quasiparticle vacua are not eigenstates of the particle number operator

$$\langle (\Delta\hat{N})^2 \rangle \equiv \langle \mathrm{HFB}|\hat{N}^2|\mathrm{HFB}\rangle - \langle \mathrm{HFB}|\hat{N}|\mathrm{HFB}\rangle^2 = 4\sum_{k>0} u_k^2 v_k^2$$

HF+BCS as an approximation to HFB where one assumes that ρ is diagonal in the basis of eigenstates of $\hat{h}$. This approximation fails in the limits of weak binding and when time-reversal symmetry is broken.

See Chapter 3 of Schunck [ed.], *Energy Density Functional Methods for Atomic Nuclei*, IoP Publishing Ltd (2019).

Hartree-Fock-Bogoliubov: HFB equations

Total energy

$$\mathcal{E} = \sum_{ij} t_{ij}\rho_{ji} + \frac{1}{2}\sum_{ijkl}\bar{v}_{ijkl}\rho_{lj}\rho_{ki} + \frac{1}{4}\sum_{ijkl}\bar{v}_{ijkl}\kappa^*_{ij}\kappa_{kl}\,.$$

Variation of the energy (under the constraints that quasiparticle states are orthogonal and that the particle number is fixed at some value N) leads to the HFB equations

$$\mathcal{H}'\begin{pmatrix} U \\ V \end{pmatrix}_\mu = \begin{pmatrix} h-\lambda & \Delta \\ -\Delta^* & -h^*+\lambda \end{pmatrix}\begin{pmatrix} U \\ V \end{pmatrix}_\mu = E_\mu \begin{pmatrix} U \\ V \end{pmatrix}_\mu$$

that can also be recast into the form

$$\left[\mathcal{H}', \mathcal{R}\right] = 0$$

In a single-particle basis of dimension Ω, there are 2Ω solutions of the HFB equations that come in pairs with $\pm E_\mu = \mp E_{\bar{\mu}}$

$$\mathcal{H}'\begin{pmatrix} U \\ V \end{pmatrix}_{\bar{\mu}} = \mathcal{H}'\begin{pmatrix} V^* \\ U^* \end{pmatrix}_\mu = -E_\mu\begin{pmatrix} V^* \\ U^* \end{pmatrix}_\mu = -E_\mu\begin{pmatrix} U \\ V \end{pmatrix}_{\bar{\mu}}$$

which have different eigenvalues of $\mathcal{R}$

$$\mathcal{R}\begin{pmatrix} U \\ V \end{pmatrix}_\mu = 0\begin{pmatrix} U \\ V \end{pmatrix}_\mu \quad , \quad \mathcal{R}\begin{pmatrix} V^* \\ U^* \end{pmatrix} = 1\begin{pmatrix} V^* \\ U^* \end{pmatrix}$$

One has

$$\beta_{\bar{\mu}} = \beta^\dagger_\mu \quad , \quad \beta^\dagger_{\bar{\mu}} = \beta_\mu$$

Dobaczewski, Nazarewicz, in
Fifty Years of Nuclear BCS, page 40 (2013)

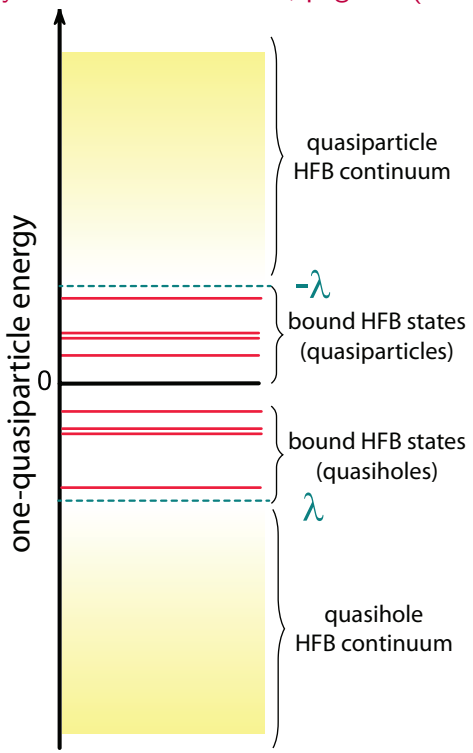

See Chapter 3 of Schunck [ed.], *Energy Density Functional Methods for Atomic Nuclei*, IoP Publishing Ltd (2019).

Even-even, odd and odd-odd nuclei

- Lowest fully paired solution is the one that is constructed from quasiparticle states with

$$|\mathrm{HFB}\rangle = \prod_{\mu} \beta_{\mu}|-\rangle \qquad \text{with} \qquad \beta_{\mu}|\mathrm{HFB}\rangle = 0$$

  for which $\beta^{\dagger}_{\mu}$ create quasiparticle states with positive E_{μ}.
- One can then create 1-quasi-particle excitations on top of that vacuum as

$$|1qp\rangle = \beta^{\dagger}_{\mu}|\mathrm{HFB}\rangle$$

  which can be recast into a quasiparticle vacuum where one quasiparticle refers to a quasiparticle vacuum on which one can create a quasiparticle with negative quasiparticle energy.
- Similar for 2-quasi-particle excitations etc.
- Solving the HFB equations for a blocked configuration is numerically more complicated (and therefore comparatively unpopular).
- Blocked quasiparticle-vacua are in general not time-reversal invariant.
- There is an "equal-filling approximation" to blocking that is a statistical mixing of blocked states and their time-reversed which leads to vanishing time-odd fields in the HFB equation.

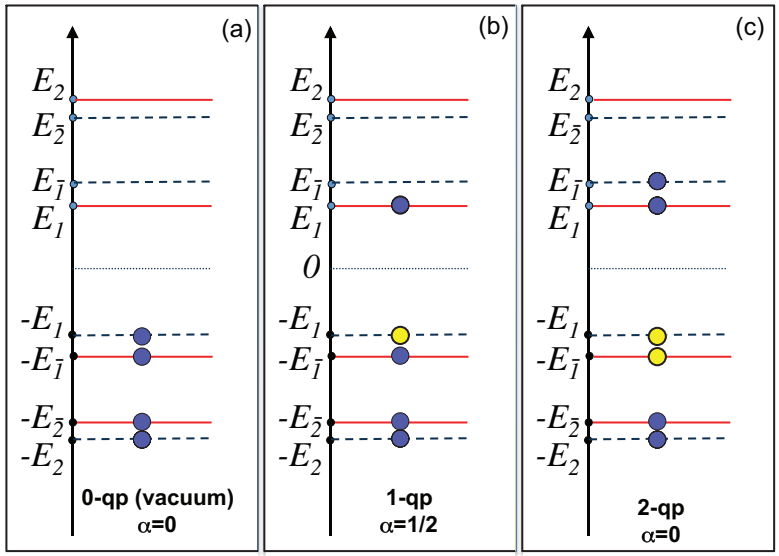

Bertsch, Dobaczewski, Nazarewicz, Pei, PR70 (2009) 043602

Mapping energy landscapes: constrained HFB

- By itself, the HFB equations converge to a minimum reachable from the initialisation of the code run.
- To map energy curves or surfaces, one has to add a *constraint* that enforces an auxiliary condition, or a set of auxiliary conditions
- This is achieved minimising a *Routhian*

$$\delta\Big(E - \lambda_c \langle \mathrm{HFB}|\hat{C}|\mathrm{HFB}\rangle = 0$$

where (ideally) λ_c is adapted such that at convergence

$$\langle \mathrm{HFB}|\hat{C}|\mathrm{HFB}\rangle = C$$

- One has

$$\lambda_c = \frac{\partial E}{\partial C}$$

- One can use many operators as constraint
- particle number (mandantory in HFB, see above!): The chemical potential of HFB satisfies $\lambda_q = \partial E/\partial N$. When λ_q is negative, one gains binding energy when adding nucleons. For positive λ_q one looses binding when adding nucleons.
- multipole moments (deformation)
- mean-square radius
- angular momentum (rotational bands)

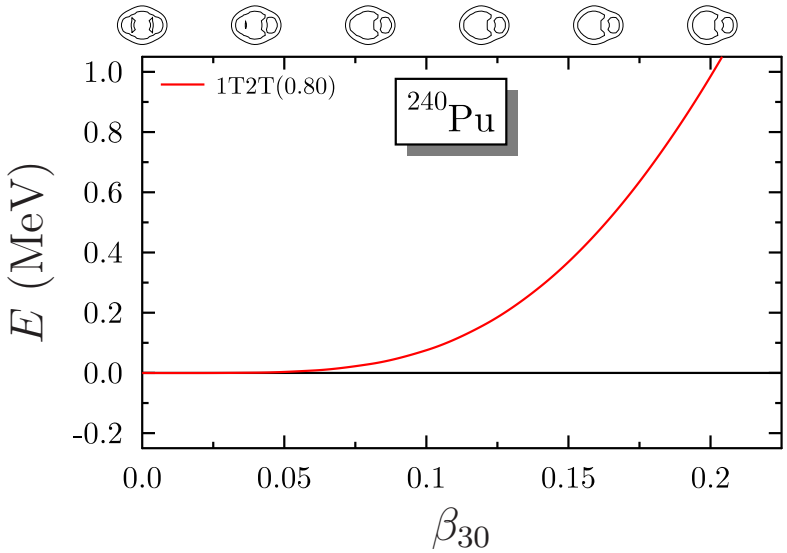

simplified plot from da Costa et al, PRC 109 (2024) 034316

- Some constraints can be mandatory in certain codes: in a code that allows for reflection-asymmetric solutions (broken parity), the centre-of-mass of the nucleus has to be fixed at the origin with a constraint on the mass dipole moment
- So there were two constrained multipole moments needed to generate the figure, and two constrained chemical potentials.

Examples of constrained HFB calculations

(2d) energy surfaces

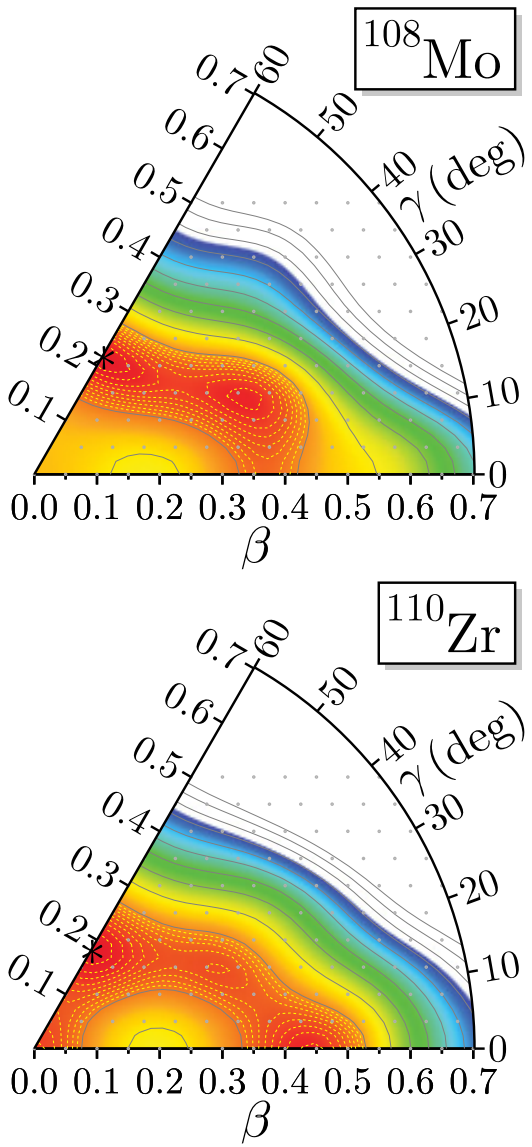

M. Bender, unpubliched vcalculation with 1T2T(0.80) aka SLy7* (2026)

paths through higher-dimensional energy surfaces

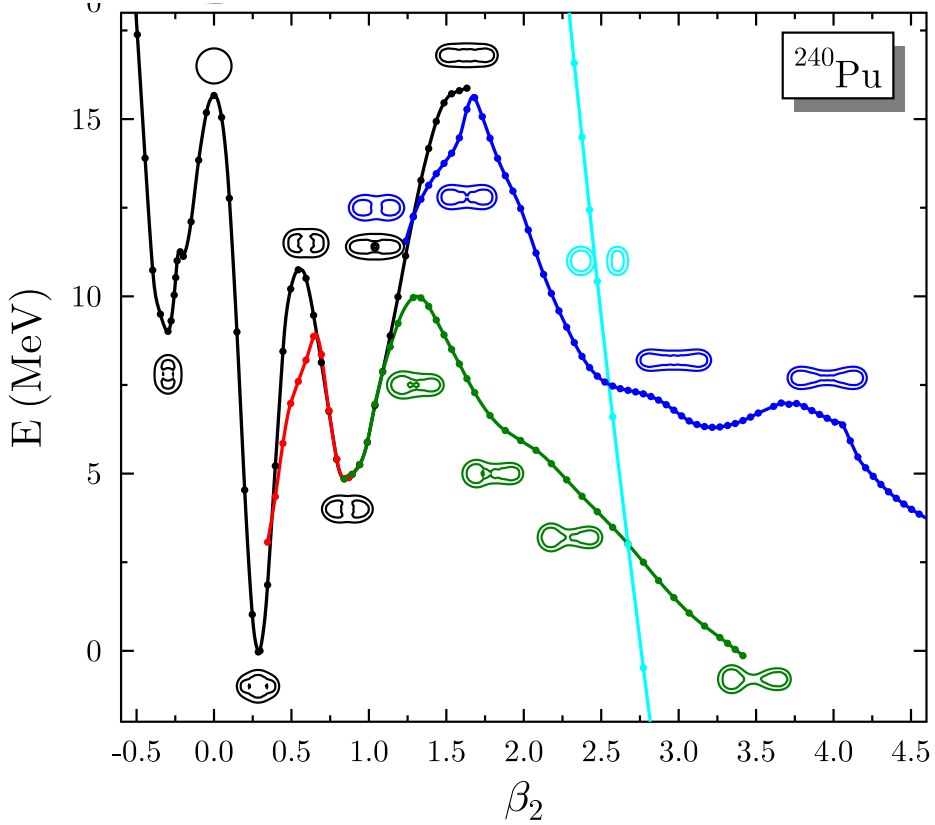

M. Bender, unpublished calculation from the 2010s

A few words on solvers

- Solver: a code to solve the self-consistent HF/HF+BCS/HFB equations
- imposed symmetry:
  - 1d spherical
  - 2d axial with or w/o parity breaking and with or w/o time-reversal symmetry
  - 3d with or w/o various plane- and/or point-reflection symmetries and with or w/o time-reversal symmetry
- Note: these symmetries are those of the densities (and by extension the potentials), not (necessarily) those of the actual single-particle states.
- coordinate-space vs basis expansion
- different strategies to solve HFB
- different strategies to update potentials

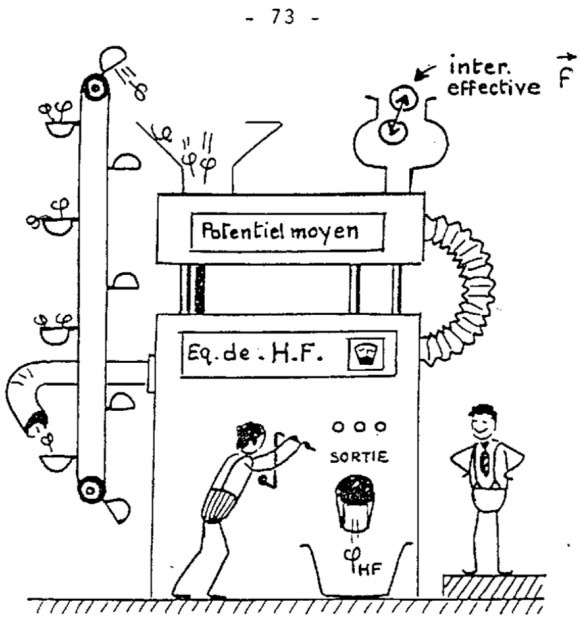

Figure 21: La résolution des équations de Hartree-Fock (J.Dechargé).

taken from the course by J.-F. Berger @ EJC 1991

(Possible) Output of a self-consistent mean-field calculation

- total binding energy + possibly its decomposition into individual terms
- single-particle matrix elements of the single-particle Hamiltonian and various other operators in some single-particle basis. Most useful (IMHO) are the two bases that diagonalise $\hat{h}$ ("HF basis") and the basis that diagonalises ρ (canonical basis).
- matrix elements of the HFB Hamiltonian and various other operators in some quasiparticle basis.
- spatial densities and currents of protons and neutrons
- moments of these spatial densities and currents
  - radial moments of the densities (mean-square radius)
  - multipole moments of the densities (as allowed by broken spatial symmetries)
  - multipole moments of the spin and current (distribution of magnetisation; as allowed by broken spatial symmetries and broken time-reversal)
  - components of the angular momentum vector (if allowed by broken time-reversal)

Role and interpretation of single-particle energies

There is "Koopman's theorem" in atomic physics that states that the eigenvalue ϵ_j of the single-particle Hamiltonian are equal to the one-nucleon separation energy to the respective state

$$S_j = E^{\mathrm{HF}(A)} - E_j^{\mathrm{HF}(A-1)}$$

with

$$\begin{aligned} E^{\mathrm{HF}(A)} &= \sum_{i=1}^{A} t_{ii} + \frac{1}{2}\sum_{i,k=1}^{A} \bar{v}_{ikik} \\ E_j^{\mathrm{HF}(A-1)} &= \sum_{\substack{i=1 \\ i\neq j}}^{A-1} t_{ii} + \frac{1}{2}\sum_{\substack{i,k=1 \\ i\neq j}}^{A} \bar{v}_{ikik} \end{aligned}$$

if

- The system is perfectly described by a Slater determinant (i.e. that there are no correlations of any kind whatsoever)
- that the single-particle states are exactly the same in the A and $A-1$ system ...
- ... meaning that the A-body system is described by the direct product of the Slater determinant of the $A-1$ system and the single-particle wave function ψ_j ...
- ... implying that rearrangement and polarization effects changing the single-particle wave functions when adding or removing a particle are negligible

Already this by itself is never found in realistic SR EDF calculations for nuclei. In addition, the presence of

- pairing correlations
- density-dependent two-body forces
- three-body forces

further breaks the equality of S_j and ϵ_j.

Empirical single-particle energies vs. eigenvalues of the single-particle Hamiltonian

Still, the eigenvalues ϵ_k of the single-particle Hamiltonian in even-even nuclei often take values that are *similar* to one-nucleon separation energies

Fully blocked self-consistent mean-field:

Rutz, Bender, Reinhard, Maruhn, Greiner, NPA634 (1998) 67

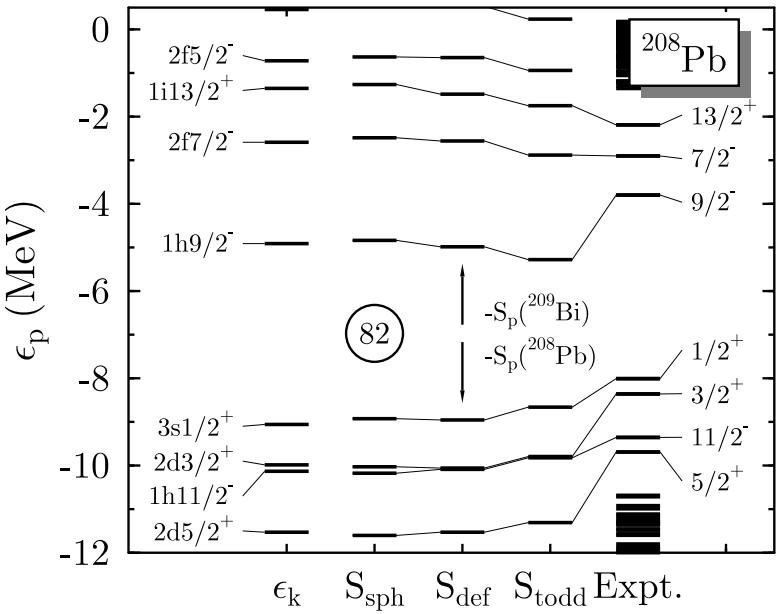

- ϵ_k from spherical HF calculations
- S_{sph} separation energy from equal filling in spherical symmetry
- S_{def} separation energy from equal filling in axial symmetry
- S_{todd} separation energy from full blocking

Particle-vibration coupling:

Litvinova and Ring, PRC 73 (2006) 044328

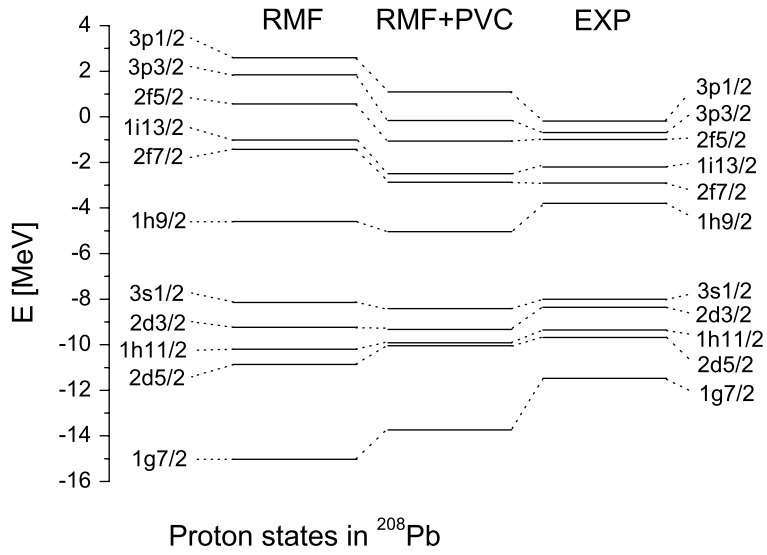

- RMF: ϵ_k from spherical HF calculations
- RMF+PVC: spectrum of low-lying states from a (spherical) particle-vibration coupling calculation (with the same parameter set)

Deformed shell structure: the example of ^{250}Fm

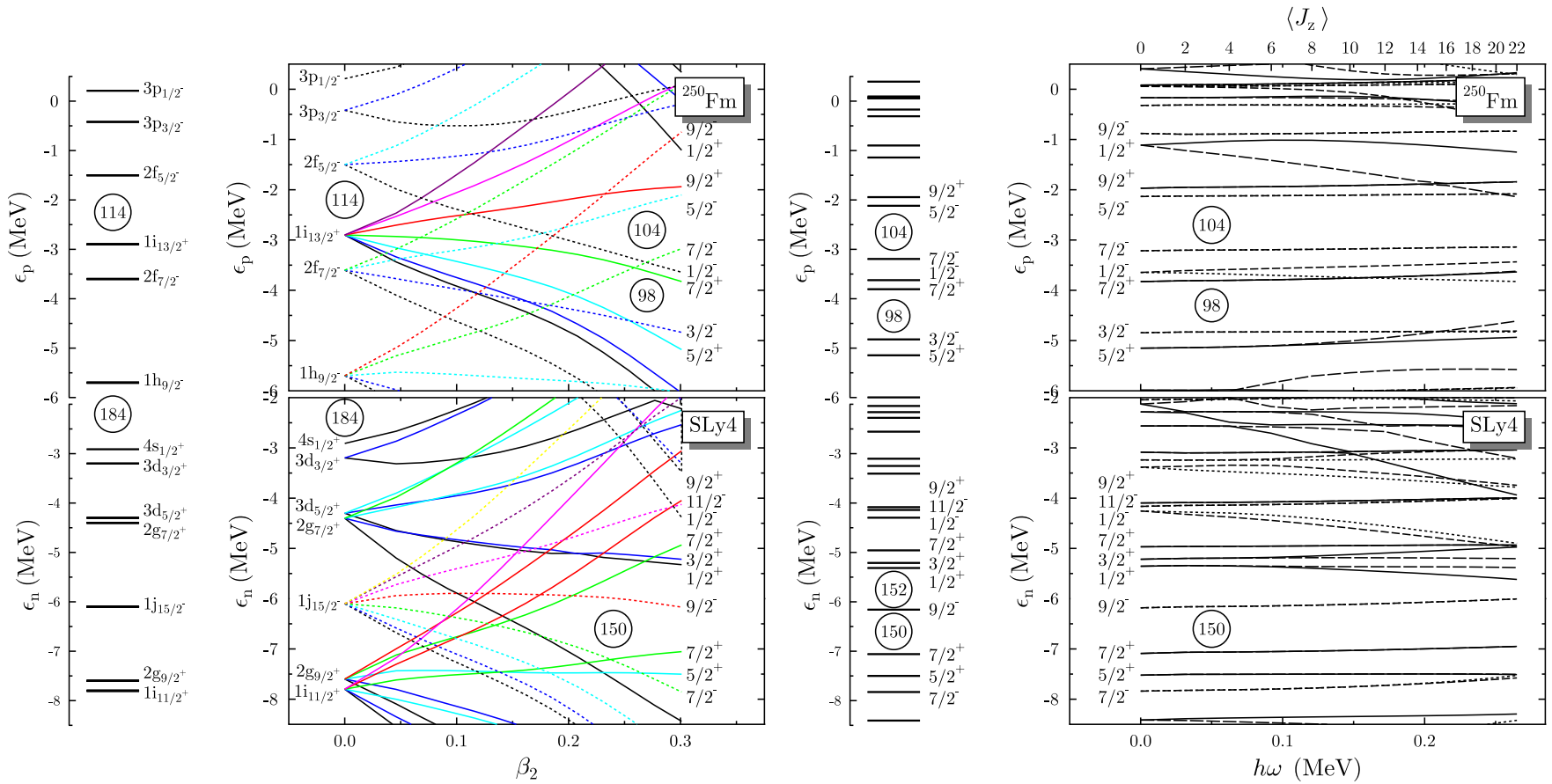

- the nucleus goes from a spherical configuration with high level density to a deformed configuration with low level density, which is more favorable (remember that at spherical shape the levels are $(2J+1)$-fold degenerate, at deformed shape they are two-fold degenerate)
- For ^{250}Fm, the energy gain from deformation (compared to the spherical mean-field state) is of the order of 25 MeV.

Why single-particle spectra determine nuclear shapes in SR EDF method

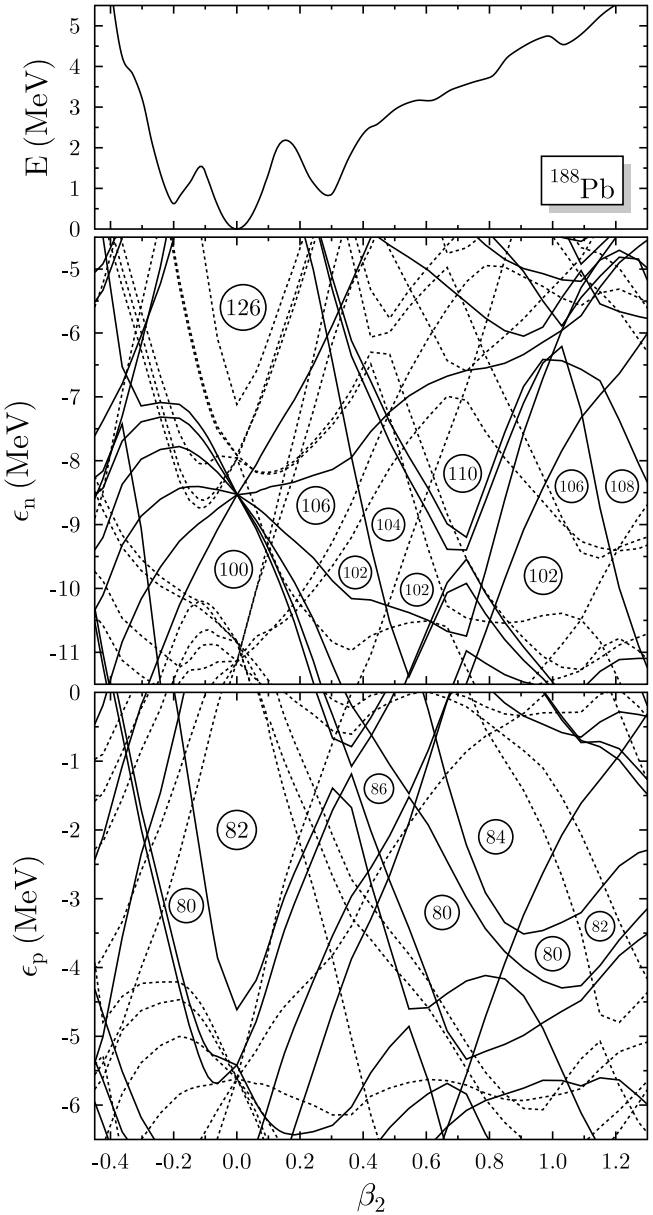

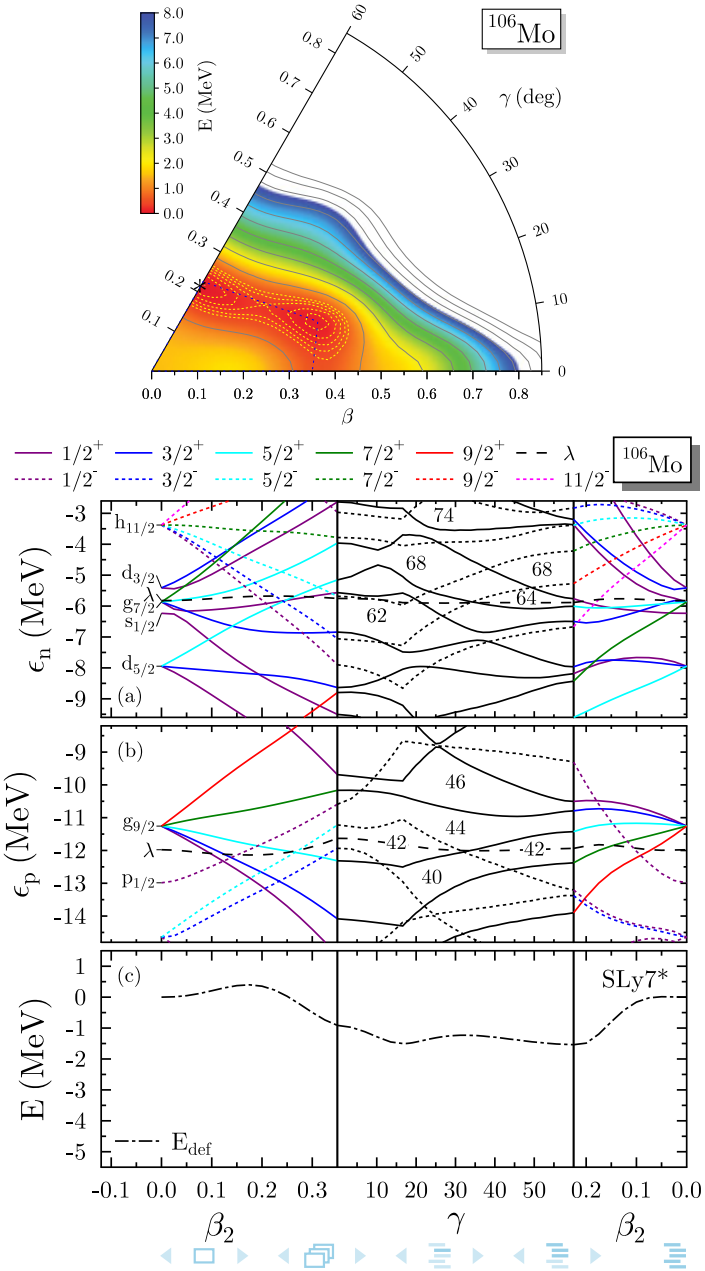

Why single-particle spectra determine nuclear shapes in SR EDF methods: Strutinski-Theorem

Energy from shell effects can be identified with the difference between the full HF(B) energy and an (LDM-like) "average energy" from averaged normal (and pair) densities

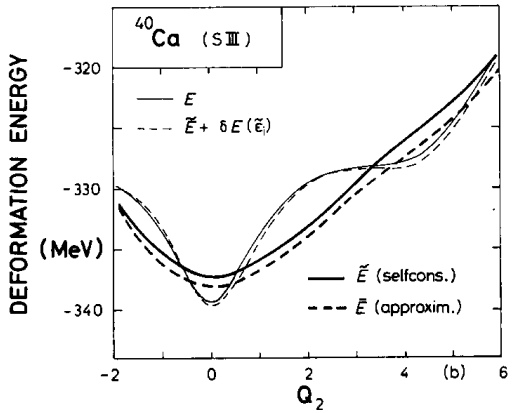

Fig. 1. Deformation energy curve for the ^{40}Ca nucleus, obtained with the Skyrme III force. Some pairing correlations have been included ($\tilde{\Delta}$ = 1 MeV). The basis of expansion of the single particle HF states corresponds for the spherical solution to 7 oscillator shells. The thin solid line is the HF energy E_{HF}, and the heavy dashed line the average energy $\bar{E}$ defined in (1). The heavy solid line is the self-consistent average energy $\tilde{E}$ defined in (2) and the thin dashed line is the approximation $\tilde{E}$ + δE_1 ($\tilde{\epsilon}_i$) to the HF energy.

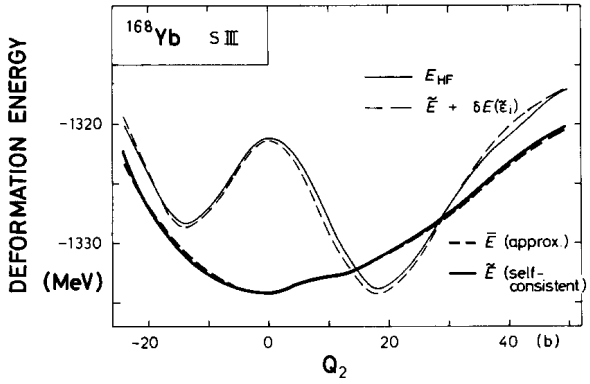

Fig. 2. The same as in fig. 1, but for the ^{168}Yb nucleus.

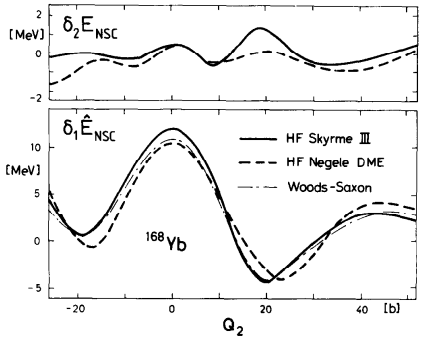

Fig. 5. First-order ($\delta_1 \hat{E}$) and second-order ($\delta_2 E$) shell-correction energies along the quadrupole deformation energy curve of ^{168}Yb. The results deduced from HF calculations are non-self-consistent and correspond to the Skyrme SIII effective force and the Negele effective force within the Negele-Vautherin [68]) density matrix expansion (DME). First-order shell corrections obtained with a Woods-Saxon parametrization [8]) of the mean field are also reported.

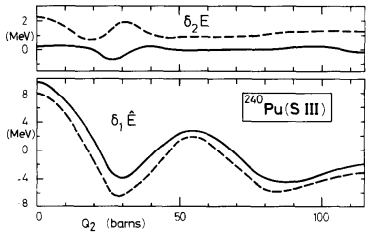

Fig. 4. First-order ($\delta_1 \hat{E}$) and second-order ($\delta_2 E$) shell-correction energies along the fission barrier of ^{240}Pu. Both self-consistent (full line) and non-self-consistent (dashed line) results are shown. The fission path was obtained by constraining the total quadrupole moment Q_2 (see also fig. 6). The Skyrme SIII effective force has been used.

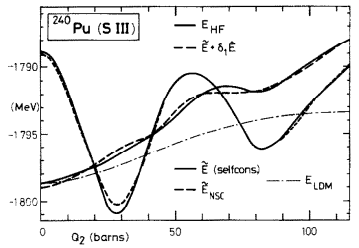

Fig. 6. Fission barrier of ^{240}Pu calculated with the Skyrme SIII effective force. The HF energy E_{HF} is compared with averaged energies $\tilde{E}$ (both self-consistent and non-self-consistent) and with its Strutinsky approximation $\tilde{E}+\delta_1 \hat{E}$. The liquid drop model [86]) estimate E_{LDM} of the fission barrier is also given. The total quadrupole moment Q_2 was constrained as in fig. 4.

Brack & Quentin, PLB 56 (1975) 421 and NPA 361 (1981) 35

Evolution of the shell correction across the chart of nuclei

Bender, Nazarewicz, Reinhard, PLB 515 (2001) 42.

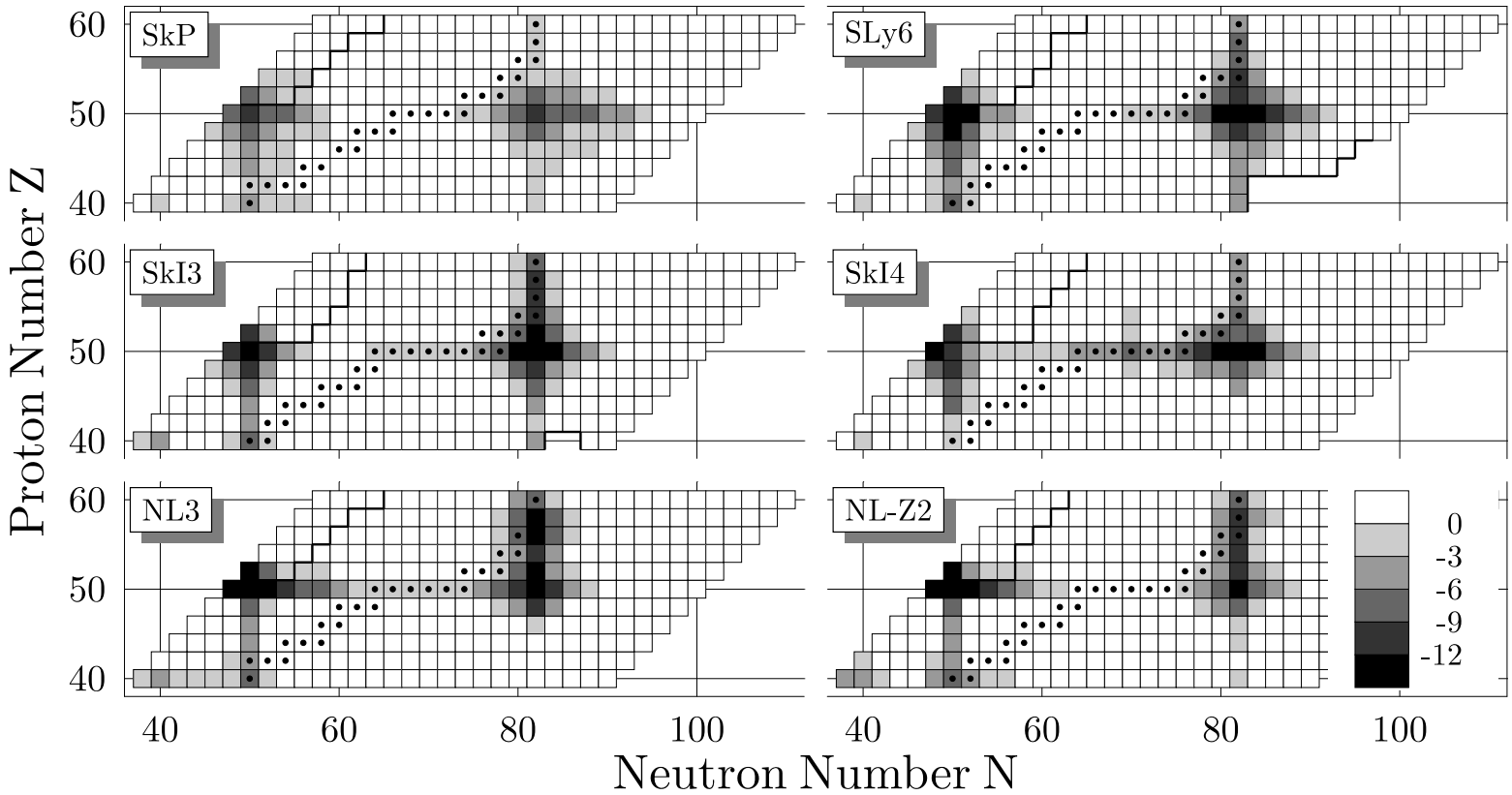

- Total shell correction energy extracted from fully self-consistent calculations assuming **spherically symmetric shapes**
- Very localized shell effect in the Sn region

Evolution of the shell correction across the chart of nuclei

Bender, Nazarewicz, Reinhard, PLB 515 (2001) 42.

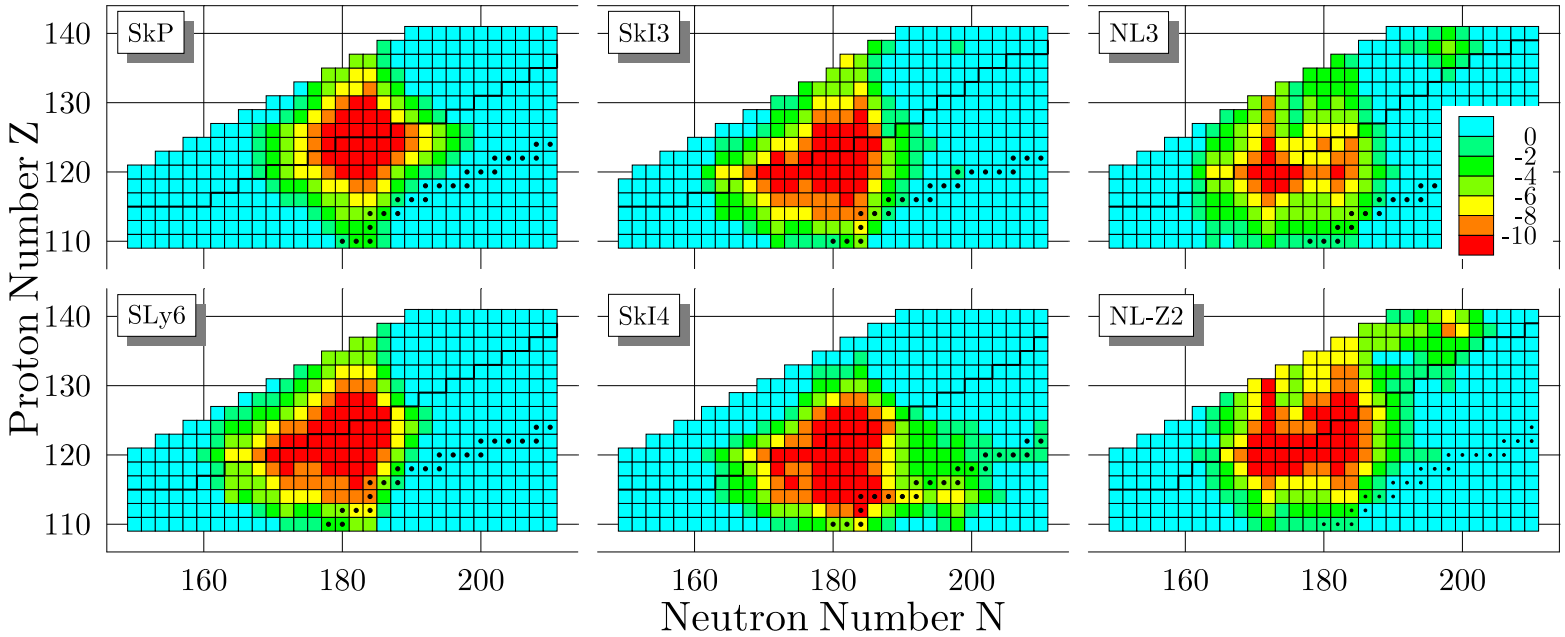

- Total shell correction energy extracted from fully self-consistent calculations assuming **spherically symmetric shapes**
- Very extended region of additional binding of spherical shapes that is in almost all cases spreads over *all* predicted spherical shell closures.
- Many of these nuclei actually are predicted to have deformed shapes for which the shell correction is then even larger . . .
- . . . in particular nuclei around the (predicted) deformed doubly-magic nuclei $^{252}_{100}\mathrm{Fm}_{152}$ and $^{270}_{108}\mathrm{Hs}_{162}$.

How important are the actual shell closures?

Bender, Nazarewicz, Reinhard, PLB 515 (2001) 42

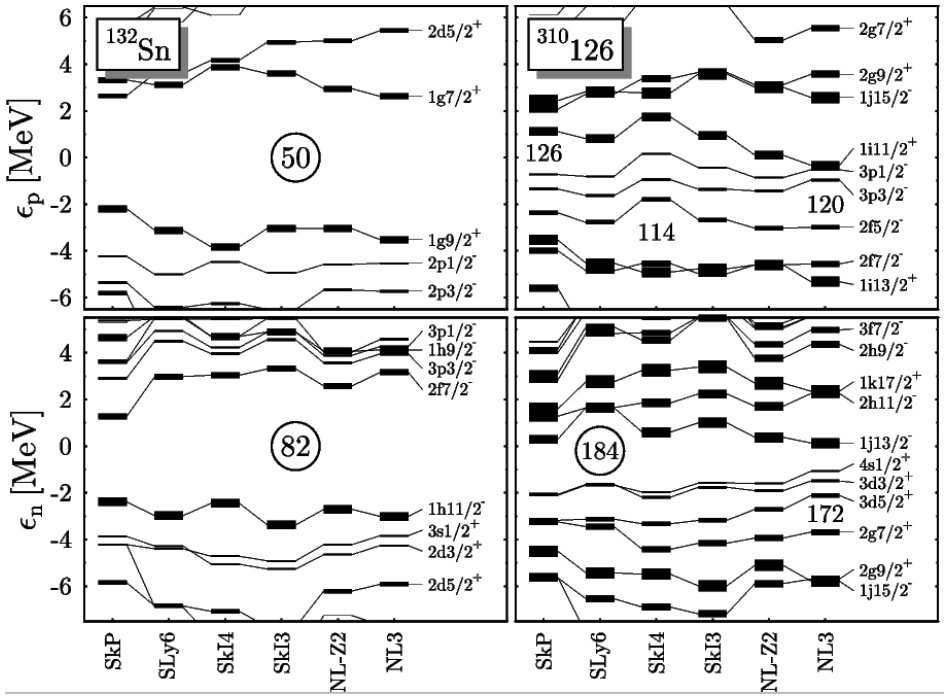

- many high-j shells
- shell effect from reduction of average level density when Fermi energy hits low-j shells
- Not the size of the shell correction counts, but how quickly it varies with deformation
- Shell effects qualitatively change when going to very heavy nuclei

How important are the actual shell closures?

Bender, Nazarewicz, Reinhard, PLB 515 (2001) 42

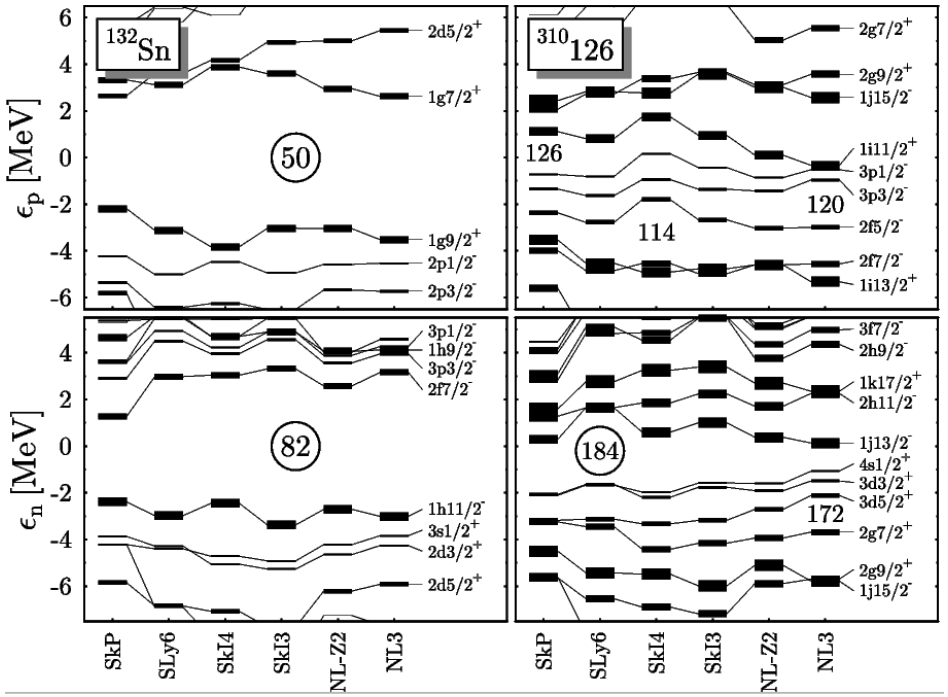

Bender and Heenen, unpublished

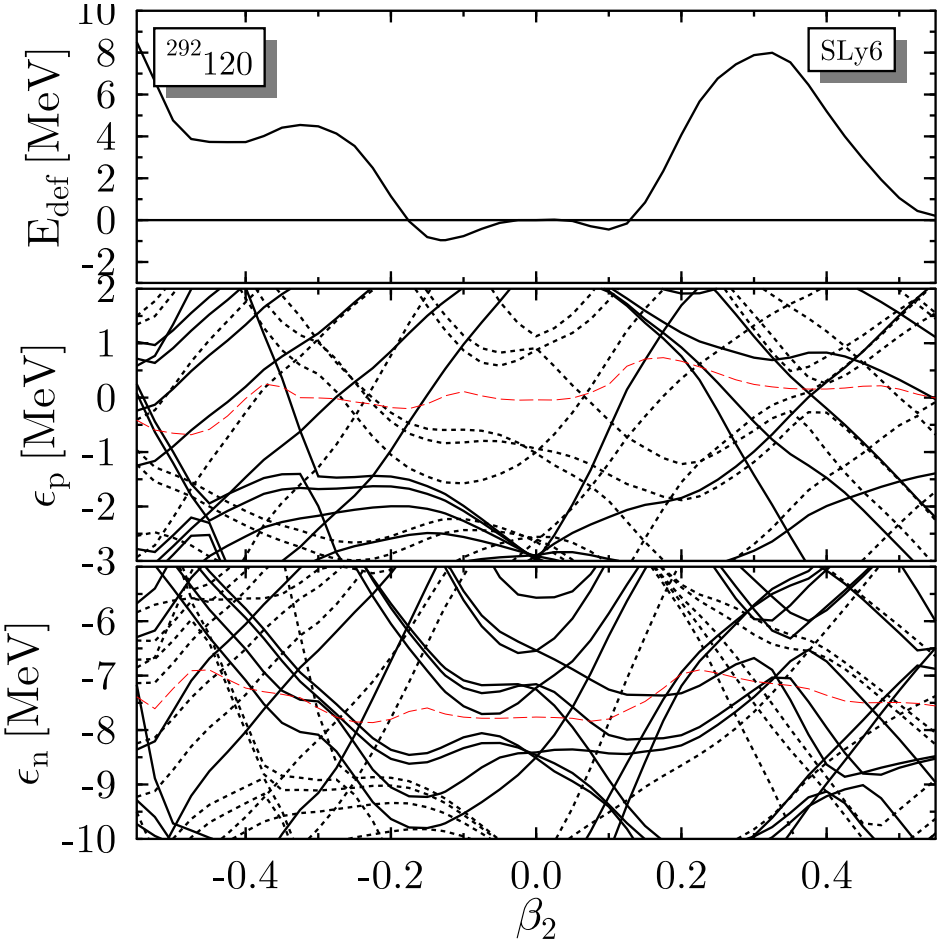

- many high-j shells
- shell effect from reduction of average level density when Fermi energy hits low-j shells
- Not the size of the shell correction counts, but how quickly it varies with deformation
- Shell effects qualitatively change when going to very heavy nuclei

Deformed odd nuclei

- Another phenomenon that is sensitive to deformation are the coexisting rotational bands of odd-mass nuclei.
- Their band heads correspond to low-lying blocked quasiparticle states
- Successful modeling requires internal consistency of deformed single-particle spectrum, moment of inertia of rotational motion and electromagnetic moments of in-band transitions.
- Similar (but more complicated) for odd-odd nuclei and single-particle excitations in even-even nuclei.
- Points that deformed shapes as obtained in (self-consistent) mean-field models describes correlations that have some "reality"

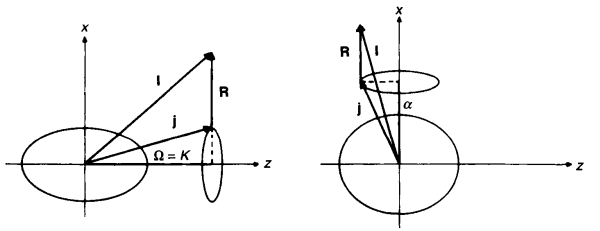

Fig. 11.3. Schematic illustration of the two extreme coupling schemes; deformation alignment (left figure) and rotation alignment (right figure) (from R.M. Lieder and H. Ryde, *Adv. in Nucl. Phys.*, eds. M. Baranger and E. Vogt (Plenum Publ. Corp., New York) vol. 10 (1978) p. 1).

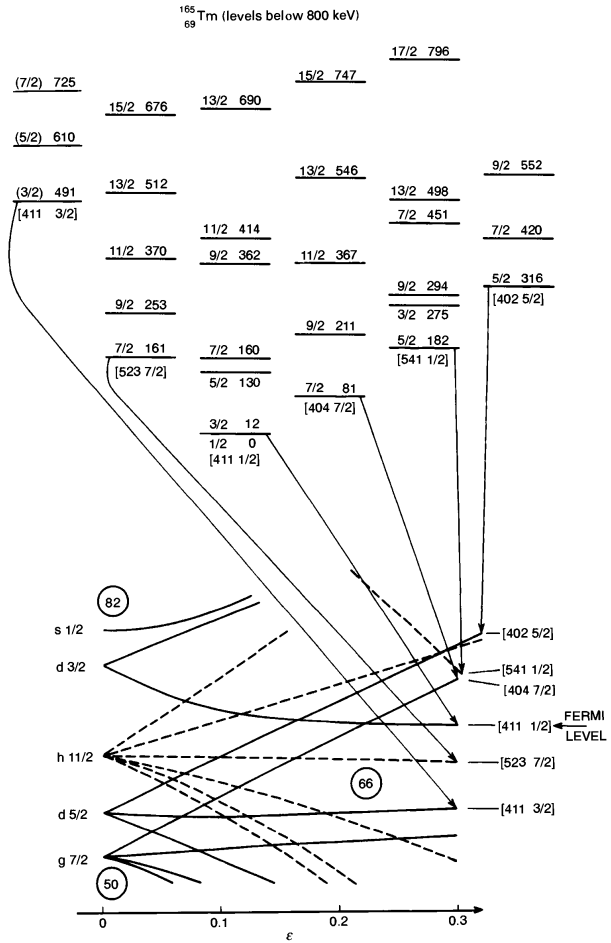

Fig. 11.4. For legend see opposite.

taken from S. G. Nilsson & I. Ragnarsson, "Shapes and Shells in Nuclear Structure", Cambridge University Press (1995).

Link to observables

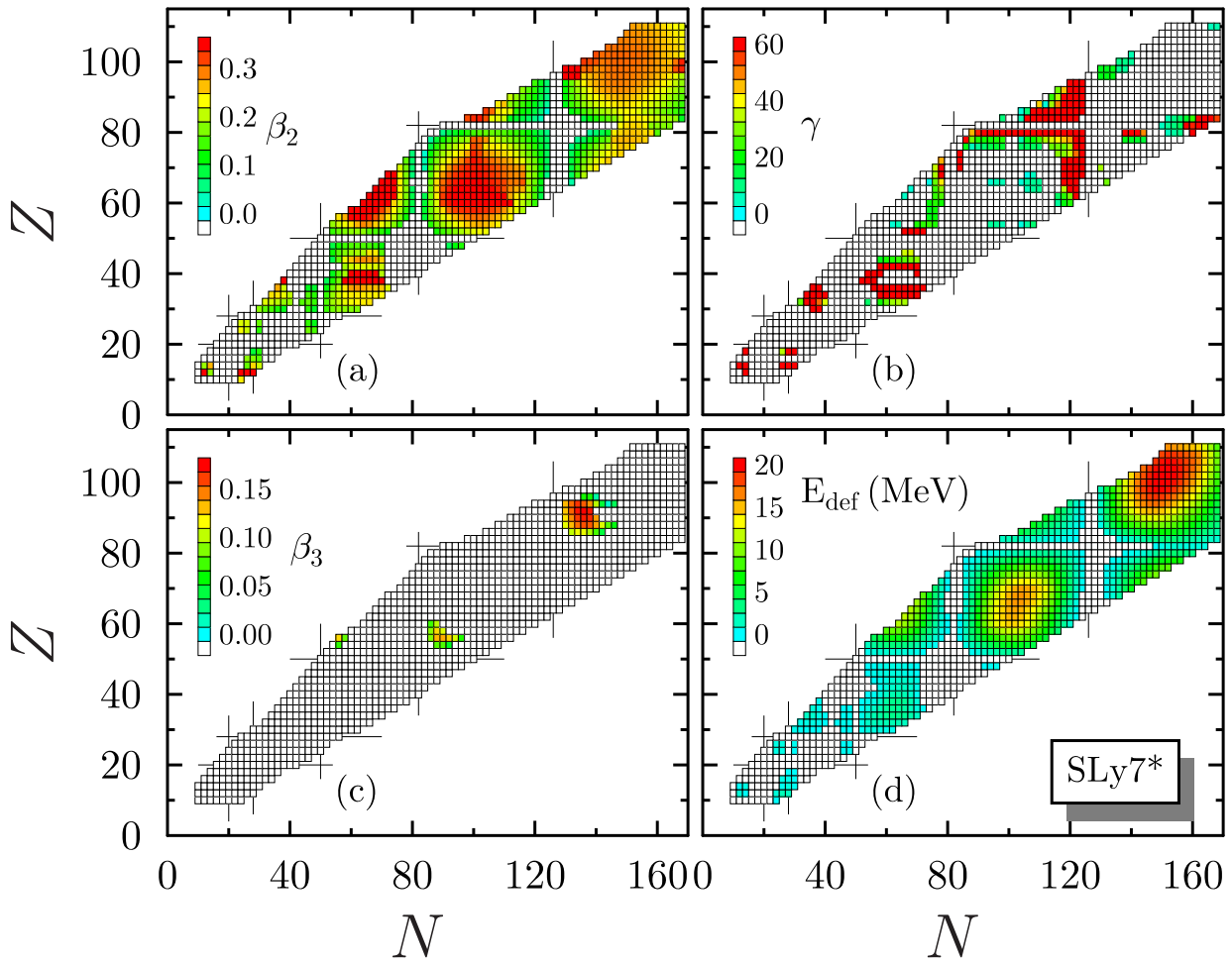

Bender, to be published

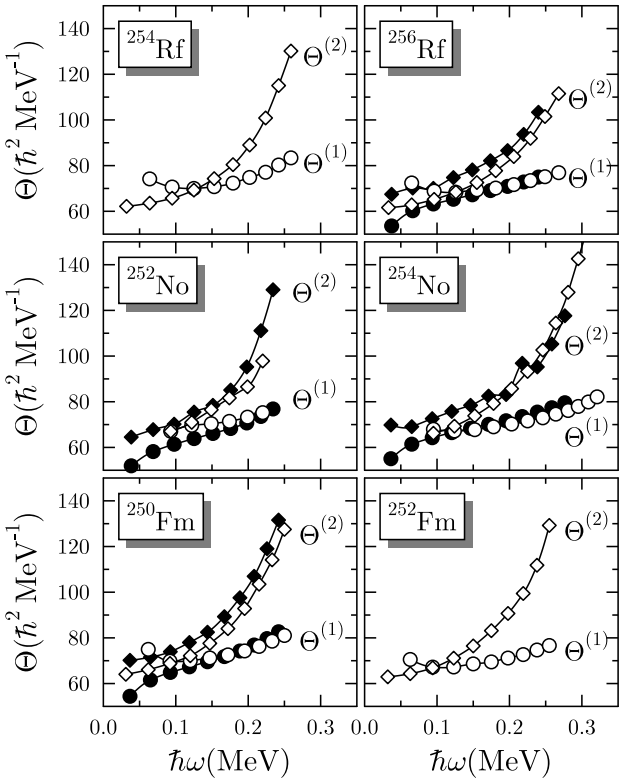

Bender and Heenen, J. Phys. Conf. Ser 420 (2013) 012002

(moments of inertia will be defined later on)

Higher-order deformations

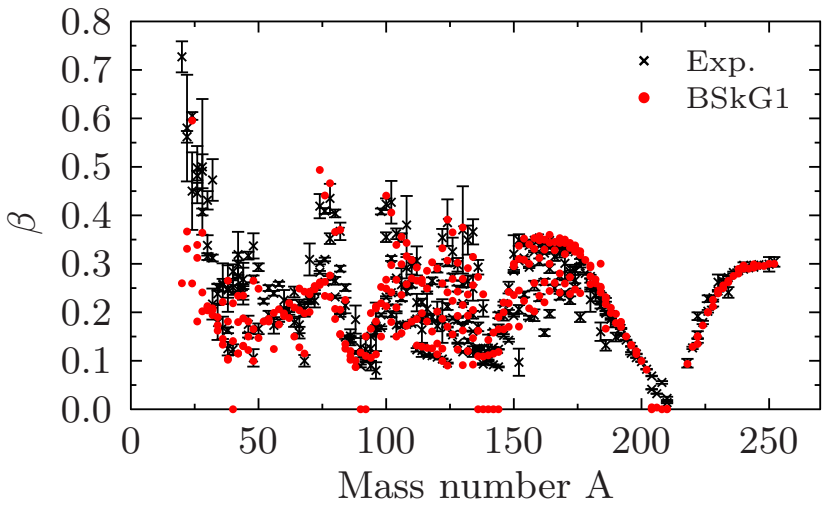

Scamps, Goriely, Olsen, Bender, Ryssens, EPJ A 57 (2021) 333

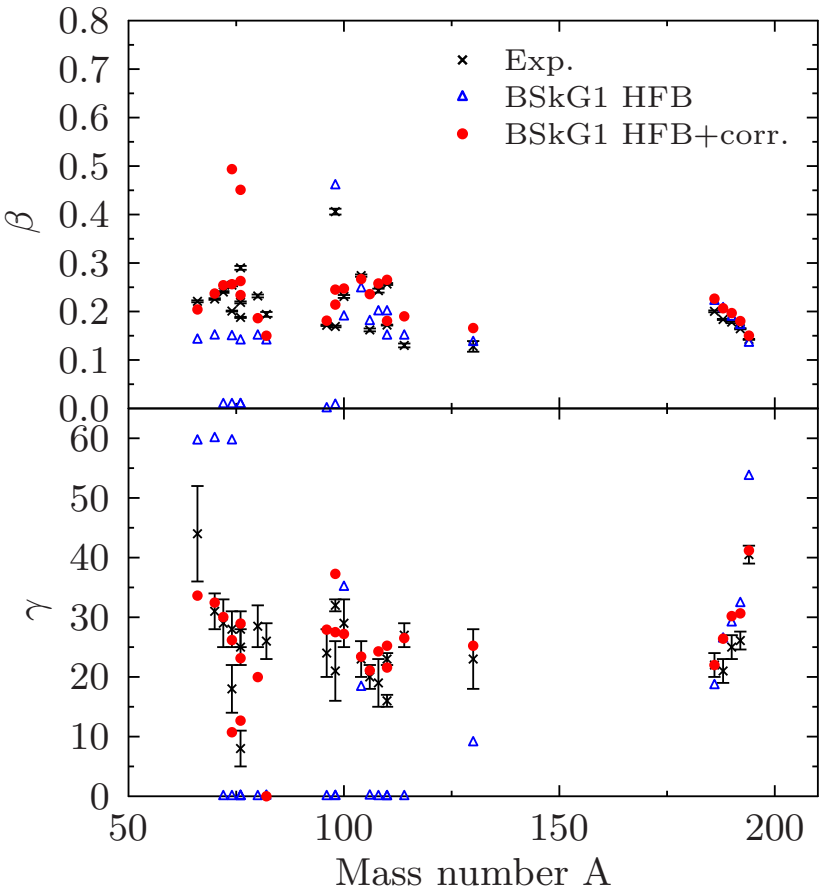

Higher-order deformations

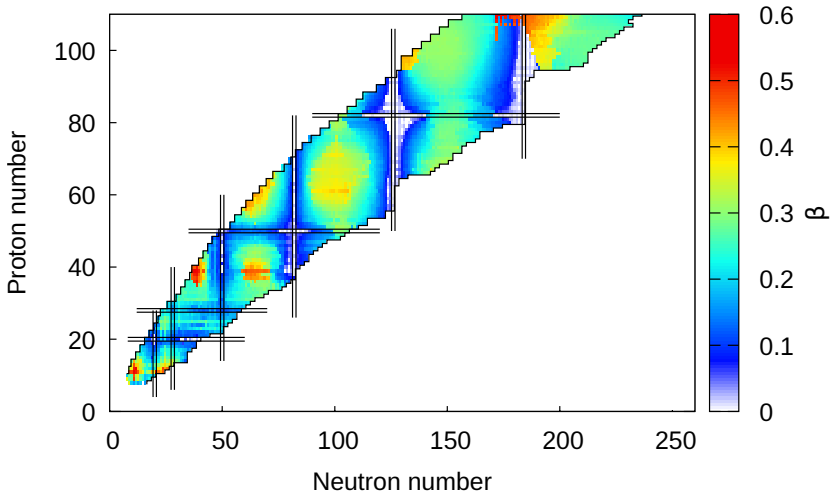

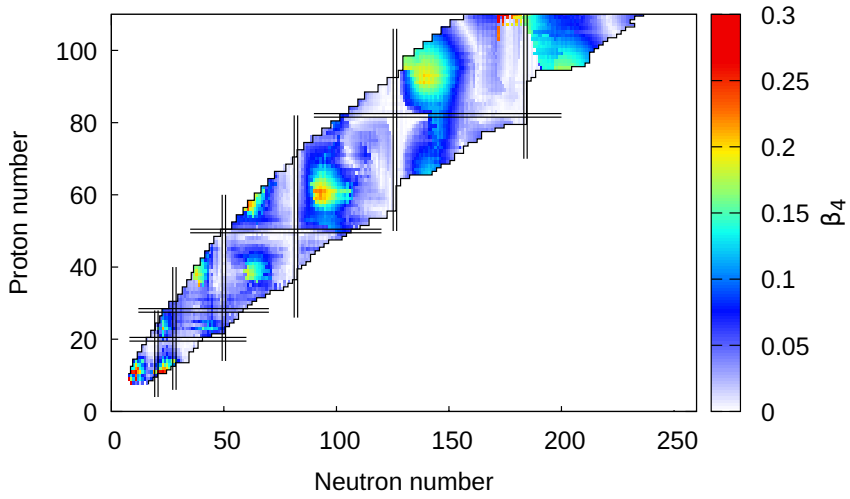

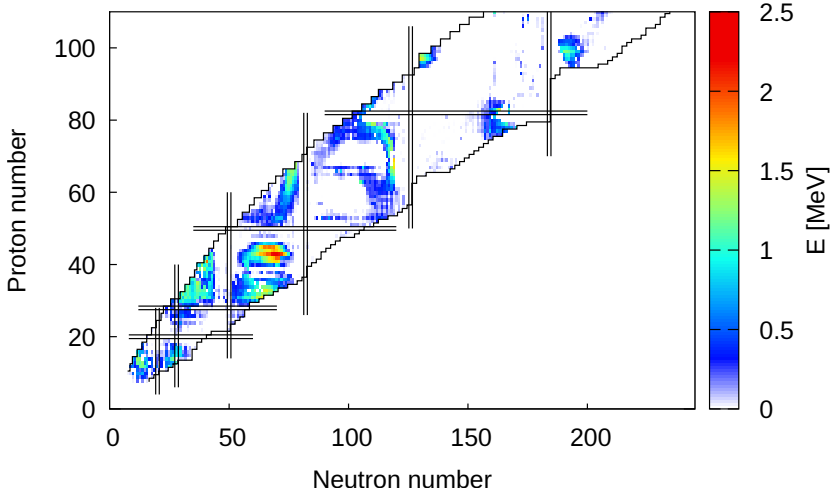

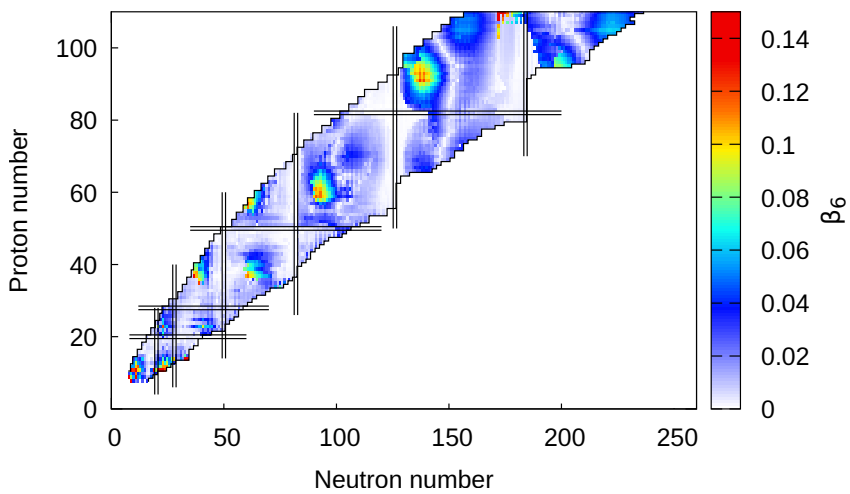

Scamps, Goriely, Olsen, Bender, Ryssens, EPJ A 57 (2021) 333

Systematics of quadrupole collectivity

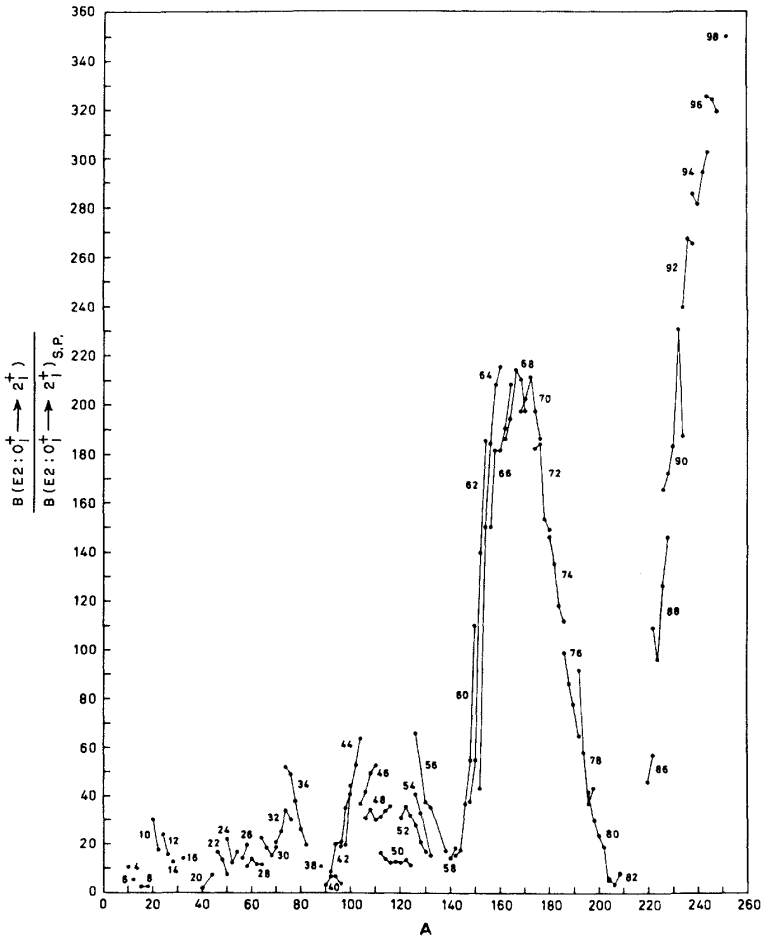

Fig. 2.16. $B(E2{:}0^+_1 \rightarrow 2^+_1)$ values for all even–even nuclei. (Bohr, 1975.)

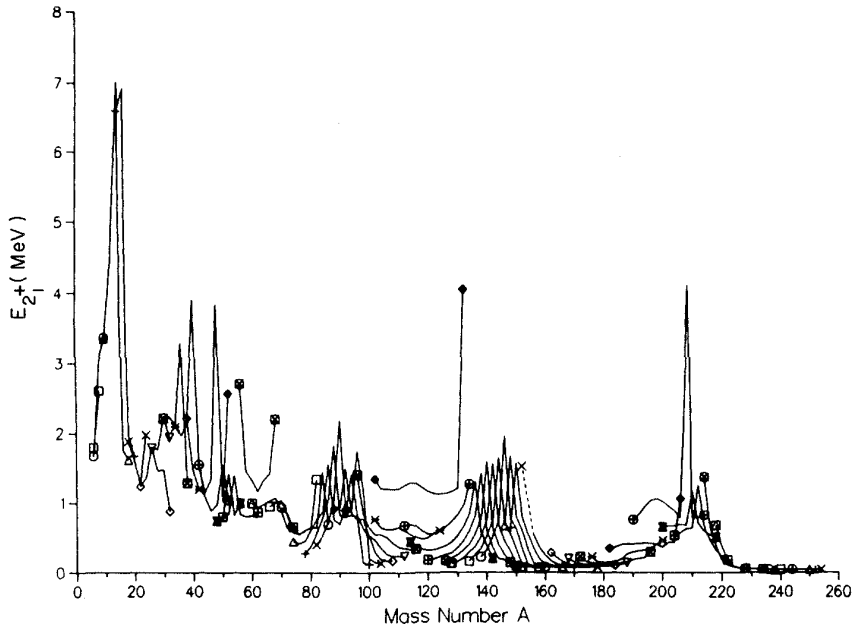

Fig. 2.12. $E_{2_1^+}$ values for all even–even nuclei (Raman, 1987).

$$E_J = \frac{J(J+1)}{2\Theta}$$

where Θ is the nuclear rotational moment of inertia, that grows with deformation.

These are "old" plots to avoid overlapping structures visible when plotting all of today's available data taken from R. Casten, "Nuclear Structure from a Simple Perspective", Oxford University Press (1990)

Deformation also depends on macroscopic properties

Liquid-drop model energy composed of volume, volume symmetry, surface and surface symmetry energies as well as direct and exchange Coulomb terms

$$
\begin{aligned}
E_{\mathrm{LDM}}(N,Z) = & \left(a_{\mathrm{vol}} + a_{\mathrm{sym}}\, I^2\right) A \\
& + \left(a_{\mathrm{surf}} + a_{\mathrm{ssym}}\, I^2\right) A^{2/3} \\
& + \frac{3\,e^2}{5\,r_0}\,\frac{Z^2}{A^{1/3}} - \frac{3\,e^2}{4\,r_0}\left(\frac{3}{2\pi}\right)^{2/3}\frac{Z^{4/3}}{A^{1/3}}
\end{aligned}
$$

- $A = N + Z$ and $I = \frac{N-Z}{N+Z}$
- The volume (a_{vol}) and volume symmetry (a_{sym}) energy coefficients can be related to properties of INM at the saturation point
- the surface (a_{surf}) and surface symmetry (a_{ssym}) energy coefficients are connected to properties of semi-infinite matter
- The radius constant r_0 entering the Coulomb energies is determined by the nuclear matter saturation density ρ_{sat} through $r_0^3 = 3/(4\pi\rho_{\mathrm{sat}})$.

In deformed nuclei, the surface, surface symmetry and Coulomb energies are deformation dependent. In general Coulomb energy decreases with deformation, surface energy increases.

Parameterisation-dependence of predictions

- While the best parameter sets of the standard forms of EDFs have similar predictive quality (and similar problems to describe certain observables and/or phenomena), there can be enormous differences between the predictions of parameter sets of a given functional.
- The following are a few representative examples for masses and deformations

Parameterisation dependence of deformation properties

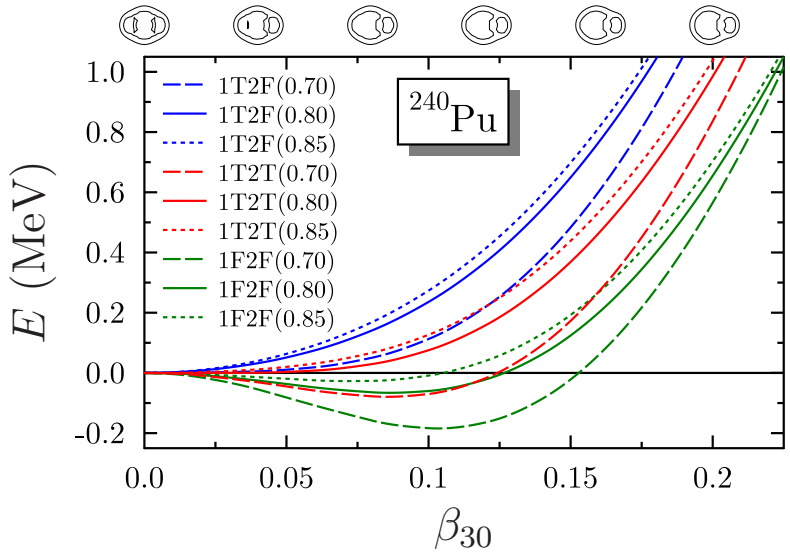

	$a^{\rm HF}_{\rm surf}$	$a^{\rm HF}_{\rm ssym}$	$a^{\rm HF}_{\rm surf,eff}$ ^{240}Pu	$a^{\rm HF}_{\rm surf,eff}$ ^{180}Hg
1T2F(0.70)	18.4	−49	16.1	17.8
1T2F(0.80)	18.2	−51	15.8	17.6
1T2F(0.85)	18.1	−51	15.7	17.5
1T2T(0.70)	17.5	−47	15.3	16.9
1T2T(0.80)	17.3	−49	15.0	16.7
1T2T(0.85)	17.2	−50	14.9	16.6
1F2F(0.70)	16.6	−44	14.5	16.1
1F2F(0.80)	16.4	−46	14.3	15.9
1F2F(0.85)	16.3	−47	14.1	15.8

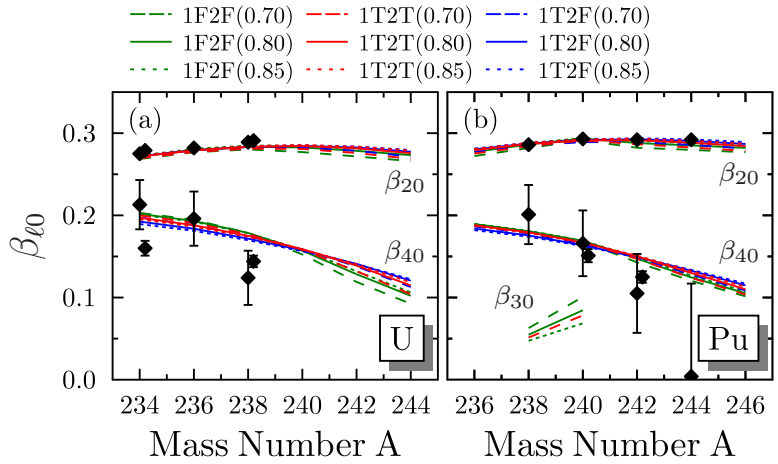

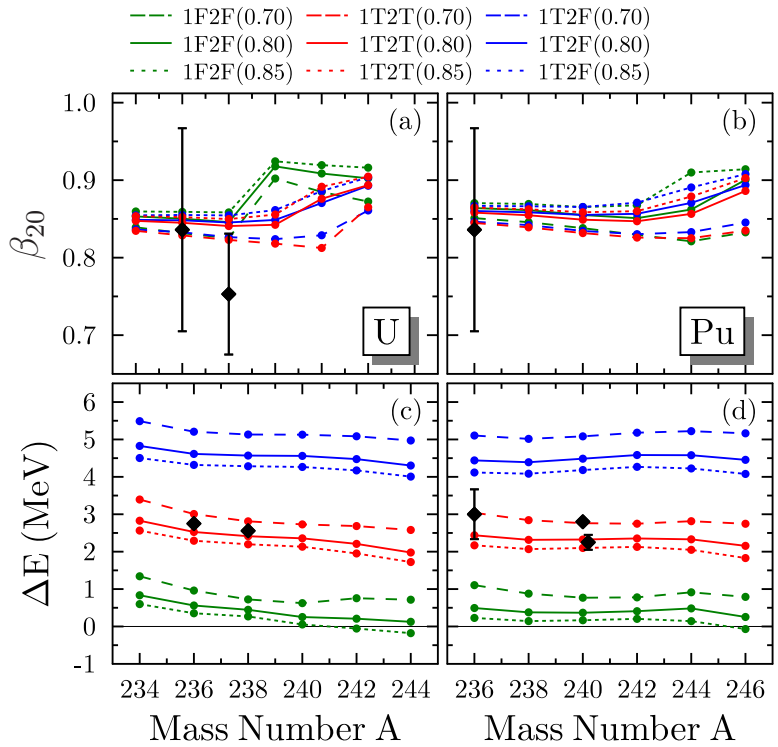

da Costa, Bennaceur, Meyer, Ryssens, Bender, PRC 109 (2024) 034316

Parameterisation dependence of deformation properties

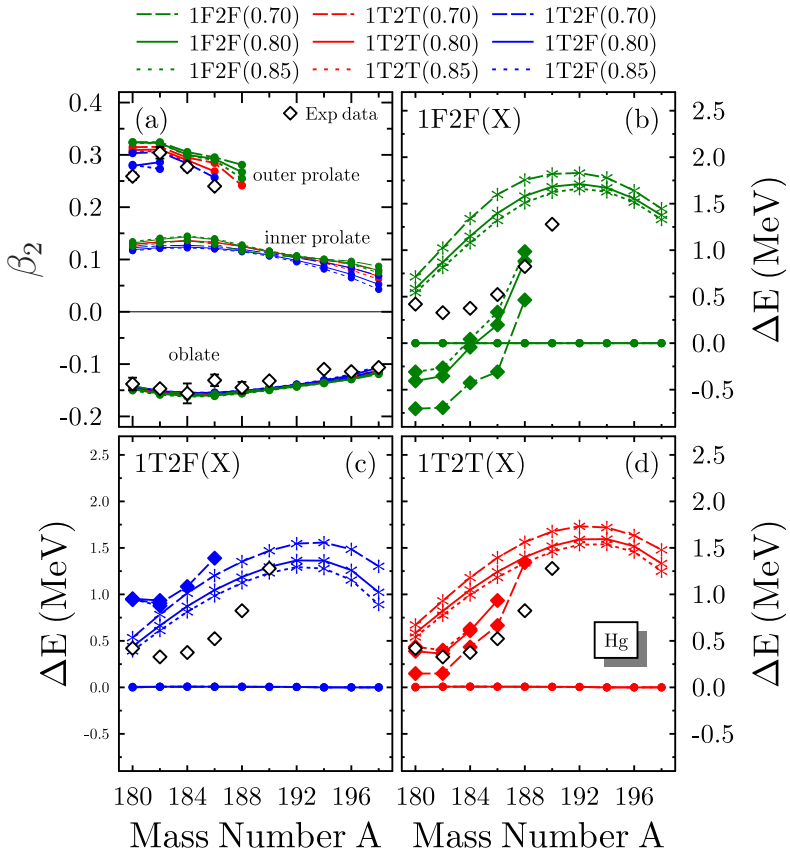

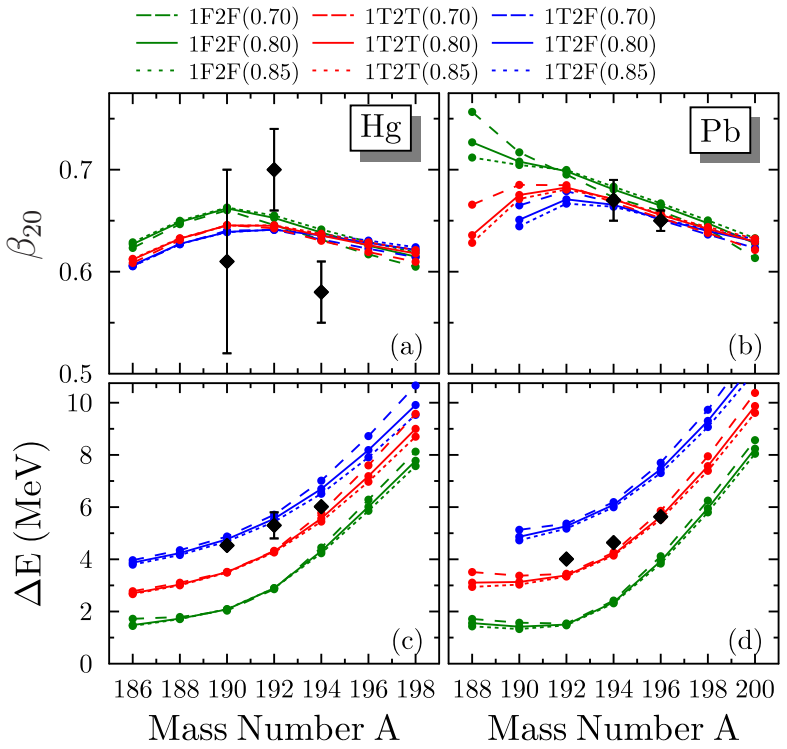

- Parameter sets adjusted with different effective mass and different surface energy
-

da Costa, Bennaceur, Meyer, Ryssens, Bender, PRC 109 (2024) 034316

Parameterisation dependence of deformation properties

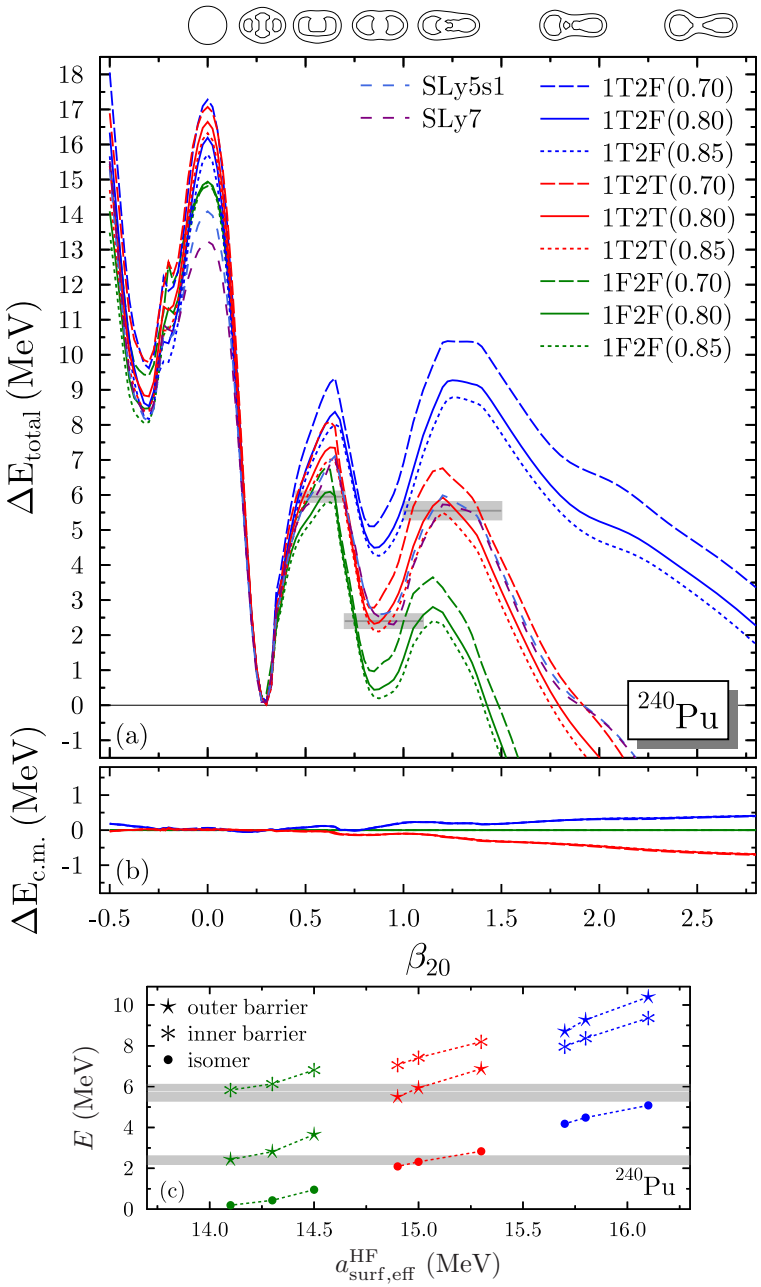

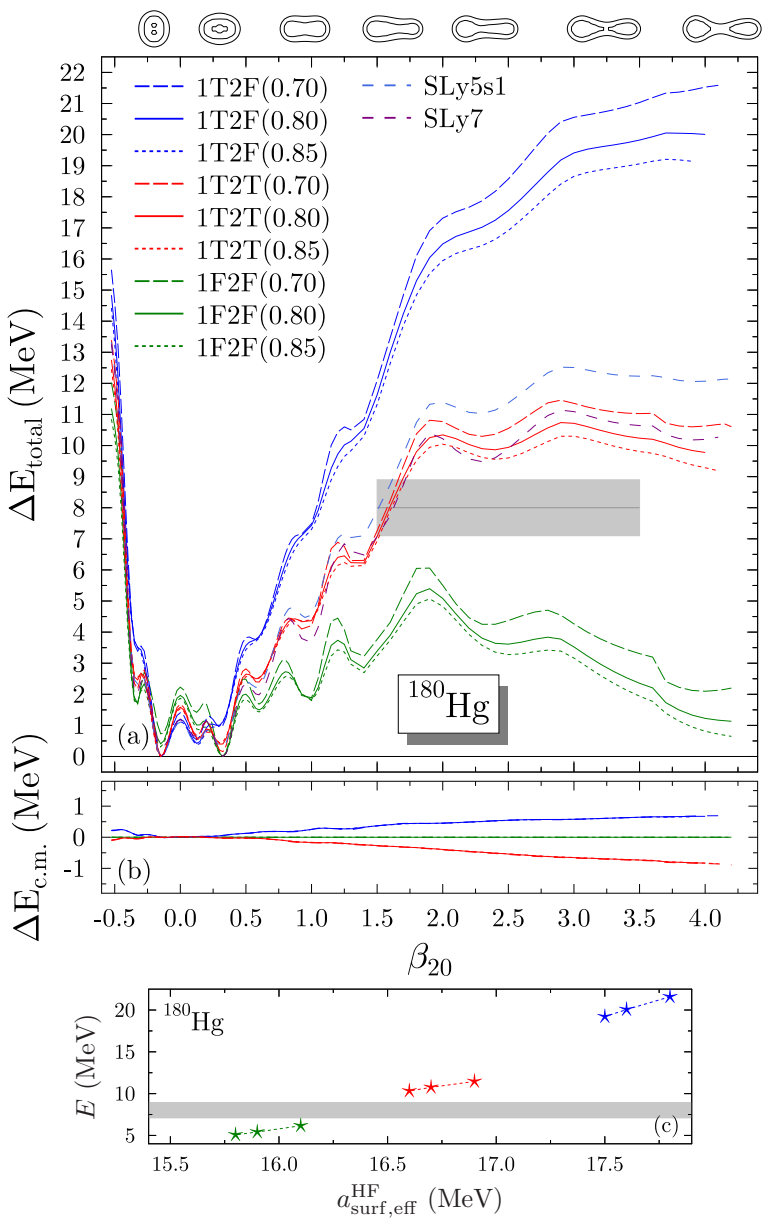

da Costa, Bennaceur, Meyer, Ryssens, Bender, PRC 109 (2024) 034316

Mass systematics - traditional parameter fits (even-even nuclei only)

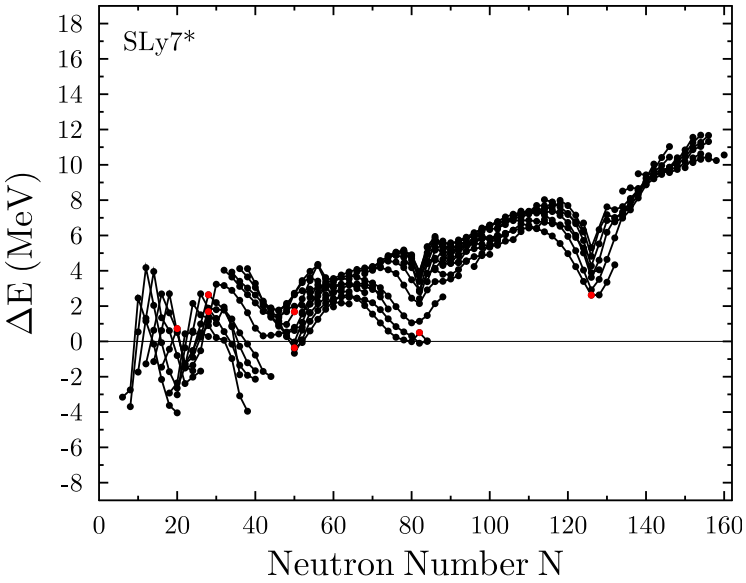

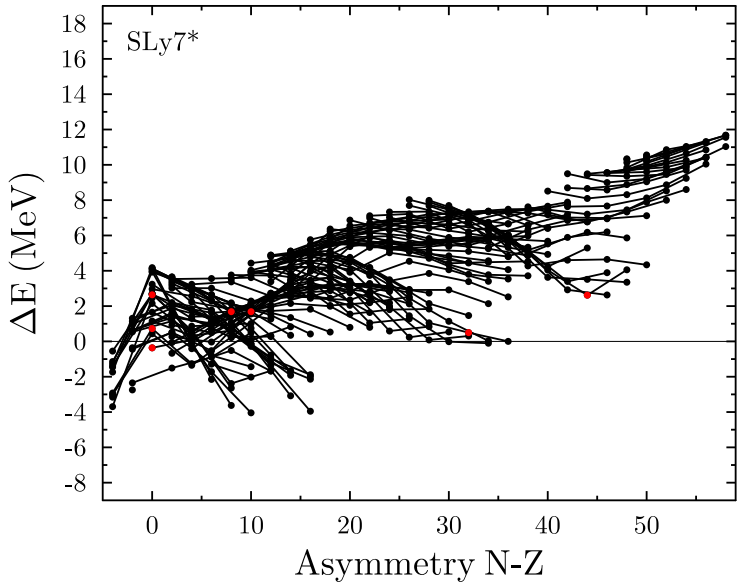

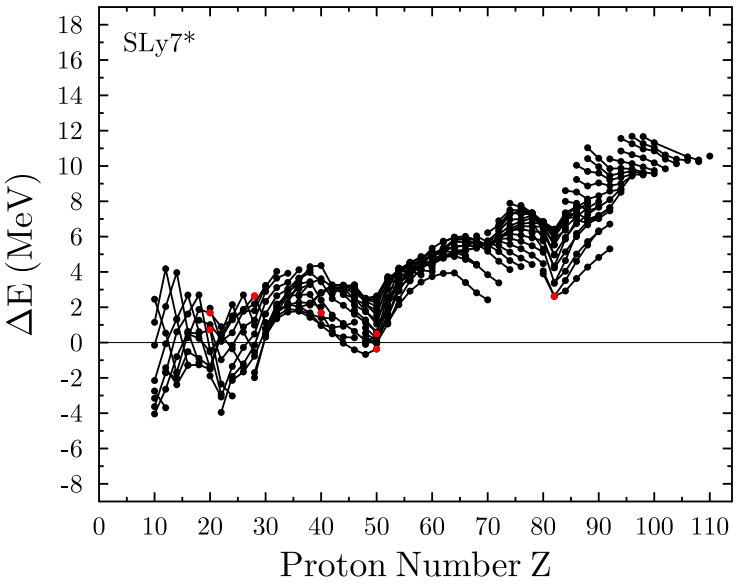

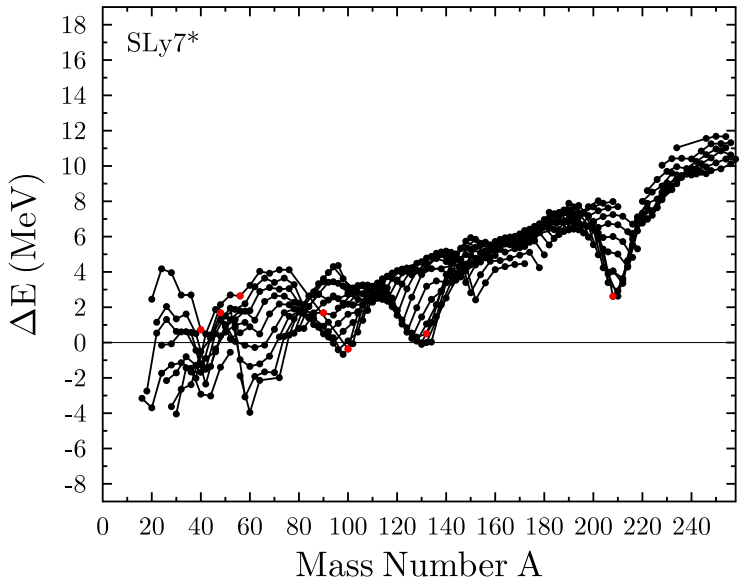

Bender et al, unpublished

Mass systematics - traditional parameter fits (even-even nuclei only)

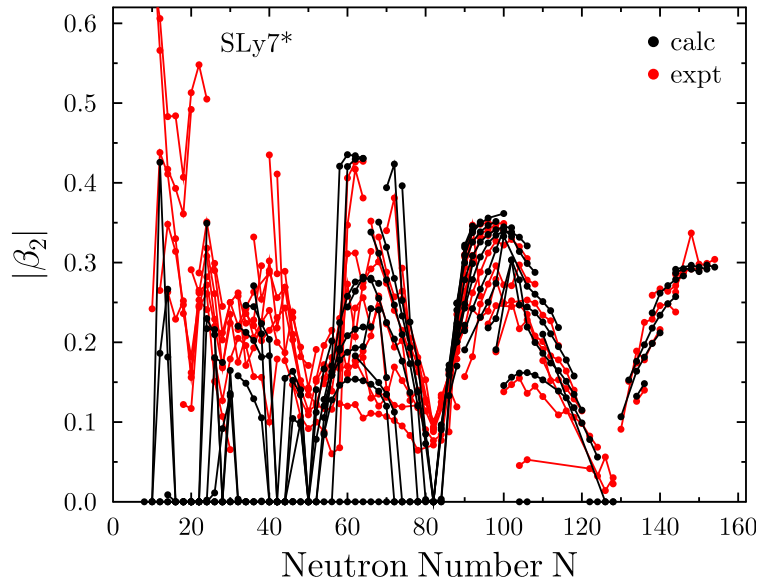

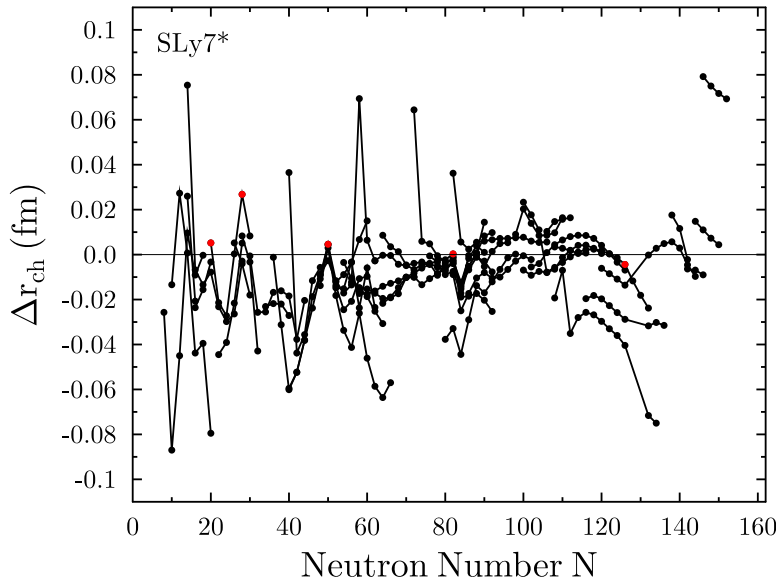

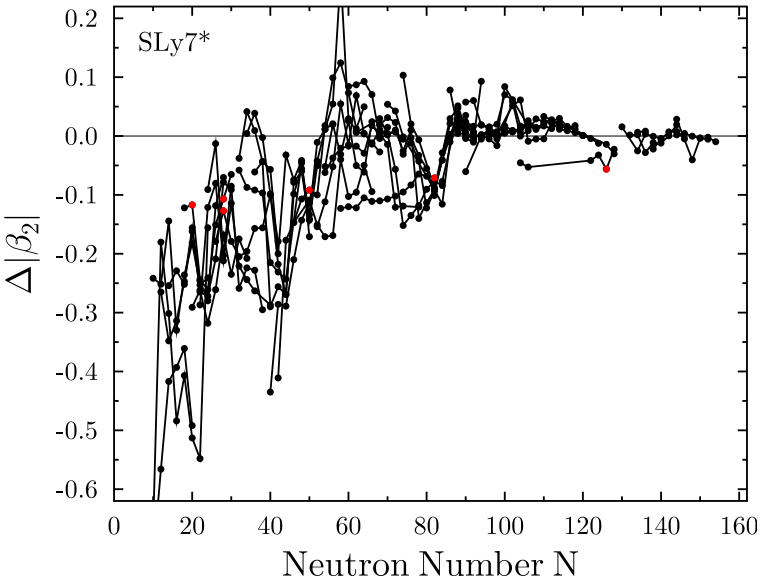

- experimental data for $|\beta|$ from Raman tables assuming that nuclei are rigid rotors
- Large differences for light nuclei
- experimental data for charge radii from
- calculated charge radii contain corrections for intrinsic charge distribution of nucleons and relativistic effects that will be explained in what follows

Bender et al, unpublished

Mass systematics - modern global fits (all nuclei)

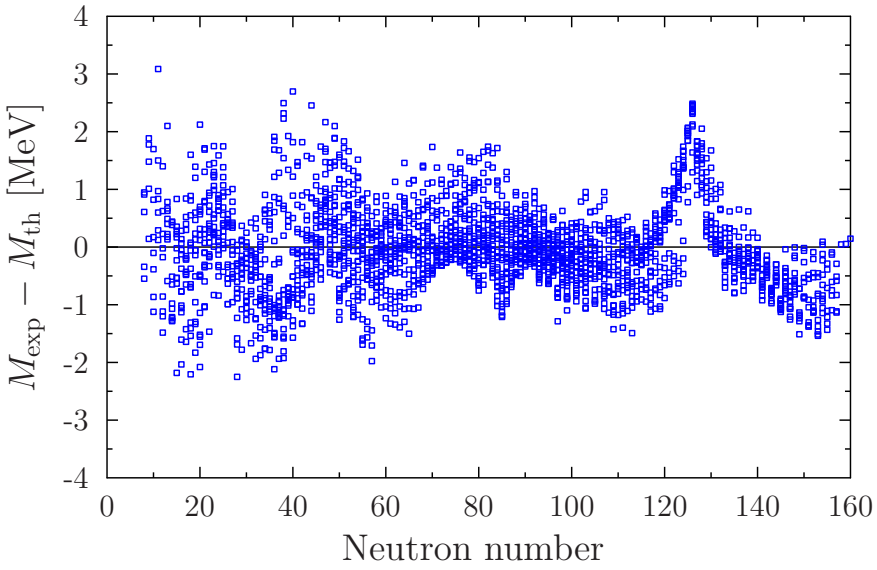

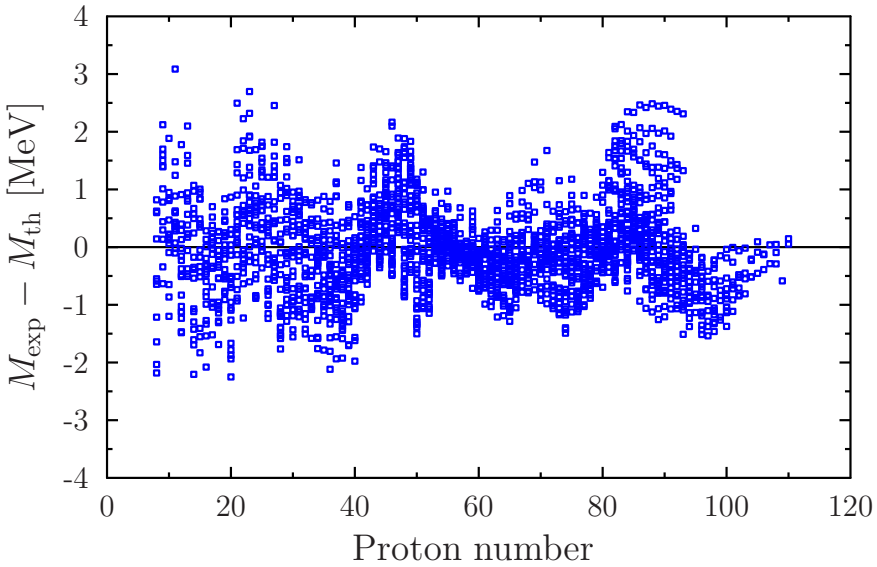

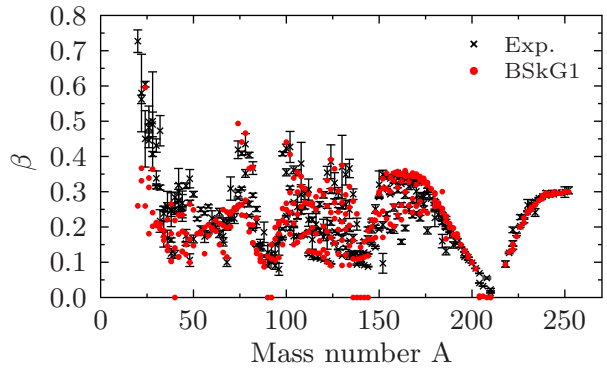

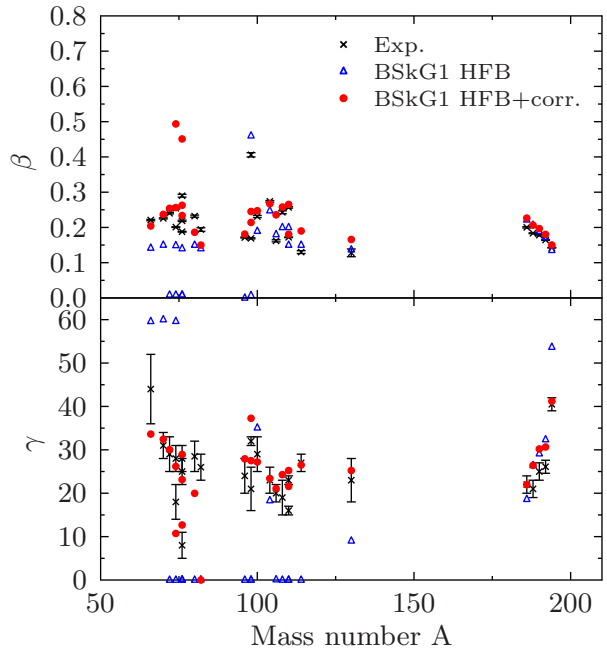

Scamps, Goriely, Olsen, Bender, Ryssens, EPJ A 57 (2021) 333

Total-binding energy differences vs single-particle energy differences

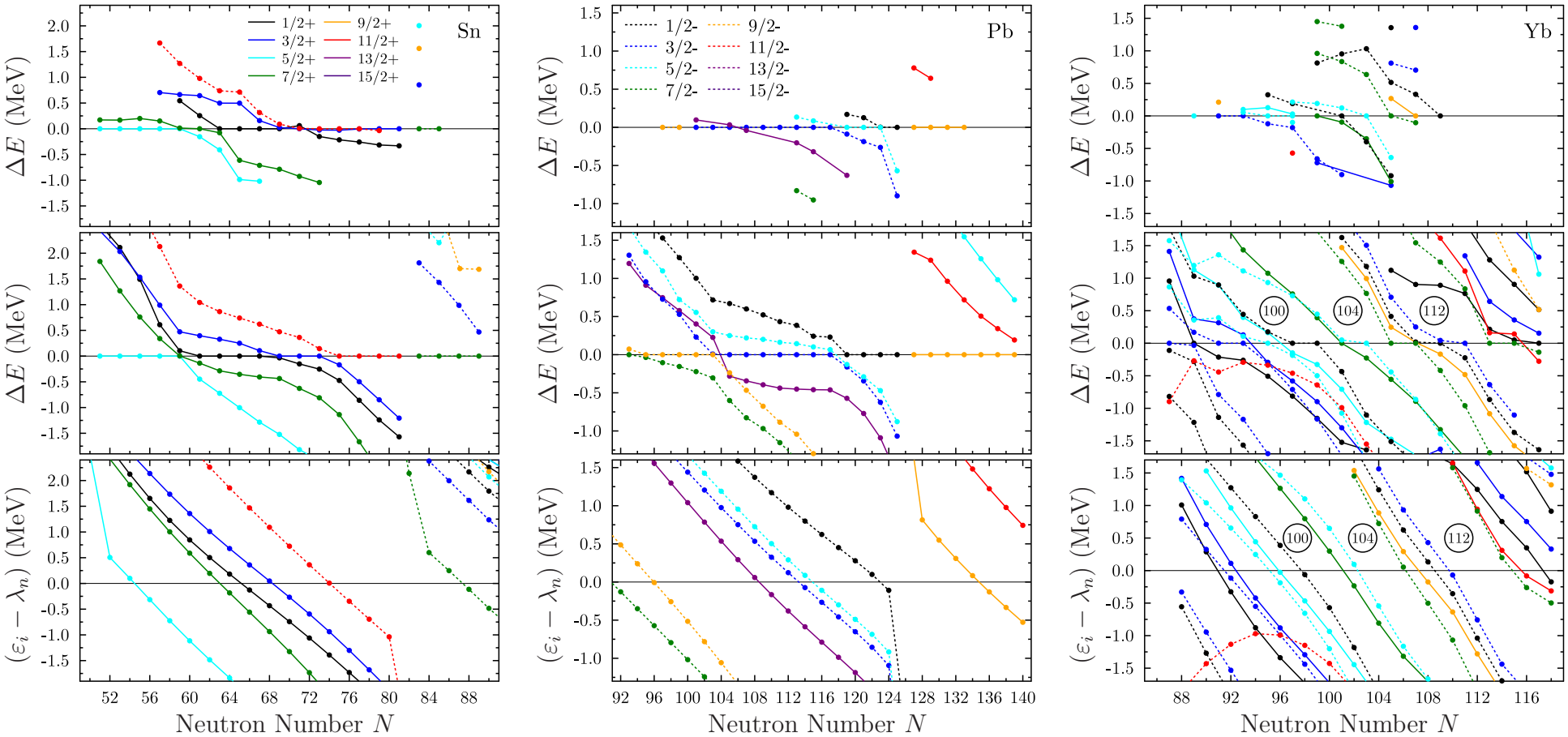

- middle: total HFB of blocked 1qp state relative to ground state. Positive (negative) sign indicates that the dominant single-particle level was above (below) λ before blocking
- top: experiment relative to ground state, sign guessed to match middle panel.
- bottom: $\varepsilon_k - \lambda$

Bender, Bennaceur, Guillon, arXiv:2603.13164

Separation energies

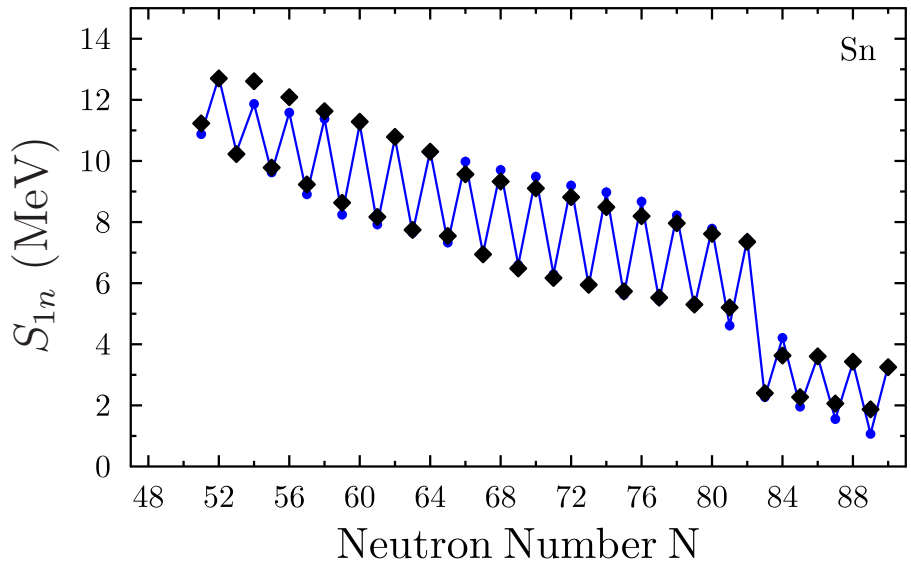

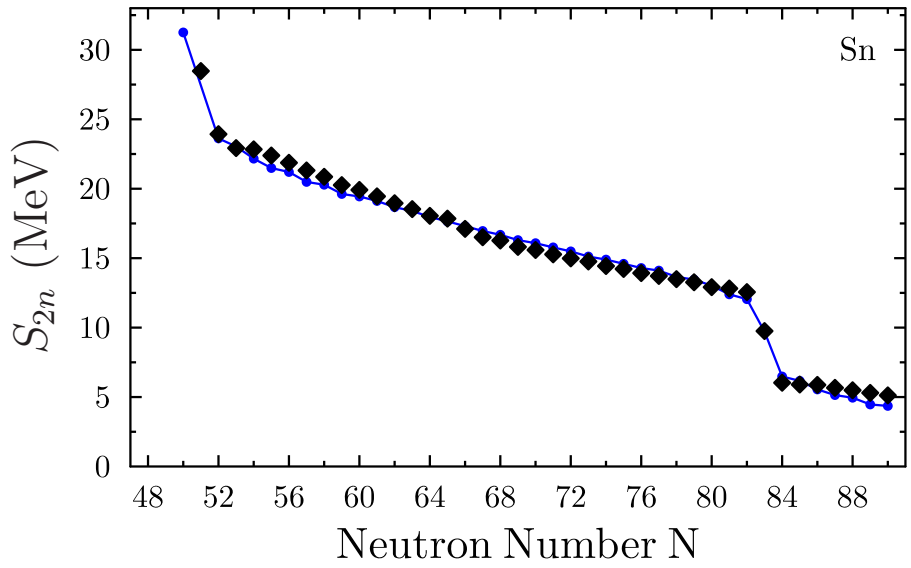

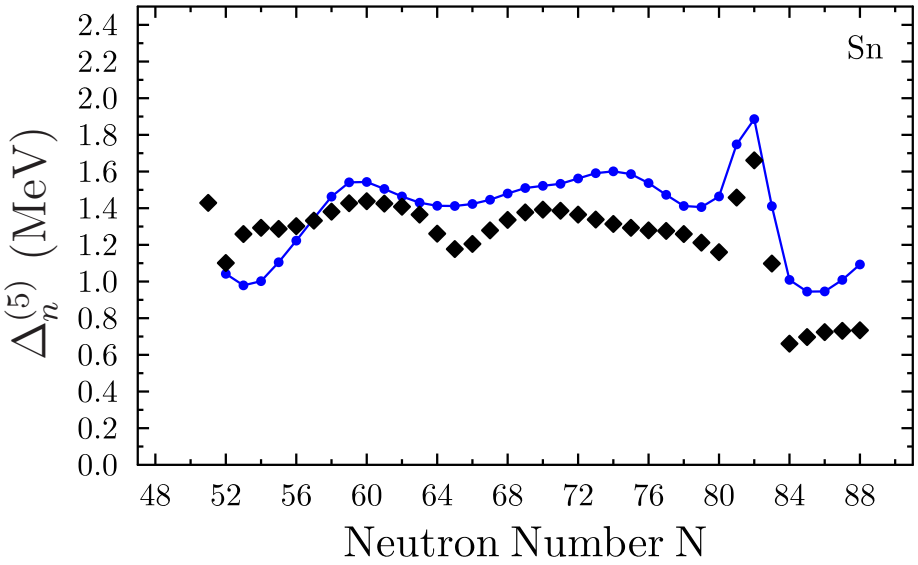

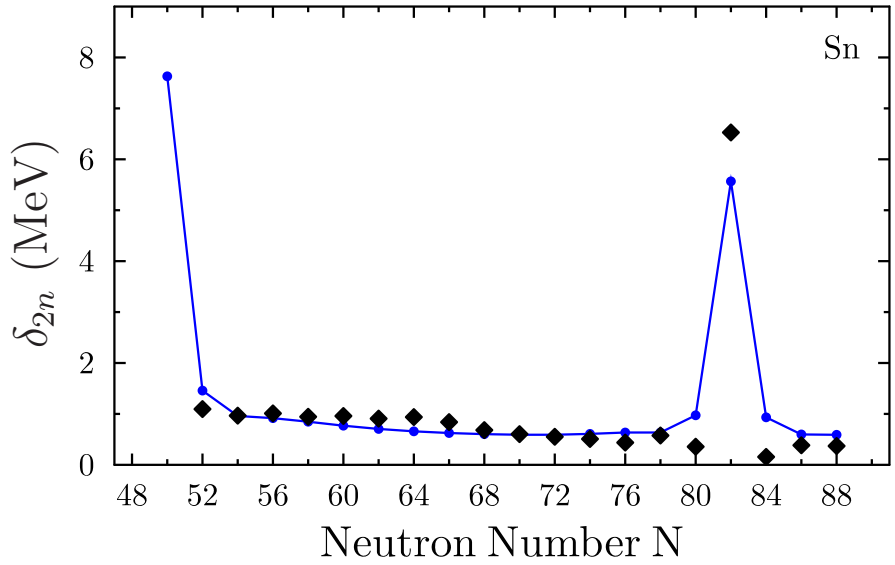

Bender, prepared from the calculations made for Bender, Bennaceur, Guillon, arXiv:2603.13164

Separation energies

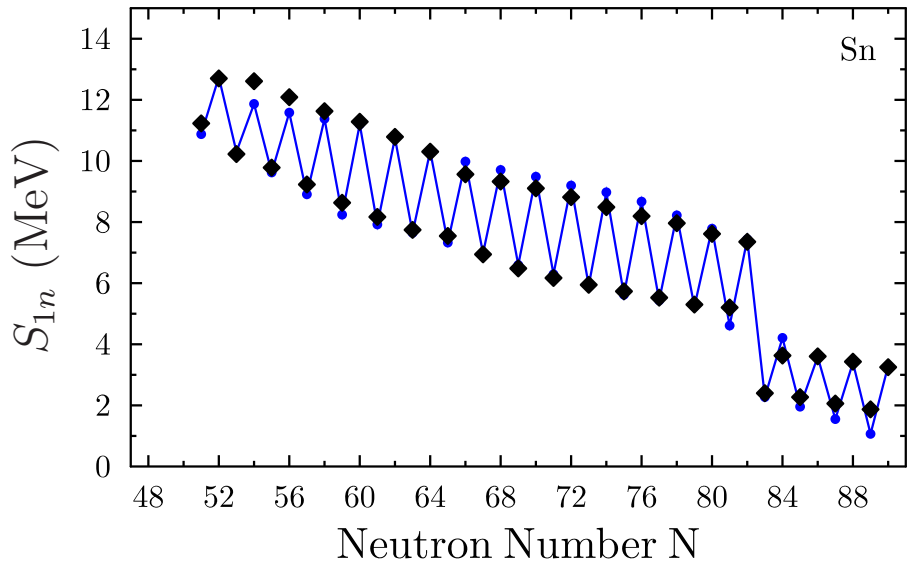

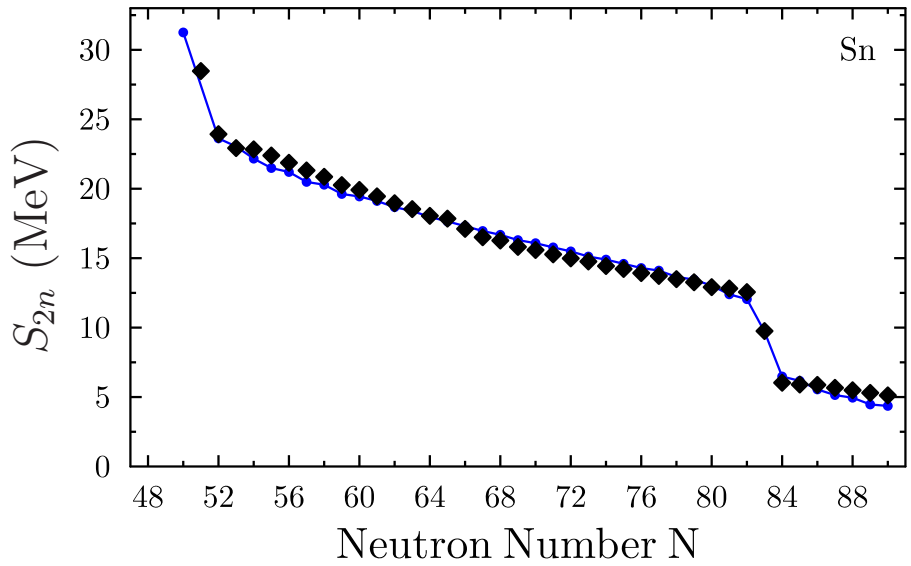

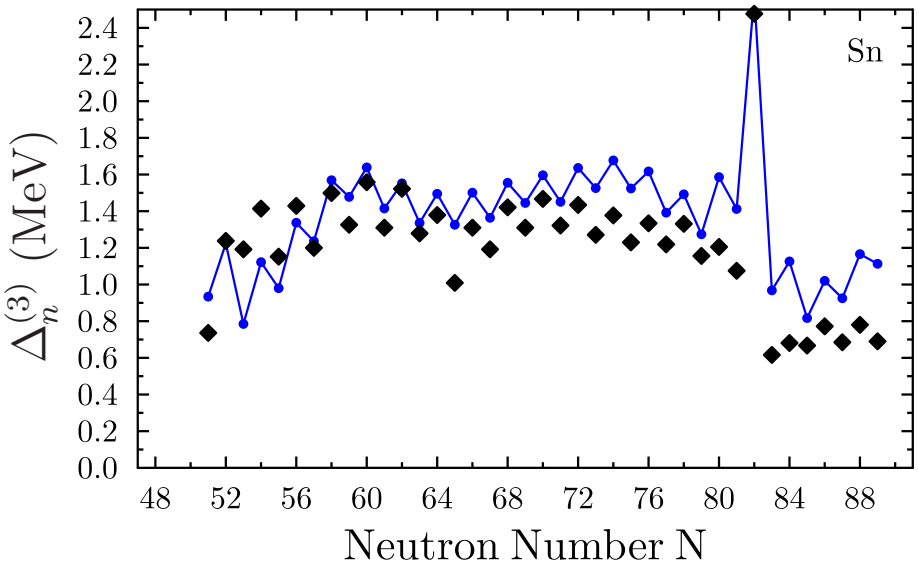

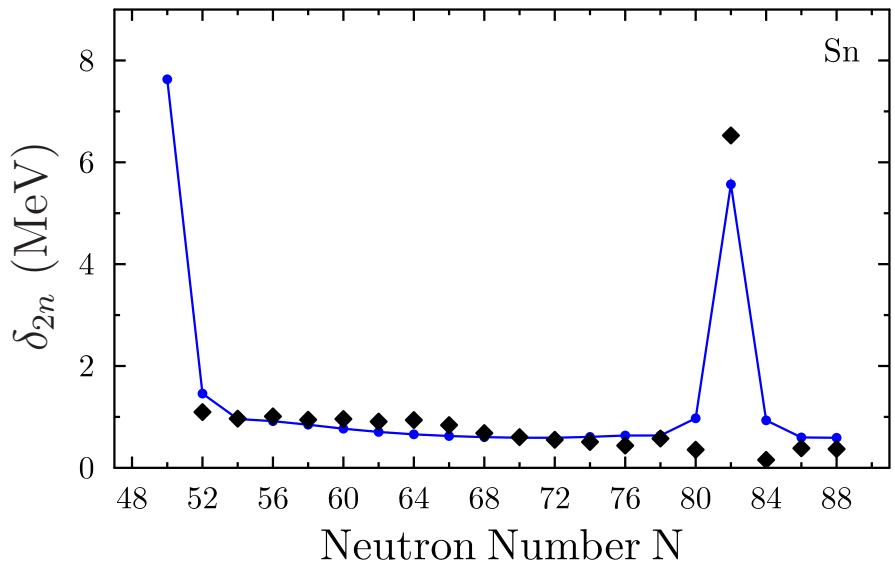

Bender, prepared from the calculations made for Bender, Bennaceur, Guillon, arXiv:2603.13164

Separation energies

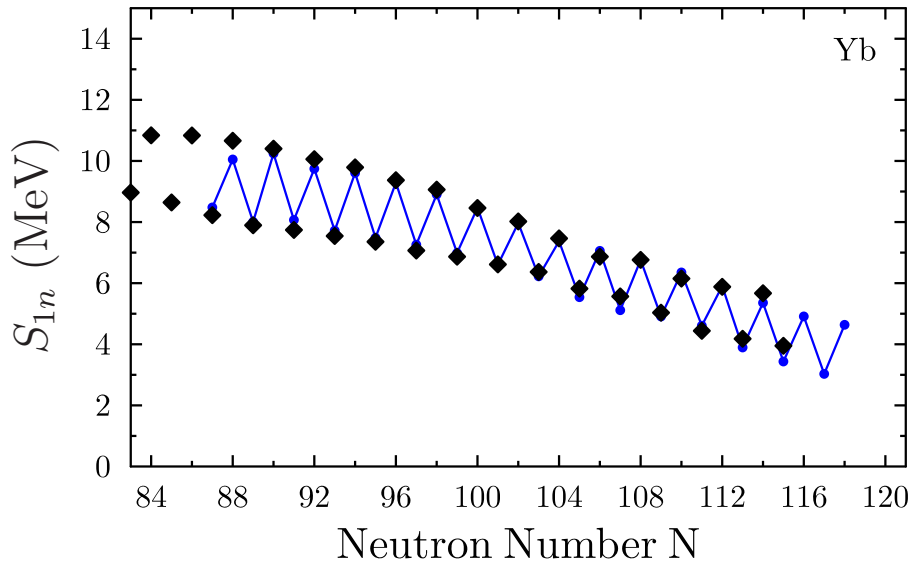

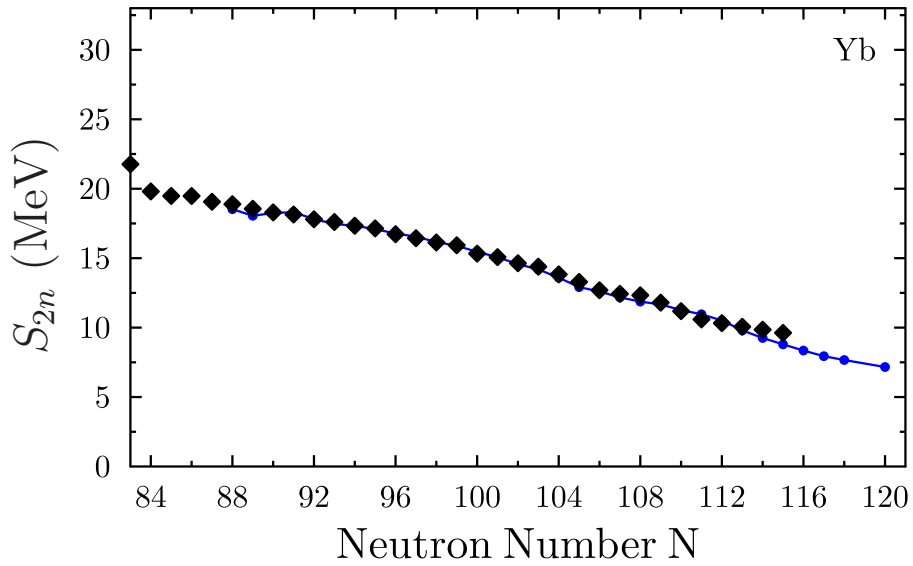

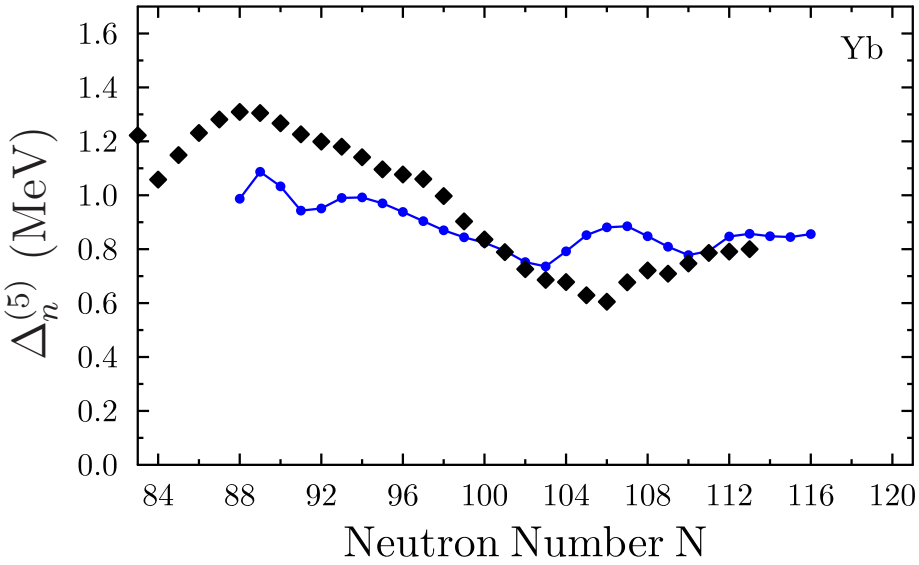

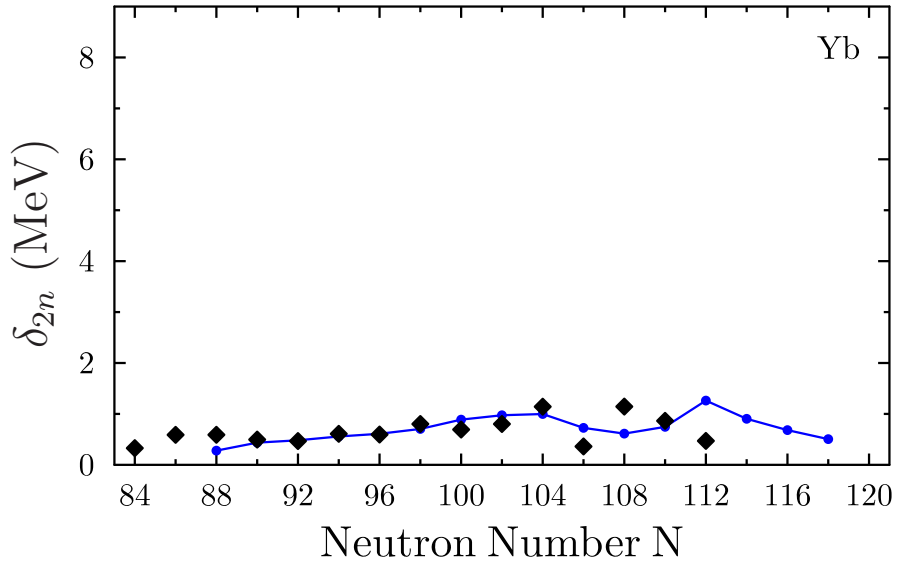

Bender, prepared from the calculations made for Bender, Bennaceur, Guillon, arXiv:2603.13164

Separation energies

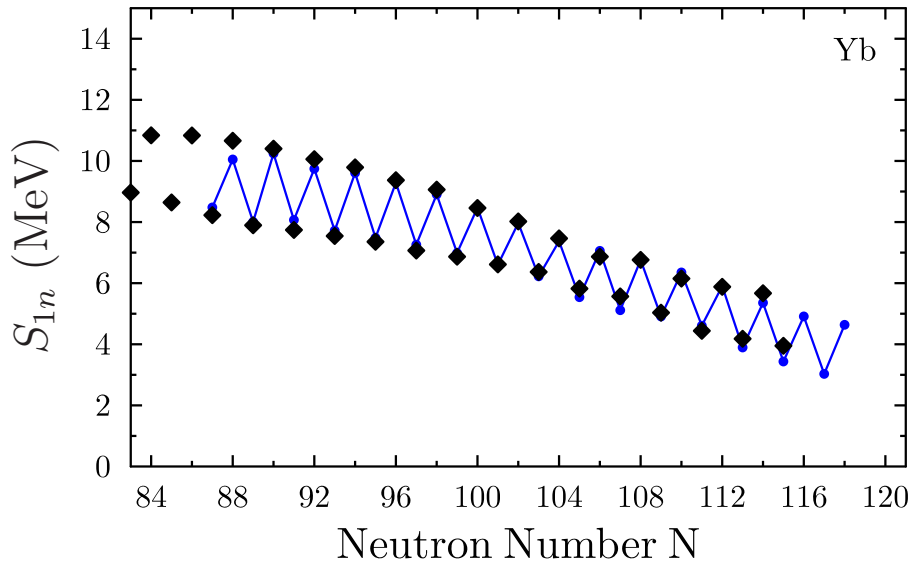

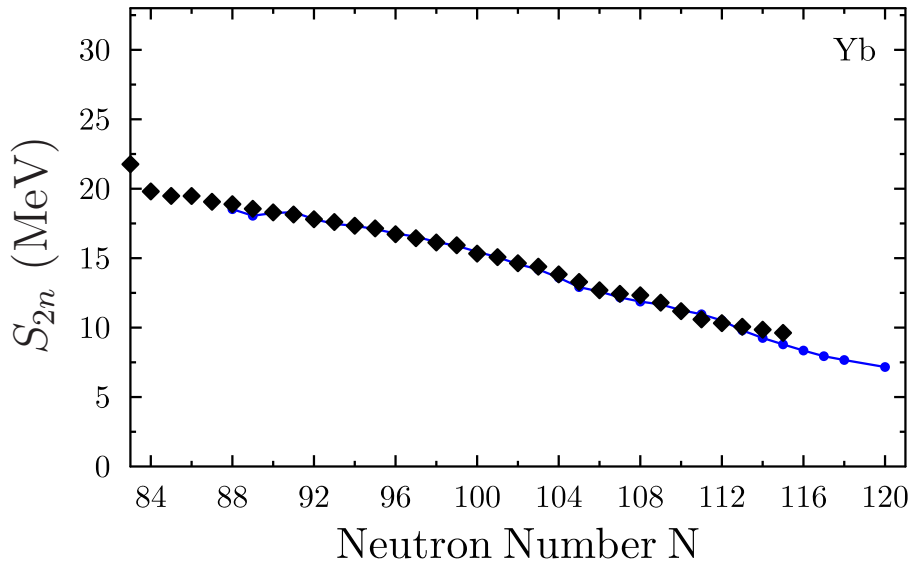

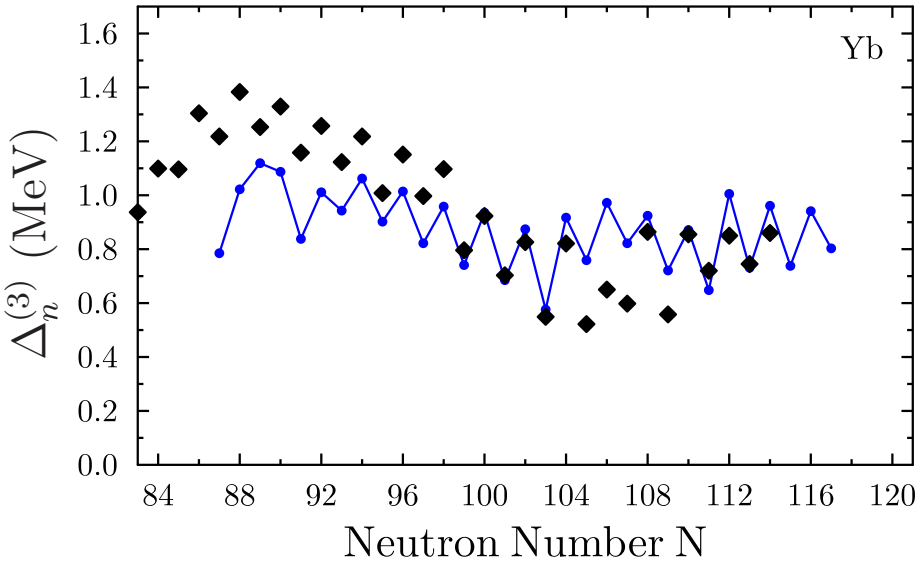

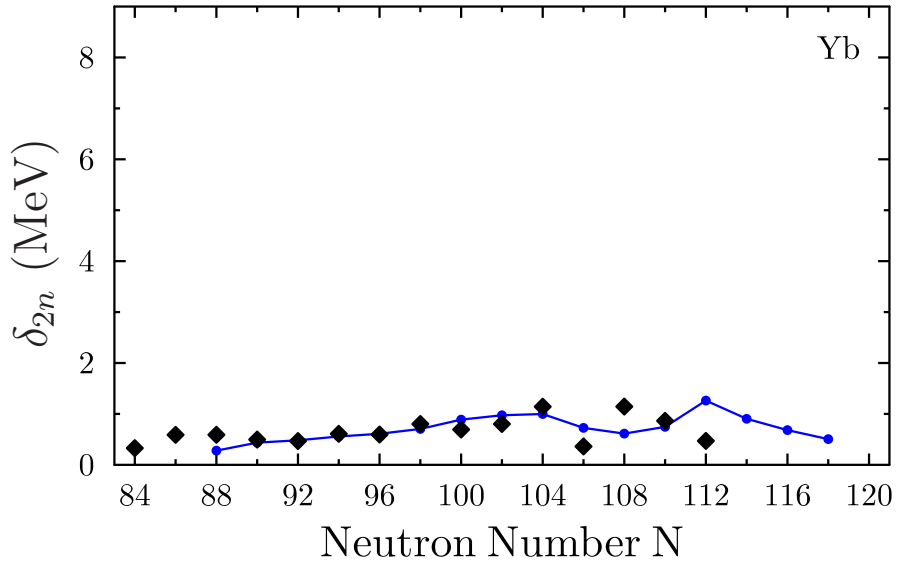

Bender, prepared from the calculations made for Bender, Bennaceur, Guillon, arXiv:2603.13164

Two-nucleon separation energy vs λ_q

$$S_{2n}(Z,N) \quad = \quad E(Z-2,N) - E(Z,N) \approx -2\lambda_n(Z,N)$$

- markers: $S_{2n}(Z,N)$
- lines: $-2\lambda_n(Z,N)$

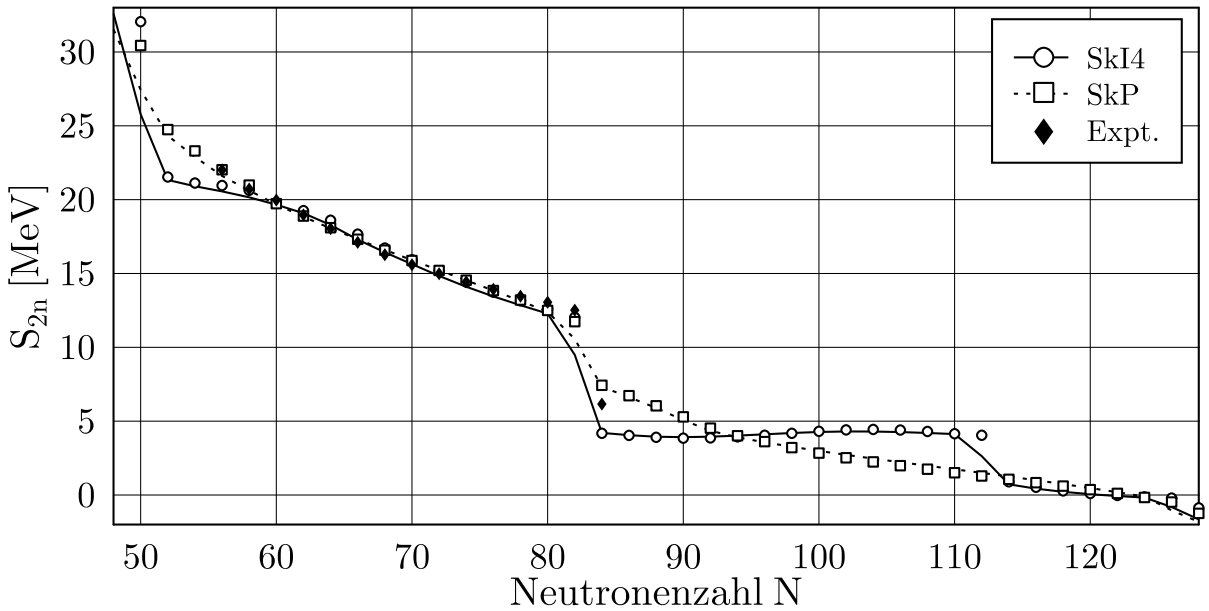

Bender, Doktorarbeit (1998)

Two-nucleon gaps

$$\delta_{2p}(Z,N) = S_{2p}(Z,N) - S_{2p}(Z-2,N) = E(Z+2,N) - 2E(Z,N) + E(Z-2,N)$$
$$\approx -2\big[\lambda_p(Z+2,N) - \lambda_p(Z,N)\big]$$

Solid line: $\delta_{2p}(Z,N)$ dotted line: $2\varepsilon_{3p_{1/2}} - 2\varepsilon_{2f_{5/2}}$ dashed line: $2\varepsilon_{1i_{11/2}} - 2\varepsilon_{2f_{5/2}}$

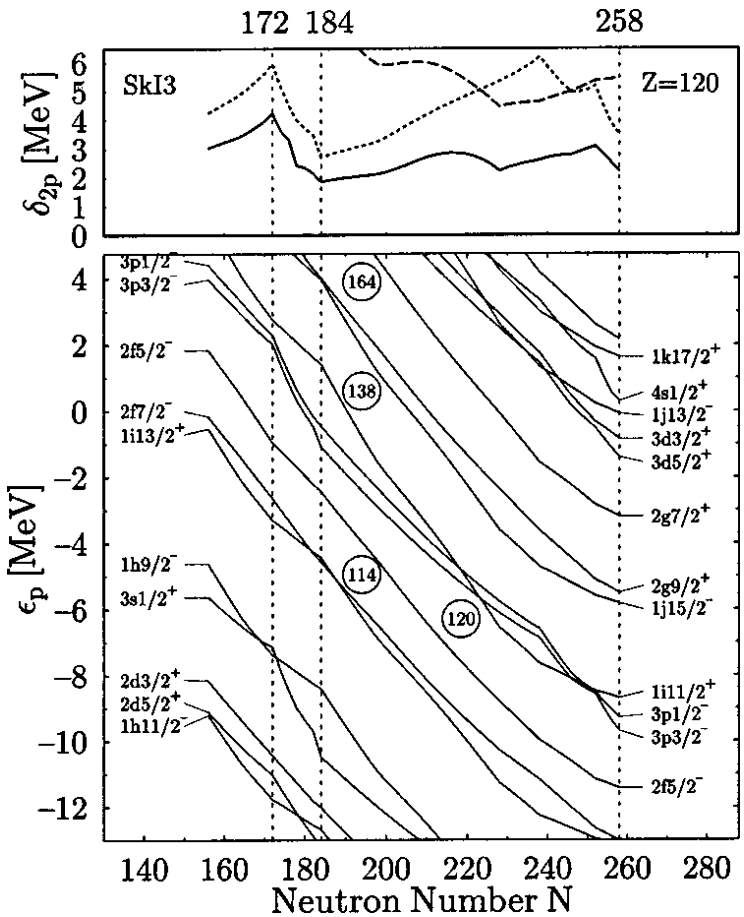

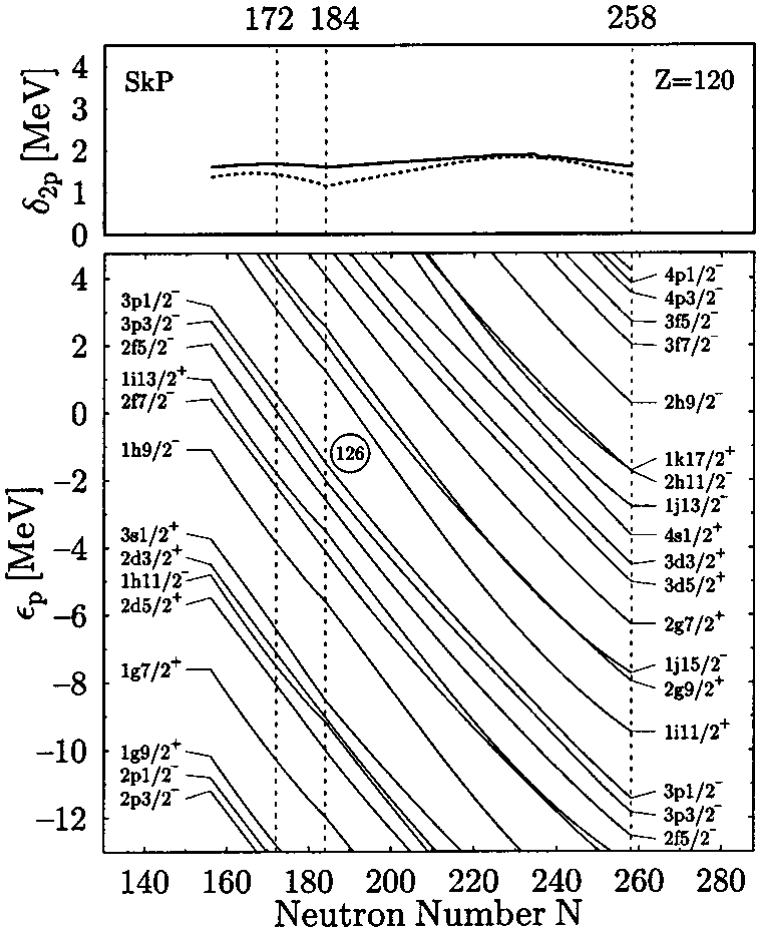

Bender, Rutz, Reinhard, Maruhn, Greiner PRC60 (1999) 034304

Beyond mean-field methods: Symmetry restoration

particle-number restoration operator

$$\hat{P}_{N_0} = \frac{1}{2\pi} \int_0^{2\pi} d\phi_N \; e^{i\phi_N(\hat{N}-N_0)}$$

angular-momentum restoration operator

$$\hat{P}^J_{MK} = \frac{2J+1}{16\pi^2} \int_0^{4\pi} d\alpha \int_0^{\pi} d\beta \; \sin(\beta) \int_0^{2\pi} d\gamma \; \mathcal{D}^{*J}_{MK}(\alpha,\beta,\gamma)\hat{R}(\alpha,\beta,\gamma)$$

K is the z component of angular momentum in the body-fixed frame. Projected states are given by

$$|JMq\rangle = \sum_{K=-J}^{+J} f_J(K) \; \hat{P}^J_{MK} \; \hat{P}^Z \; \hat{P}^N \; |q\rangle = \sum_{K=-J}^{+J} f_J(K) \; |JMKq\rangle$$

$f_J(K)$ is the weight of the component K and determined variationally

Axial symmetry (with the z axis as symmetry axis) allows to perform the α and γ integrations analytically, whereas the sum over K collapses, $f_J(K) \sim \delta_{K0}$

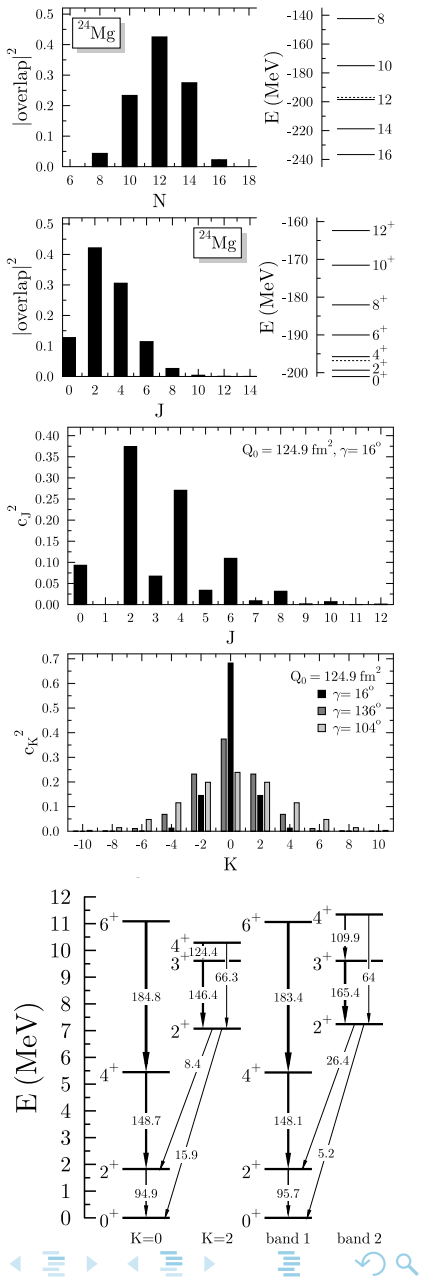

plots from Bender, EPJ ST156 (2008) 217 & Bender, Heenen PRC78 (2008) 024309

Superposition of angular-momentum projected SCMF states

$$|JM\nu\rangle = \sum_q \sum_{K=-J}^{+J} f_{J\nu}(q,K)\,|JMqK\rangle \qquad \begin{cases} |JMqK\rangle & \text{projected mean-field state} \\ f_{J\nu}(q,K) & \text{weight function} \end{cases}$$

$$\frac{\delta}{\delta f^*_{J\nu}(q,K)} \frac{\langle JM\nu|\hat{H}|JM\nu\rangle}{\langle JM\nu|JM\nu\rangle} = 0 \quad \Rightarrow \quad \text{Hill-Wheeler-Griffin equation}$$

$$\sum_{q'} \sum_{K'=-J}^{+J} \left[\mathcal{H}_J(qK,q'K') - E_{J,\nu}\,\mathcal{I}_J(qK,q'K')\right] f_{J,\nu}(q'K') = 0$$

with

$$\mathcal{H}_J(qK,q'K') = \langle JMqK|\hat{H}|JMq'K'\rangle \quad \text{energy kernel}$$
$$\mathcal{I}_J(qK,q'K') = \langle JMqK|JMq'K'\rangle \quad \text{norm kernel}$$

Angular-momentum projected GCM gives the

- correlated ground state for each value of J
- spectrum of excited states for each J

Horizontal vs. vertical expansion of correlations

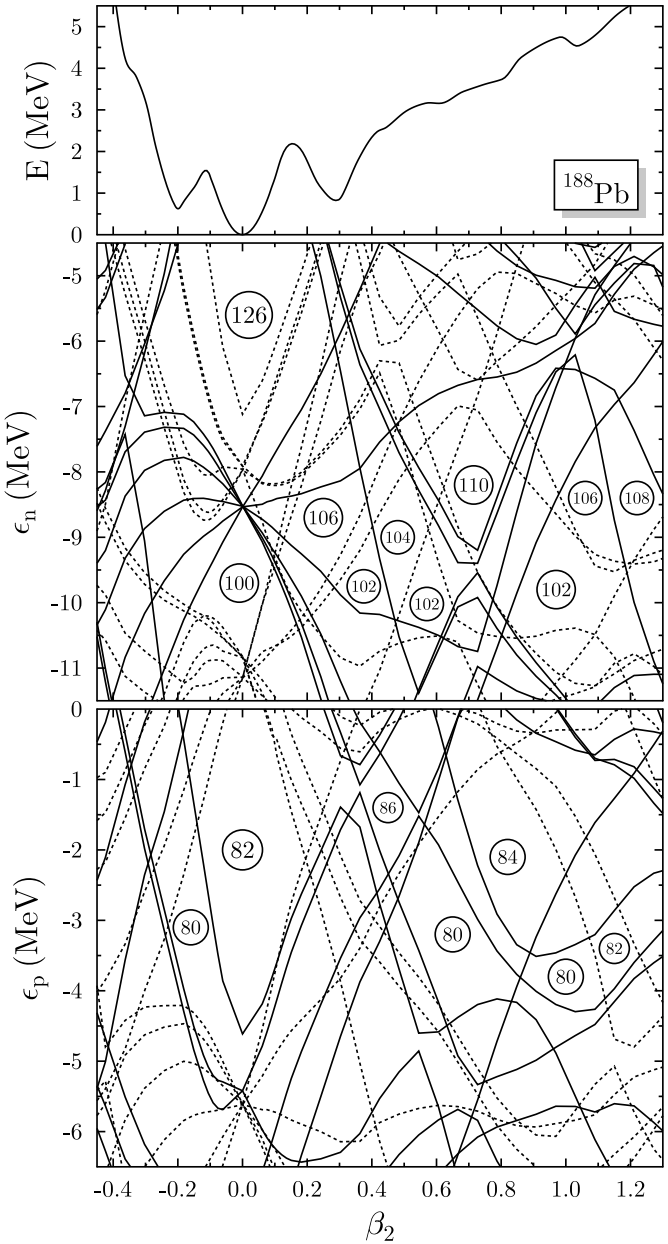

- Single-particle spectra change with deformation.
- avoidance of degenerate many-body states $\Rightarrow$ in the absence of pairing correlations, all open-shell nuclei are deformed.
- GCM as "horizontal expansion" that is to be contrasted with the "vertical expansion" of RPA.
- Original idea formulated in Dönau *et al*, NPA496 (1989) 333.
- coexisting minima correspond to shapes with low density of single-particle levels of either neutrons or protons (or both) near the respective Fermi surface

Horizontal vs. vertical expansion of correlations

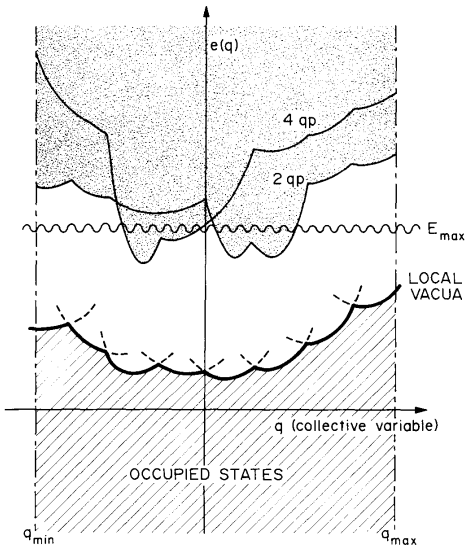

Fig. 1. Schematic plot of the energy versus the collective variable. The dark envelopes show the positions of the local vacua. The domain of the collective variable is defined by q_{min}, q_{max} and the energy cut E_{max}.

Dönau et al, NPA496 (1989) 333

- Single-particle spectra change with deformation.
- avoidance of degenerate many-body states $\Rightarrow$ in the absence of pairing correlations, all open-shell nuclei are deformed.
- GCM as "horizontal expansion" that is to be contrasted with the "vertical expansion" of RPA.
- Original idea formulated in Dönau *et al*, NPA496 (1989) 333.
- coexisting minima correspond to shapes with low density of single-particle levels of either neutrons or protons (or both) near the respective Fermi surface

Spectroscopy from MR EDF – the example of ^{188}Pb

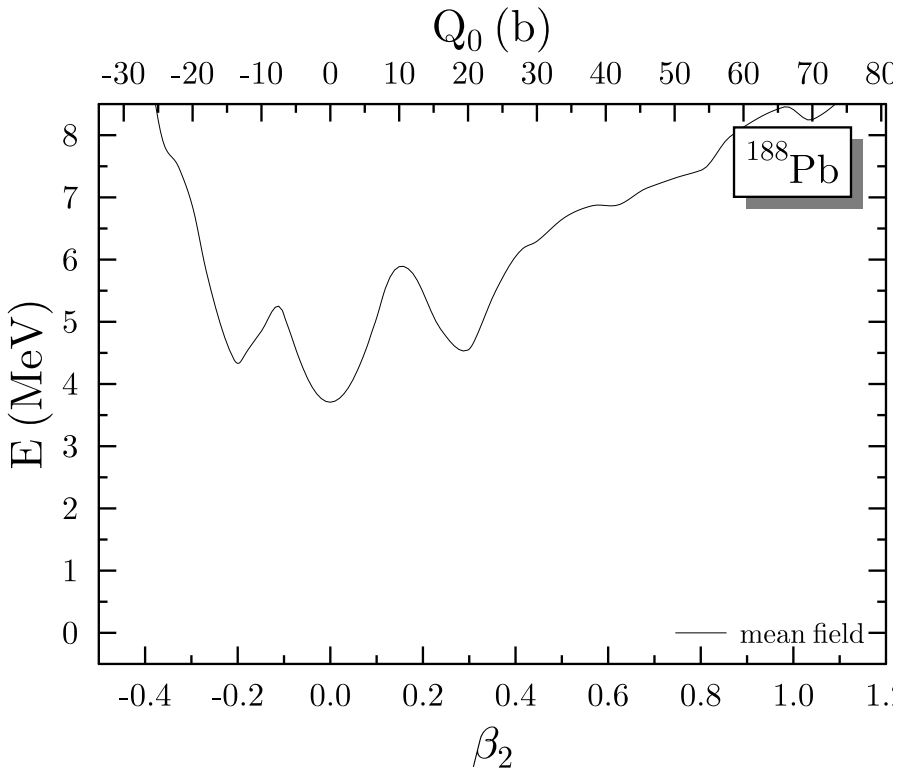

M. Bender, P. Bonche, T. Duguet, P.-H. Heenen, Phys. Rev. C 69 (2004) 064303.

Spectroscopy from MR EDF – the example of ^{188}Pb

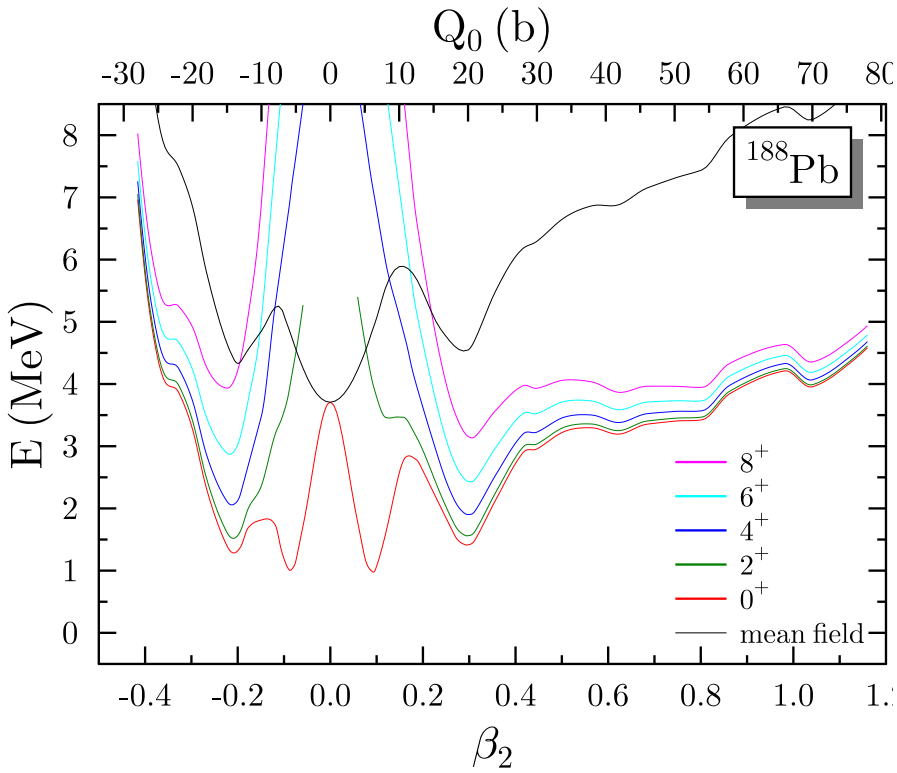

M. Bender, P. Bonche, T. Duguet, P.-H. Heenen, Phys. Rev. C 69 (2004) 064303.

Spectroscopy from MR EDF – the example of ^{188}Pb

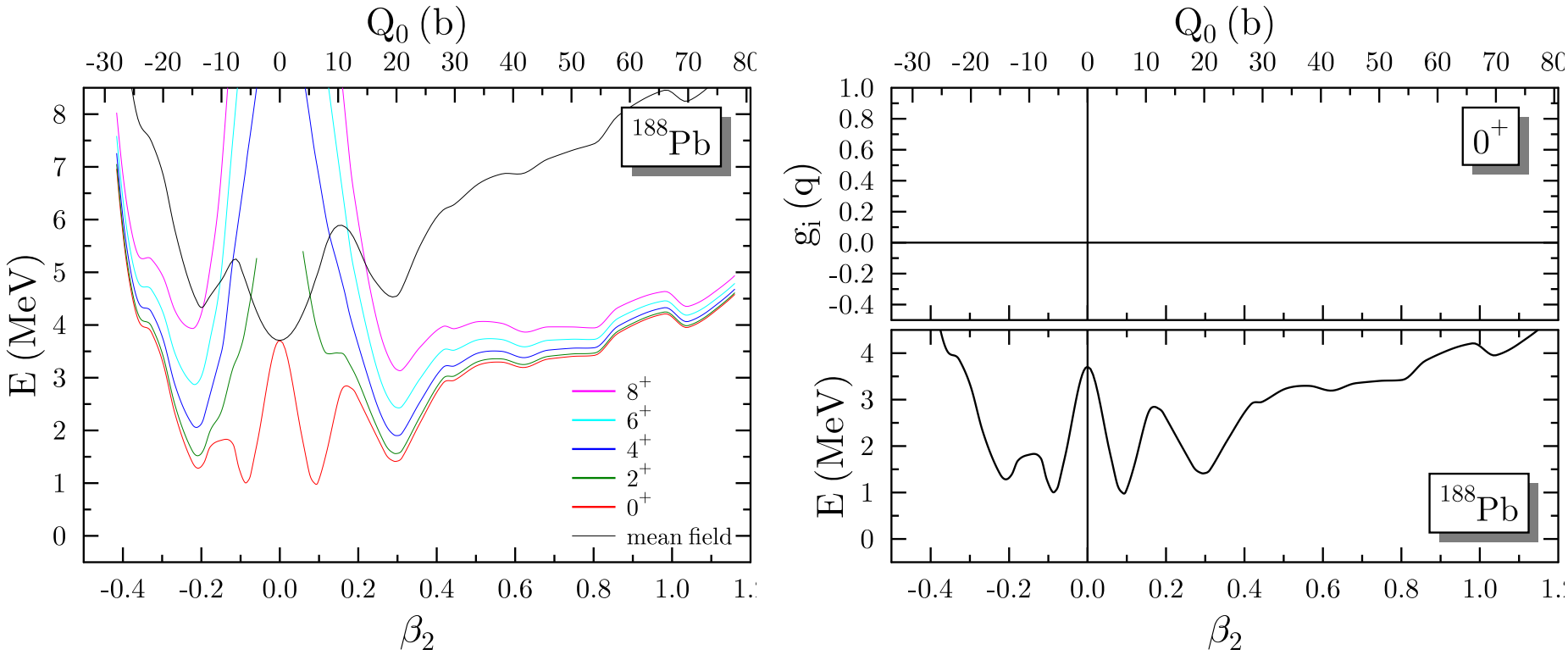

M. Bender, P. Bonche, T. Duguet, P.-H. Heenen, Phys. Rev. C 69 (2004) 064303.

Spectroscopy from MR EDF – the example of ^{188}Pb

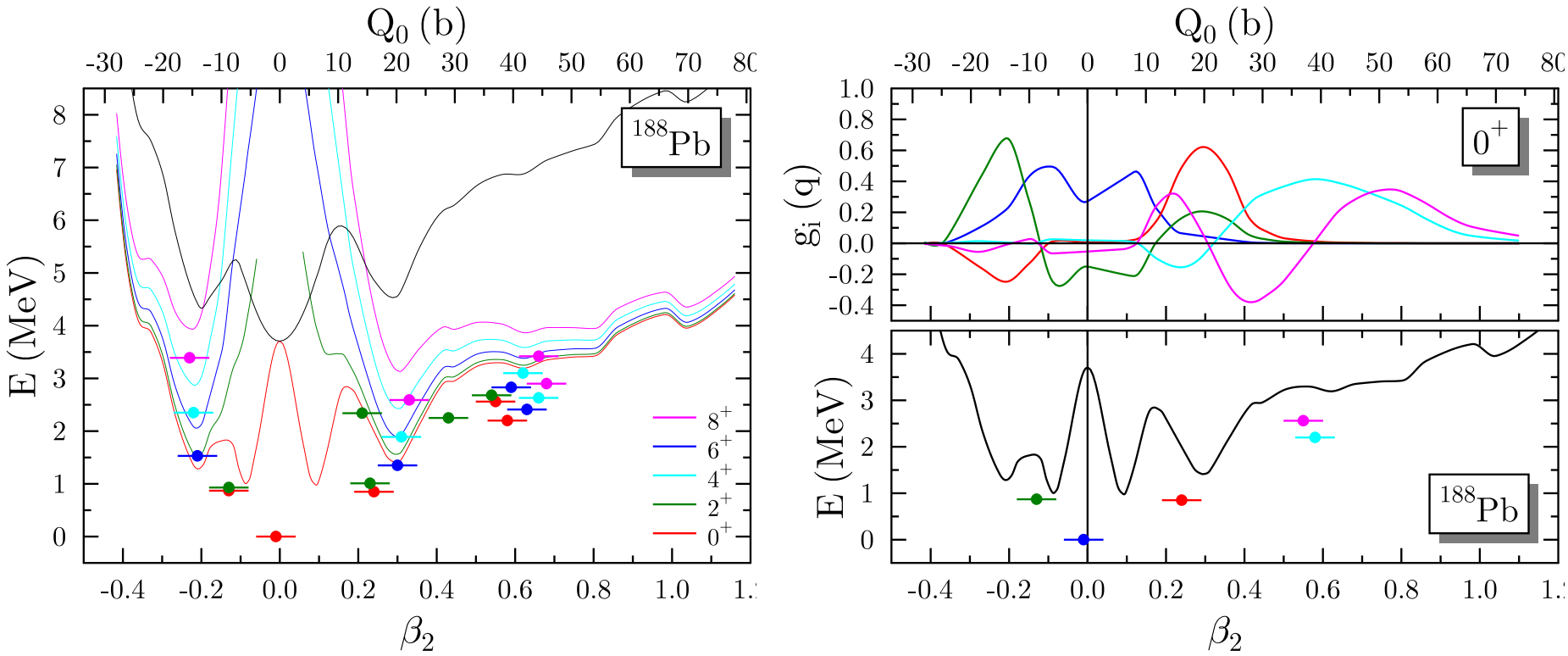

M. Bender, P. Bonche, T. Duguet, P.-H. Heenen, Phys. Rev. C 69 (2004) 064303.

Attention: $g_i^2(q)$ is not the probability to find a mean-field state with intrinsic deformation q in the collective state

Spectroscopy from MR EDF – the example of ^{188}Pb

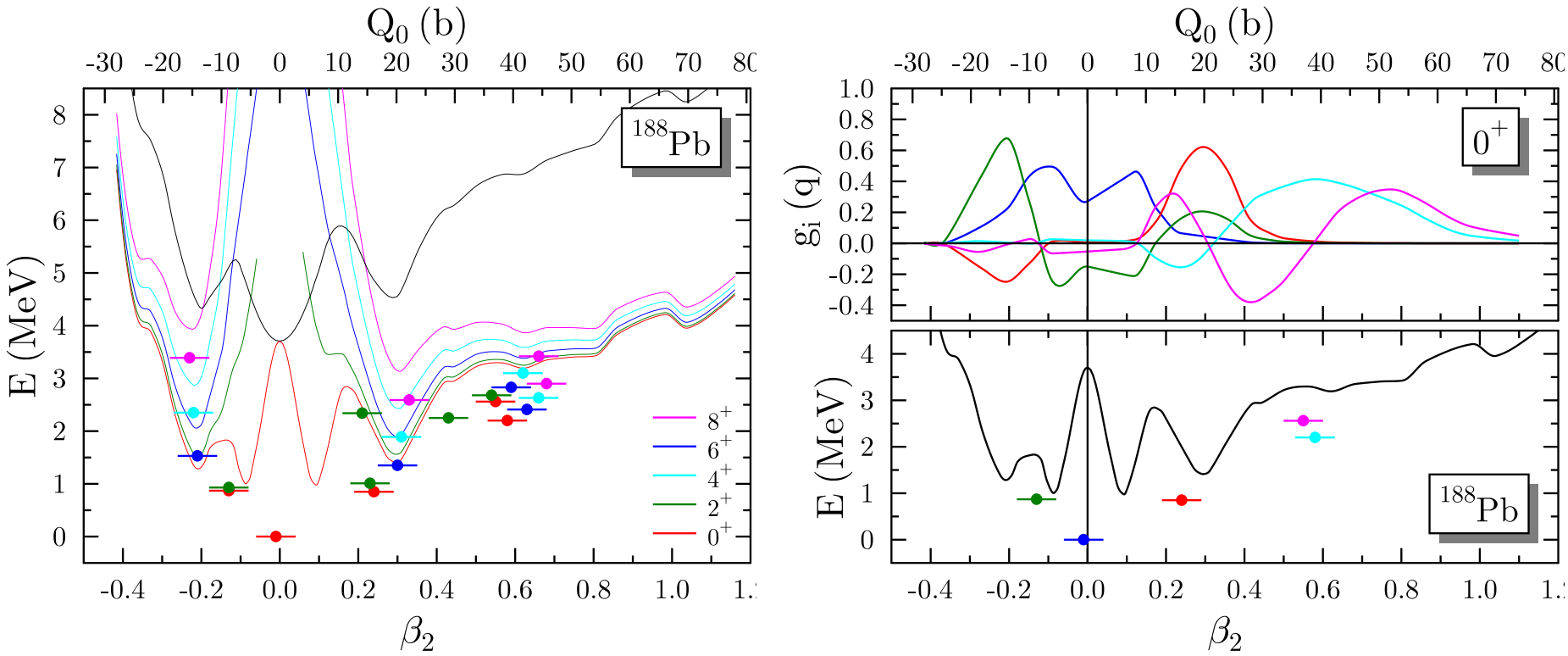

M. Bender, P. Bonche, T. Duguet, P.-H. Heenen, Phys. Rev. C 69 (2004) 064303.

Attention: $g_i^2(q)$ is not the probability to find a mean-field state with intrinsic deformation q in the collective state

Spectroscopy from MR EDF: Transition moments

M. Bender, P. Bonche, T. Duguet, P.-H. Heenen, Phys. Rev. C 69 (2004) 064303.
Experiment: T. Grahn *et al*, Phys. Rev. Lett. **97** (2006) 062501

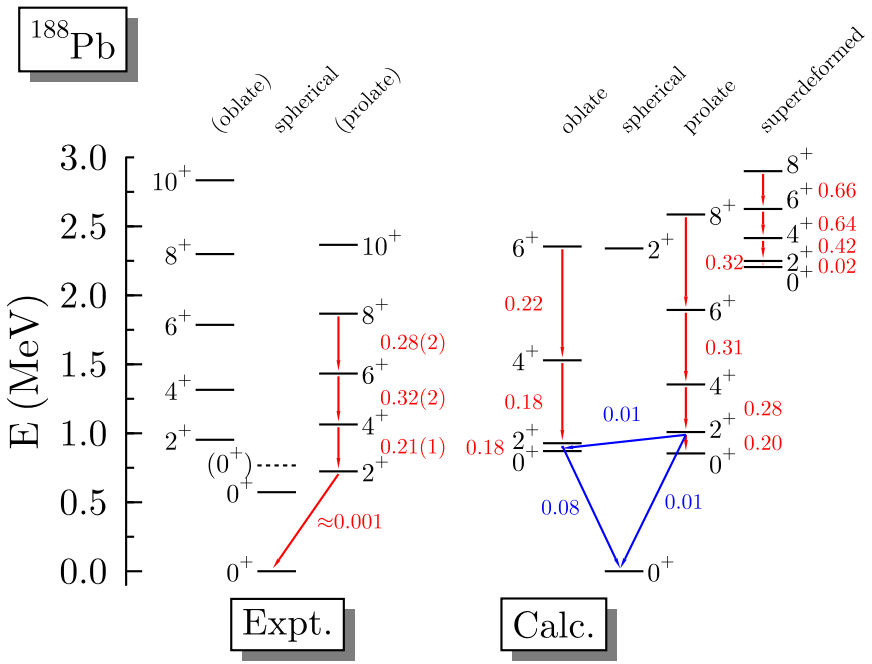

- in-band and out-of-band $E2$ transition moments directly in the laboratory frame with correct selection rules
- full model space of occupied particles
- only occupied single-particle states contribute to the kernels ("horizontal expansion")
- $\Rightarrow$ *no effective charges necessary*
- *no adjustable parameters*

$$B(E2; J'_{\nu'} \to J_\nu) = \frac{e^2}{2J'+1} \sum_{M=-J}^{+J} \sum_{M'=-J'}^{+J'} \sum_{\mu=-2}^{+2} |\langle JM\nu|\hat{Q}_{2\mu}|J'M'\nu'\rangle|^2$$

$$\beta_2^{(t)} = \frac{4\pi}{3R^2A}\sqrt{\frac{B(E2; J \to J-2)}{(J\,0\,2\,0\,|(J-2)\,0)^2 e^2}} \quad \text{with} \quad R = 1.2\,A^{1/3}$$

Typical Situations

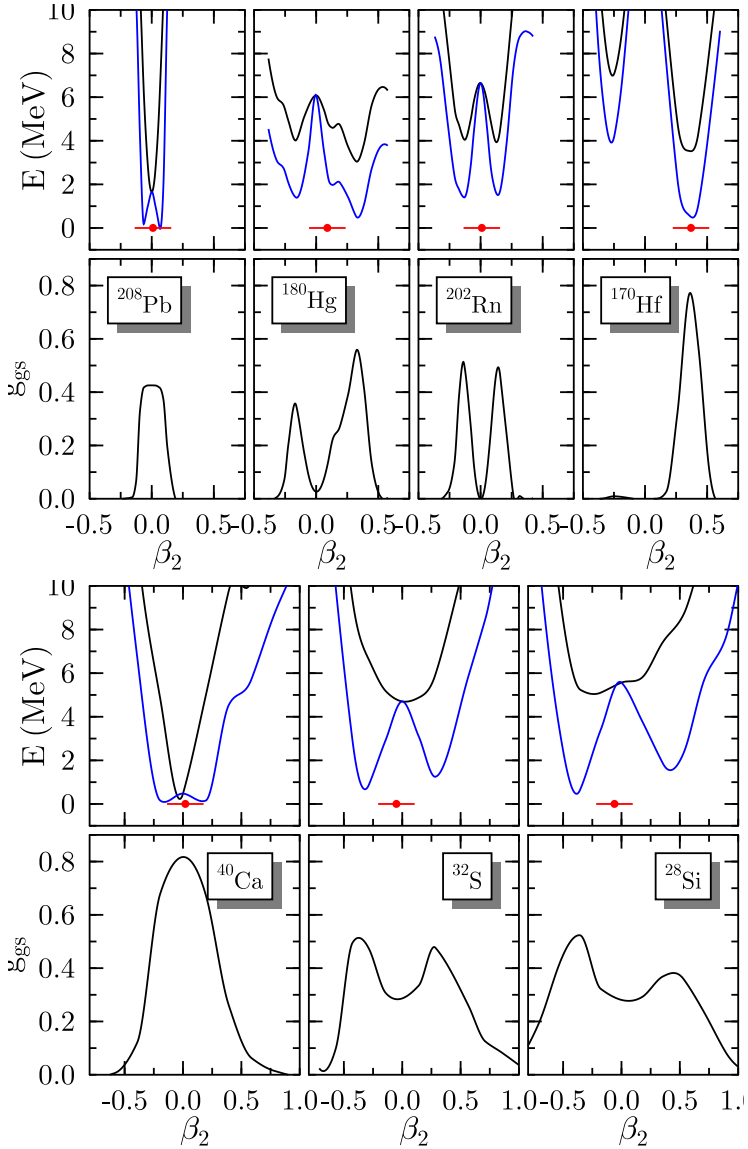

nucleus	E_{def}	$E_{J=0}$	E_{GCM}	E_{corr}
^{208}Pb	0.0	1.7	0.0	1.7
^{180}Hg	3.0	2.6	0.5	3.1
^{170}Hf	12.2	2.9	0.5	3.4
^{202}Rn	2.6	2.7	1.4	4.0
^{48}Ca	0.0	1.4	0.7	2.0
^{32}S	0.0	3.8	0.9	4.7
^{28}Si	0.7	4.2	0.6	4.9

- E_{def}: static deformation energy
- $E_{J=0}$: energy gain from projection
- E_{GCM}: energy gain from mixing projected states
- $E_{\text{corr}} = E_{J=0} + E_{\text{GCM}}$: total dynamical correlation energy

Bender, Bertsch, Heenen, PRC 73 (2006) 034322

How is the evolution of shell structure related to systematics of masses?

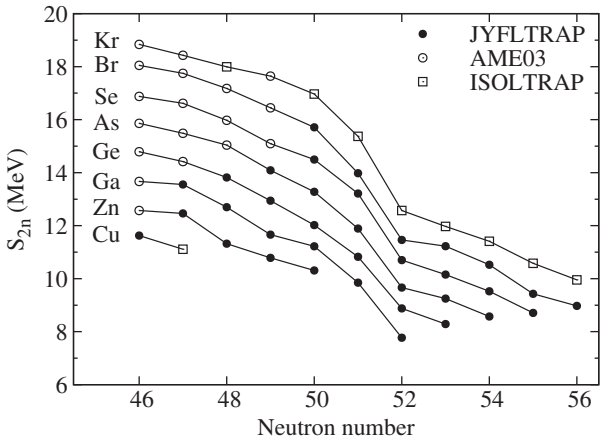

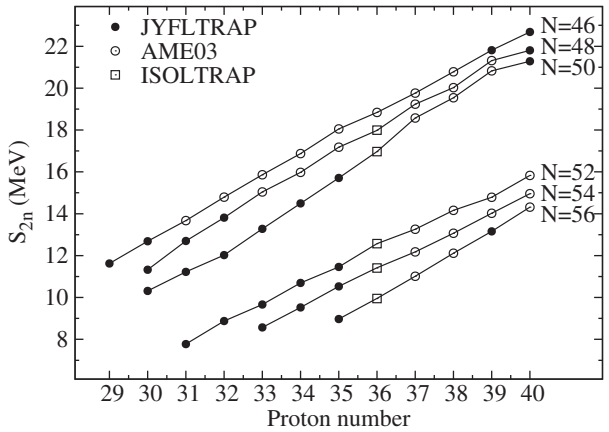

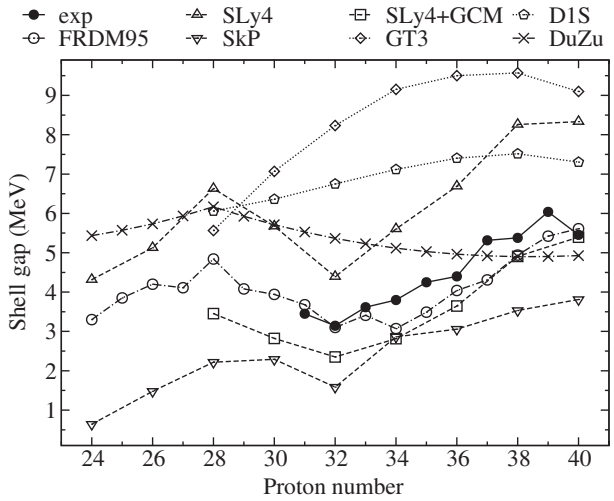

$$S_{2n}(Z,N) = E(Z-2,N) - E(Z,N)$$
$$\delta_{2n}(Z,N) = S_{2n}(Z,N) - S_{2n}(Z,N+2) = E(Z,N-2) - 2E(Z,N) + E(Z,N+2)$$

Hakala et al, PRL 101 (2009) 052502

Impact of of static deformation and fluctuations in collective degrees of freedom on separation energies around shell closures

- even-even nuclei
- intrinsic shapes constrained to axial symmetry
- projection on particle number and angular momentum
- mixing of configurations with different intrinsic deformation
- Skyrme interaction SLy4 + density-dependent zero-range pairing interaction

Intrinsic Deformation and Quadrupole Correlation Energy

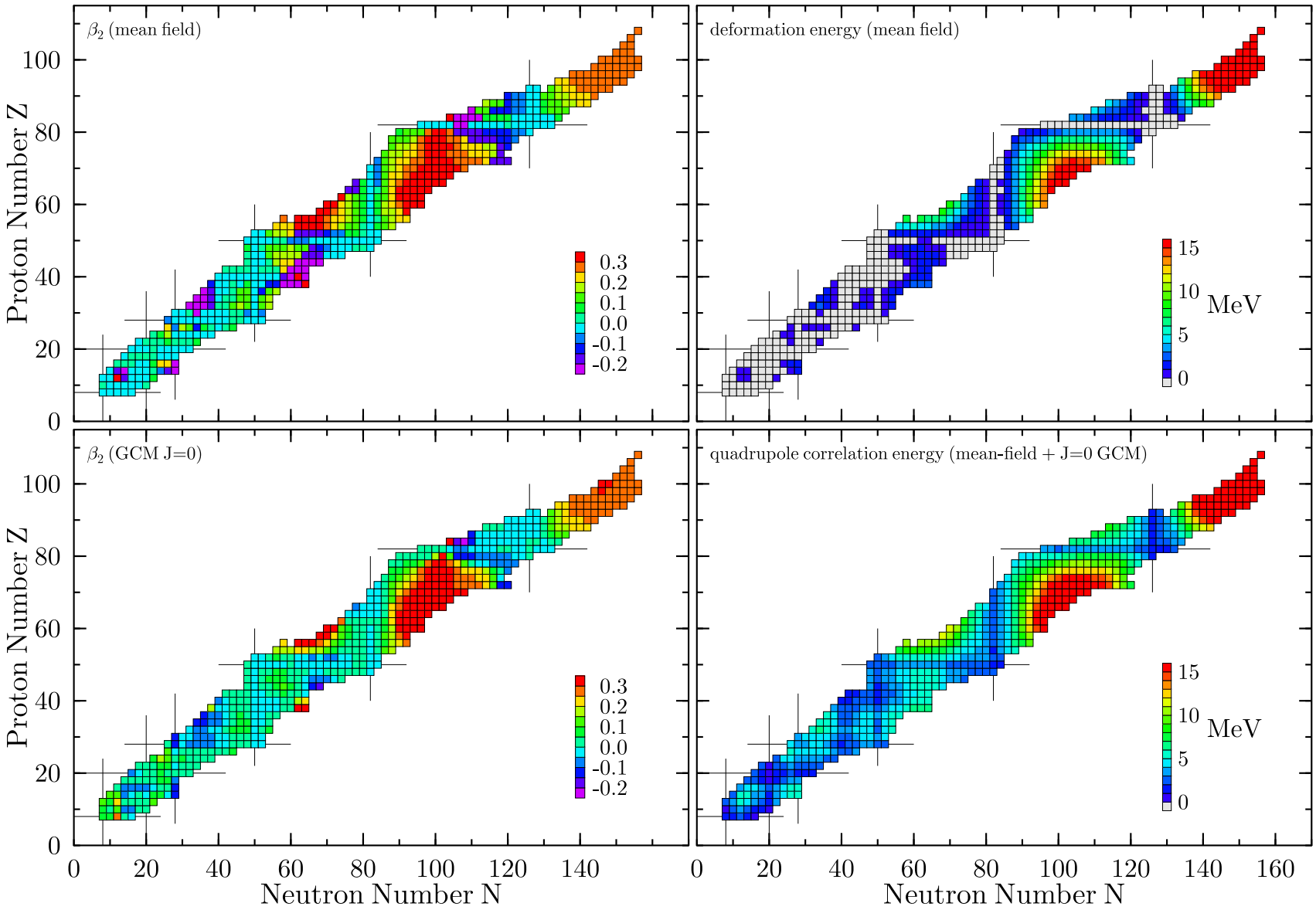

Bender, Bertsch, Heenen, PRC 73 (2006) 034322

Static and dynamic quadrupole correlation energies

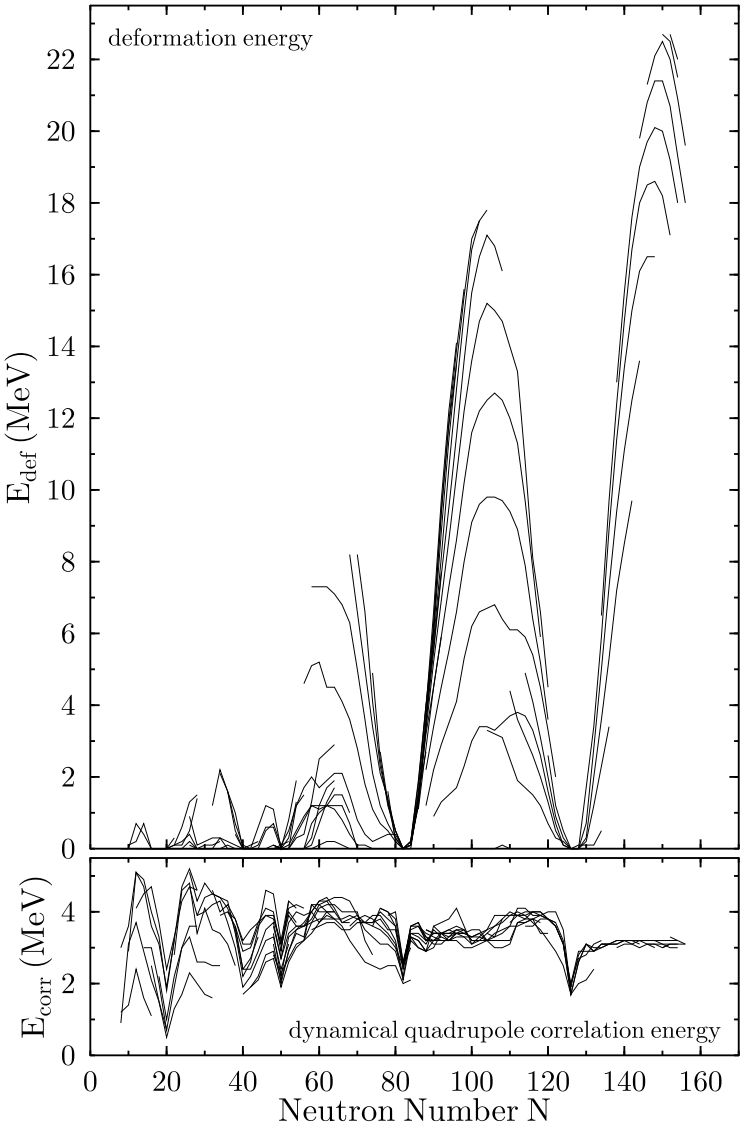

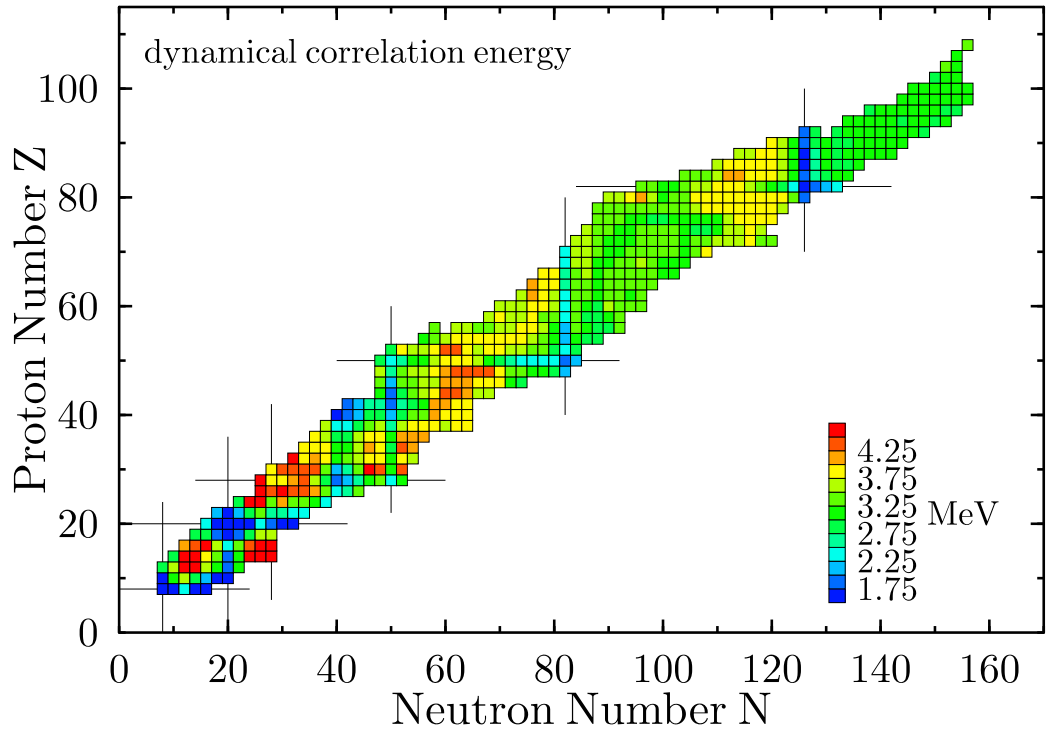

Bender, Bertsch, Heenen, PRC 73 (2006) 034322

Mass residuals

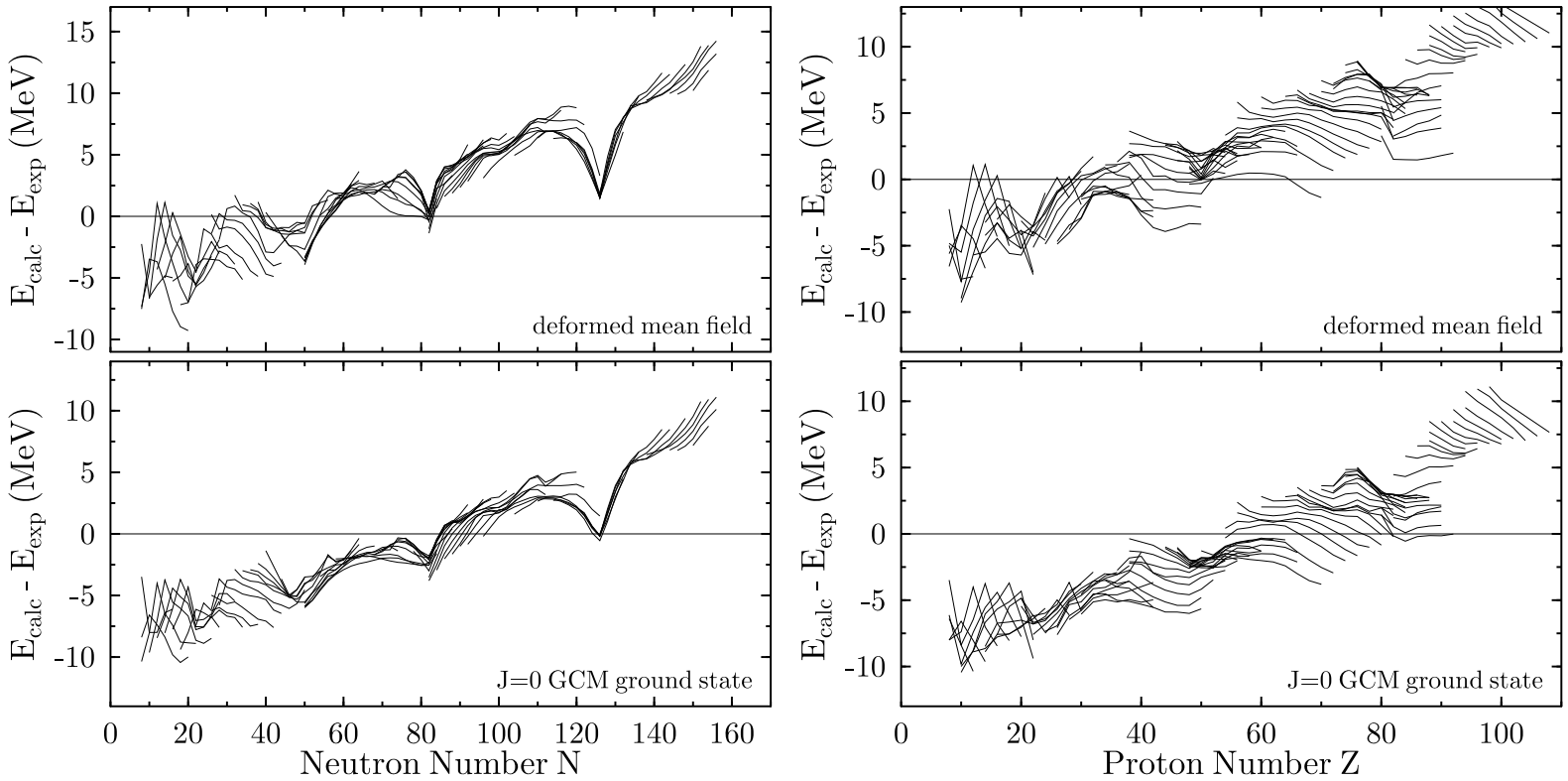

- Shell effects are not overestimated in general, they are overestimated for neutrons
- This might well be a problem with the effective interaction, not so much with large missing correlations

Bender, Bertsch, Heenen, PRC 73 (2006) 034322

Collectivity-enhanced quenching of signatures of shell closures

Bender, Bertsch, Heenen, PRC 78 (2008) 054312

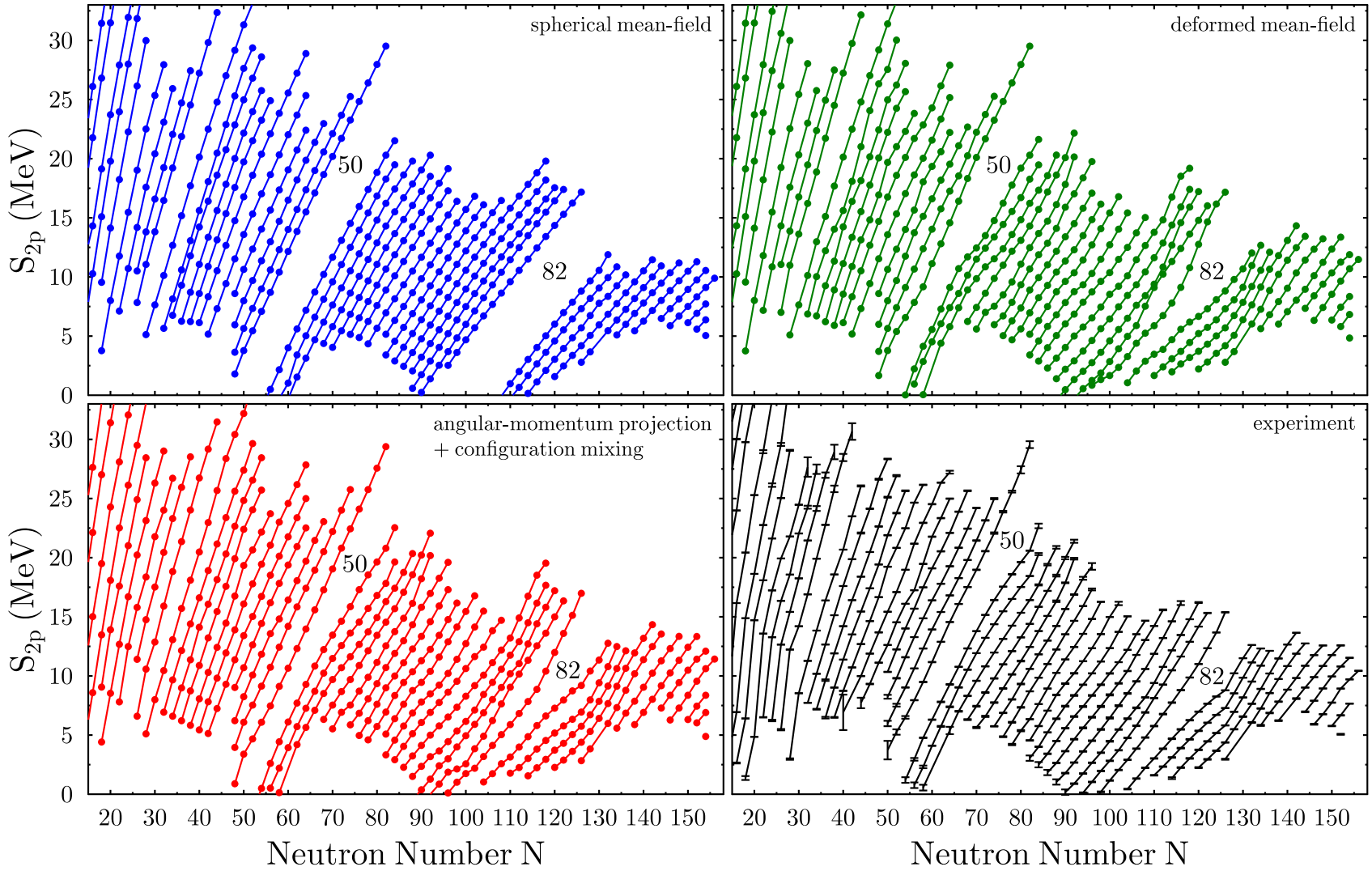

Collectivity-enhanced quenching of signatures of shell closures

Bender, Bertsch, Heenen, PRC 78 (2008) 054312

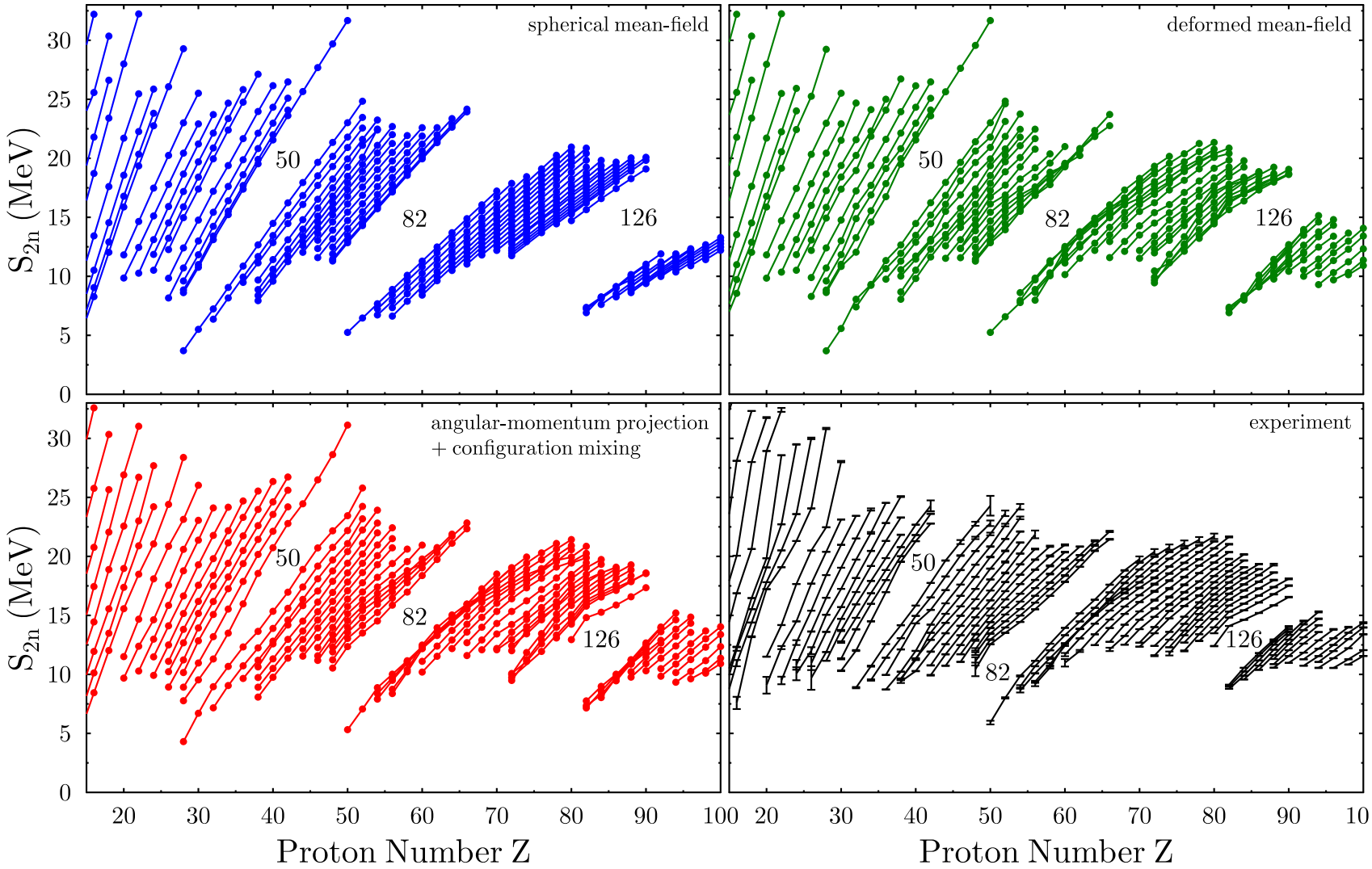

Collectivity-enhanced quenching of signatures of shell closures

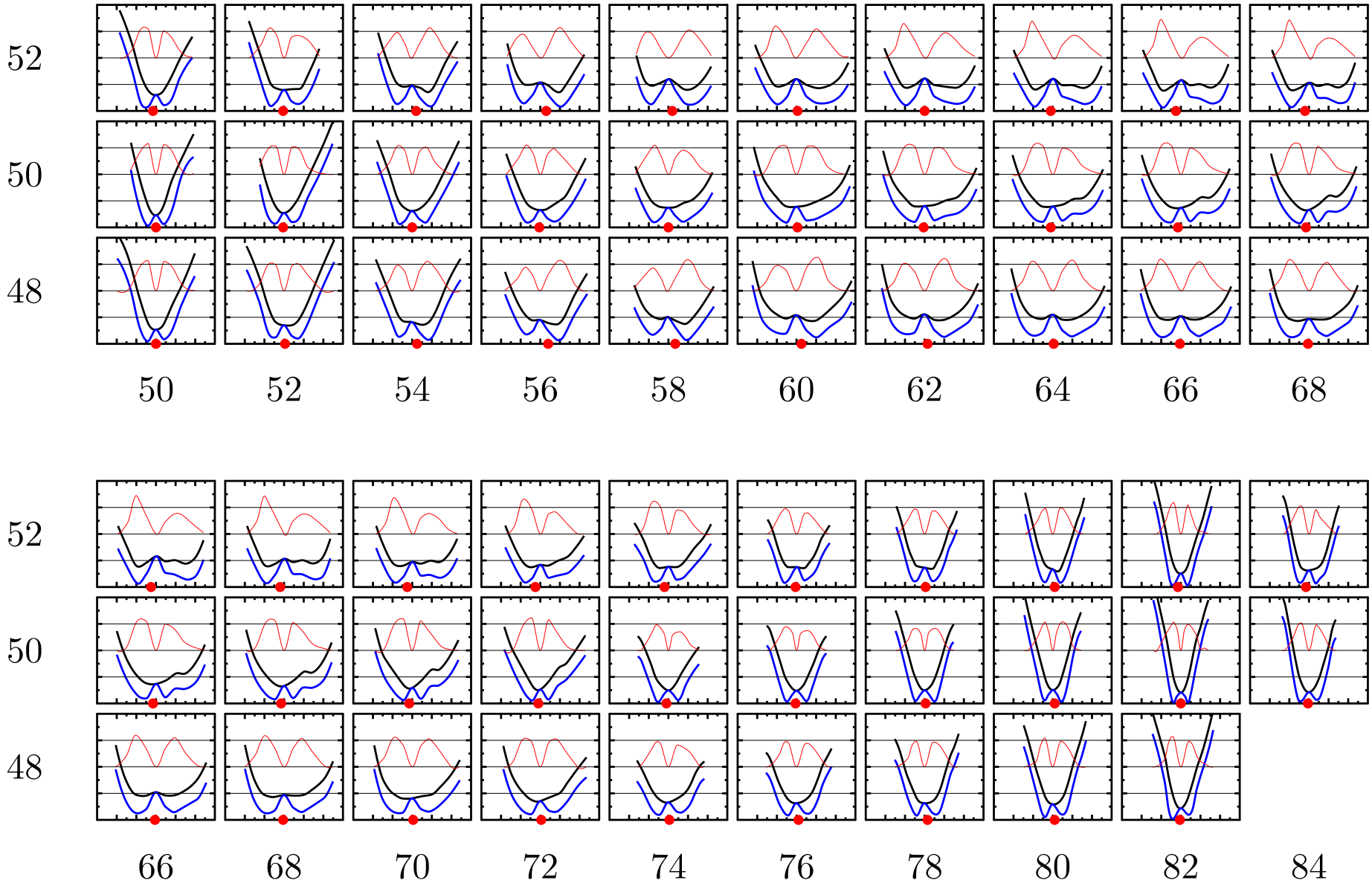

Bender, Bertsch, Heenen, unpublished material for PRC 73 (2006) 034322

Eigenvalues of the single-particle Hamiltonian vs. S_{2q}

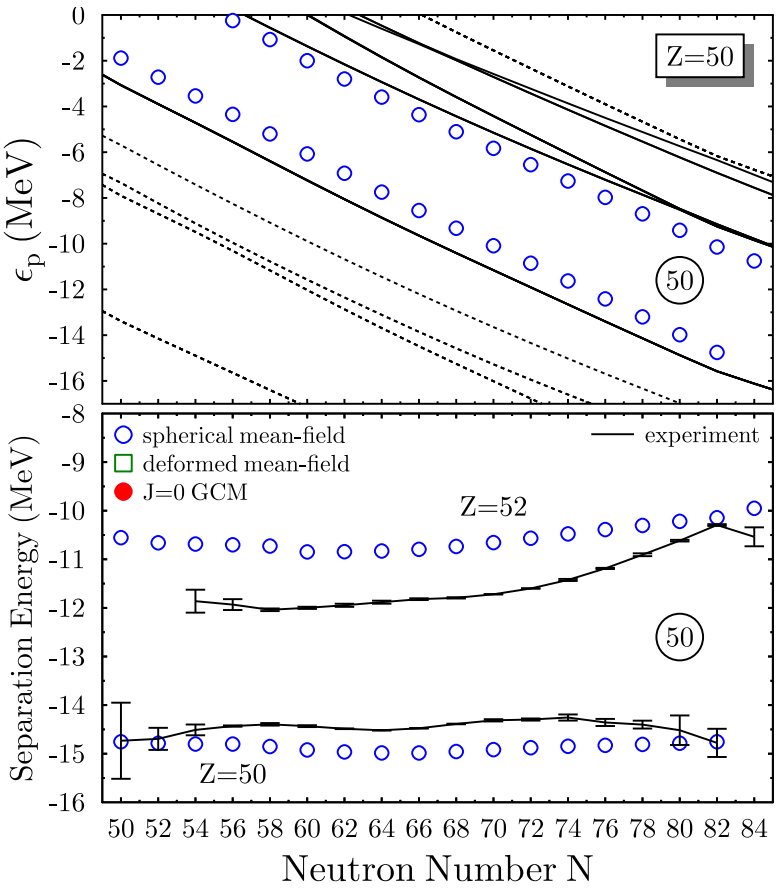

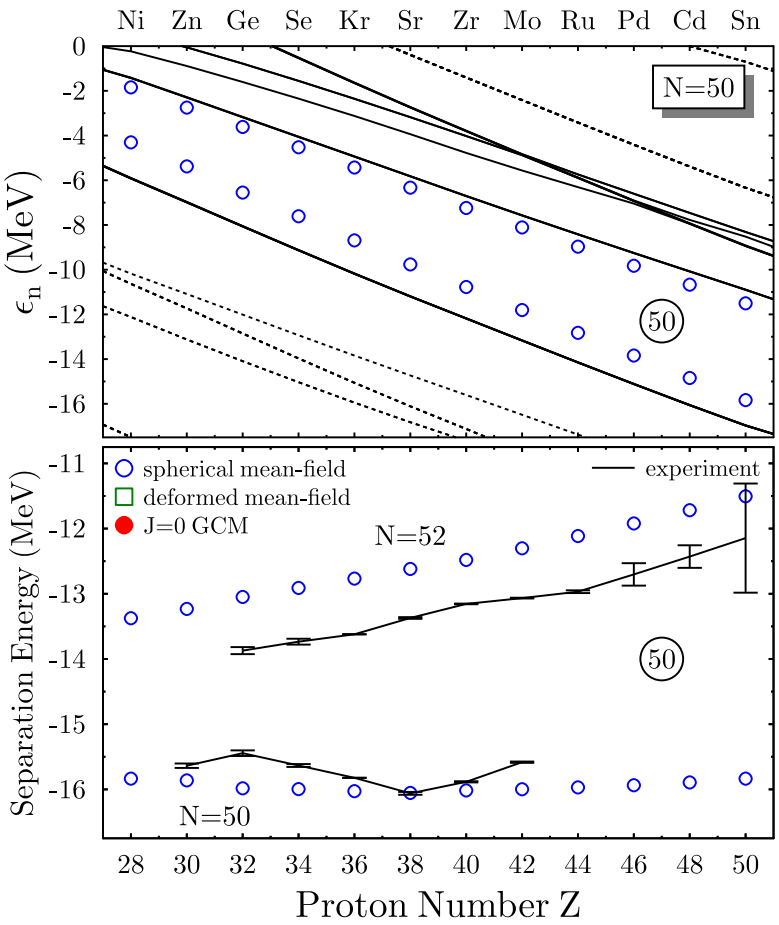

lower panel: $-S_{2p}(Z=50, N)/2$
The global linear trend is taken out subtracting
$\frac{N-82}{2}\,[S_{2p}(Z{=}50, N{=}50) - S_{2p}(Z{=}50, N{=}82)]$
using the spherical mean-field S_{2p}
Bender, Bertsch, Heenen, PRC 78 (2008) 054312

lower panel: $-S_{2n}(Z, N=50)/2$
The global linear trend is taken out subtracting
$\frac{N-50}{2}\,[S_{2n}(Z{=}28, N{=}50) - S_{2n}(Z{=}50, N{=}50)]$
using the spherical mean-field S_{2n}